5-22-2012

# The dependence of CD4 T cell development and activation on the kinetics of the TCR:pMHC interaction

Jennifer Nicole Lynch
*Washington University in St. Louis*

WASHINGTON UNIVERSITY IN ST. LOUIS

Division of Biology and Biomedical Sciences

Pathology and Immunology

Dissertation Examination Committee:
Paul Allen, Chair
Ted Hansen
Chyi Hsieh
Yina Huang
Andrey Shaw
Wojciech Swat

# The dependence of CD4 T cell development and activation on the kinetics of the TCR:pMHC interaction

by

Jennifer Nicole Lynch

A dissertation presented to the
Graduate School of Arts and Sciences
of Washington University in
partial fulfillment of the
requirements for the degree
of Doctor of Philosophy

August 2012

Saint Louis, Missouri

Two T cells, alike in specificity
*In vivo* and *in vitro* to describe
From common sequence t'new affinity
Where effects to increased $k_{on}$ ascribe

From forth the thymi of transgenic mice
The T cells develop with different ends.
The one, too strong for peptide ends its life
If it escapes responsiveness suspends.

The weaker one proliferates in spades
But responds to fewer altered peptides,
A consequence of kinetic downgrades
Though cell signaling is maintained inside.

The differences twixt the T cells are clear
The details of which are described in here.

ABSTRACT OF THE DISSERTATION

The kinetics of TCR:pMHC interactions regulate CD4 T cell selection and activation

By

Jennifer N. Lynch

Doctor of Philosophy in Immunology

Washington University in St Louis, 2012

Professor Paul M. Allen, Chairperson

The T cell is a critical player in the adaptive immune response. T cells function by stimulating antibody production by B cells, secreting cytokines to attract other immune cells, regulating the response of other T cells, and directly killing infected or damaged targets. The role of the adaptive immune response depends on the specific recognition of foreign antigenic epitopes by the T cell.

A T cell's specificity for antigen is conferred by the T cell receptor (TCR). The TCR is designed to bind a peptide antigen presented on an MHC molecule by an antigen presenting cell (APC). The strength of this interaction is determined by the ratio of the rate of dissociation ($k_{off}$) and the rate of association ($k_{on}$) between the TCR and the pMHC. The overall affinity of the complex must be sufficient for productive transmission of signals through the TCR to activate a T cell. However, the precise regulation of this event is not fully understood. Structural changes are thought to occur once the TCR encounters pMHC. Because of the energetics involved, kinetic and thermodynamic parameters have been correlated with the pattern and strength of T cell activation but

these relationships do not explain all TCR:pMHC. The contact duration or dwell time of the TCR with pMHC takes into account the potential for rebinding events, which can enhance the signal strength and are related to the $k_{on}$ and $k_{off}$ of the complex. A faster $k_{on}$ can balance out a fast $k_{off}$ to have sufficient interaction between the TCR and pMHC for complete T cell activation. The $k_{on}$ also controls the number of rebinding events that can occur. Even so, the role of $k_{on}$ in T cell biology has not been explored independently of changes in $k_{off}$.

Presented in this thesis is a system using two TCRs with specificity for the same antigen to compare how changes in $k_{on}$ alter T cell development and function. The n3.L2 and a mutant version, M2, recognize the $Hb^{d}$(64-76) antigen presented on the I-$E^{k}$ MHC class II molecule. M2 had a 3.7 fold stronger affinity for Hb(64-76)/I-$E^{k}$ due solely to a faster $k_{on}$. As a consequence, the M2 TCR responded more strongly to a broader range of altered Hb peptide ligands (APLs). While this presumably was due to an overall increased association with the MHC molecule, which could result from increased $k_{on}$, the M2 TCR still retained antigen specificity and did not respond strongly to all Hb APLs. N3.L2 hybridomas and double positive thymocytes responded more strongly to two APLs of the P2 TCR contact residue. Therefore the changes between the n3.L2 and M2 TCR structures only allow certain residues to productively bind. By measuring the kinetics of n3.L2 and M2 in association with APL/I-$E^{k}$, the maximal IL-2 response is accurately predicted by the $k_{off}$. No kinetic parameter correlated with the amount of APL needed to stimulate IL-2 production, suggesting other factors may be involved.

Since the response to APLs can mimic the ability of a TCR to recognize selecting self-peptides in the thymus, peripheral T cell responsiveness may be developmentally

controlled. TCR transgenic mice were generated expressing either the n3.L2 or M2 TCR. M2 thymocytes had stronger recognition of endogenous peptides and were deleted through negative selection when exposed to Hb(64-76) as a self peptide. N3.L2 thymocytes underwent full development and were not completely deleted by Hb(64-76). Interestingly, this difference in T cell selection led to functional consequences in peripheral T cells. $Ca^{2+}$, an early activation signal, was more sustained in n3.L2 CD4 T cells and more oscillatory in M2 CD4 T cells. Interestingly, M2 CD4 T cells failed to proliferate in response to antigen. Therefore, the TCR sensitivity set during T cell selection leads to qualitatively different signaling cascades in the periphery and can generate an anergic population with increased $k_{on}$ for pMHC recognition.

ACKNOWLEDGEMENTS

I would first like to thank my mentor, Paul Allen, for his guidance through my final years of graduate school. Paul has been a part of the graduate careers for a large number of students over the years and I have been fortunate to be one of them. His motivation and dedication were reasons why I joined the lab in my 3rd year. Paul has been patient and understanding during the slow times (and my absences), excited about my curious results, and truly enthusiastic to watch this thesis come together.

I also want to acknowledge the support of my thesis committee. They provided the voice of reason, a needed outside perspective, and the criticism to push my thesis in a new direction, leading to the final results presented here. Andrey Shaw, Chyi Hsieh, and Wojciech Swat pushed me to think about my research in different ways and increase the impact of my research on the field. Yina Huang may just have joined my thesis committee but has provided feedback and support for the past few years, hearing my thesis in informal pieces. Ted Hansen, who has served as the chair of my thesis committee, was particularly excited to be a part of this journey. He thanked me for the opportunity to be on another committee discussing peptide presentation. Ted's enthusiasm rekindled my interest when experiments weren't working and mice weren't breeding and he was always available to discuss my conclusions and future directions, personal and scientific.

The Allen lab, both current and past members, is a dedicated and brilliant group of researchers. Without the work and support of Darren Kreamalmeyer, Donna Thompson, and Stephen Horvath, my research would not have happened. I would particularly like to thank Darren for breeding and caring for all the mice that contributed

to this work, from the original “Cheesus” to the multiple lines I used in the end. I would also like to acknowledge Terri Sherlinski of the Washington University Transgenic Mouse Core for generating the original M2 founders, which was no small amount of work. Scott Weber and Dave Donermeyer were critical in the initiation and progress of this work, both in experimental and conceptual help. They have been part of this project longer than I have and were amazing sources of knowledge. Jen Racz, Cynthia Hickman-Brecks, Celeste Morley, and Stephanie Rodriguez were always open and available for support, lunch, and discussions. They truly kept me on track throughout this journey. Melanie Puhar, Jerri Smith, Sharon Smith, and Jeanne Silvestrini provided invaluable administrative support throughout my graduate school years.

In addition to the lab support group, I have built a wonderful group of friends in St Louis. Weijen Chua, Elizabeth Miller, and Samantha McNulty were my scientist support team, always with wine and cookies. My non-scientist friends provided the relief I needed when times got rough and an escape to dance/drink beer/be artistic/silly/ creative. They remind me each day to enjoy life and have made St Louis home.

This thesis is dedicated to my family. My parents would constantly ask about my research but probably understood very little. Even so, they kept trying and were always proud of their little “Peanut’s” accomplishments. My rabbit, Spike, has been a great help in writing this thesis: he determined good papers to cite by eating them and threw many others on the ground that didn’t make his grade. Hopefully he approves of this thesis. Finally, I would like to apologize to my husband and best friend, Eric, for all the late nights, days when I was curt with him after a hard day at work, making him read piles of edits, and forcing him to listen to me practice all my talks. He has weathered it all with

love, hugs, and delicious dinners. I look forward to all the adventures we will take together now that this one is done.

TABLE OF CONTENTS

LIST OF FIGURES AND TABLES

CHAPTER 2: The CD4 T cell response to altered peptide ligand recognition correlates with kinetics of TCR:pMHC association

CHAPTER 3: $k_{on}$ of TCR pMHC affinity drives changes in selection and activation of CD4 T cells

# LIST OF ABBREVIATIONS

| | |
|---|---|
| $^3H$ | tridiated thymidine |
| AP-1 | activator protein 1 |
| APC | antigen presenting cell |
| APL | altered peptide ligand |
| CD | cluster of differentiation |
| CDR | complement determining region |
| cSMAC | central supramolecular activation cluster |
| CTLA-4 | cytotoxic T-cell antigen 4 |
| DN | double negative |
| DP | double positive |
| EAE | experimental autoimmune encephalitis |
| $EC_{50}$ | effective concentration for stimulation at 50% of max |
| ELISA | enzyme-linked immunosorbent assay |
| $E_{max}$ | dose to produce maximal effect |
| ERK, pERK | extracellular signal-regulated kinase, phosphorylated ERK |
| FCS | fetal calf serum |
| FPLC | fast performance liquid chromatography |
| GFP | green fluorescence protein |
| Grb2 | growth-factor receptor-bound protein-2 |
| Hb | hemoglobin |
| Hb(64-76)/I-$E^k$ | hemoglobin peptide bound to I-$E^k$ MHC class II |
| HEL | hen egg lysozyme |
| HPLC | high performance liquid chromatography |
| ICAM-1 | intercellular adhesion molecule 1 |
| IFNγ | interferon gamma |
| IL-10 | interleukin 10 |
| IL-2 | interleukin 2 |
| IL-4 | interleukin 4 |
| IL-7 | interleukin 7 |
| IL-7R | interleukin 7 receptor |
| IMDM | Iscove's |
| ITAM | immunoreceptor tyrosine-based activation motif |
| $K_D$ | affinity |
| $k_{off}$ | rate of dissociation, off rate |
| $k_{on}$ | rate of association, on rate |
| Lck | leukocyte-specific protein tyrosine kinase |
| LFA-1 | leukocyte function-associated molecule 1 |
| MCC | moth cytochrome C |
| MHC | major histocompatibility complex |
| MHCII | MHC class II |
| NFAT | nuclear factor of activated T cells |
| NFκB | nuclear factor κB |
| PCR | polymerase chain reaction |
| PD-1 | programmed death 1 |

| | |
|---|---|
| pMHC | peptide bound to MHC |
| RBC | red blood cell |
| scTCR | single chain T cell receptor |
| SOS | son of sevenless |
| SP | single positive |
| SPR | surface plasmon resonance |
| TCR | T cell receptor |
| TCR:pMHC | TCR bound to pMHC |
| $T_{reg}$ | regulatory T cell |
| WT | wildtype |
| ZAP-70 | zeta-chain-associated protein 70 kD |

# CHAPTER 1

# Introduction

T cells are a critical component of the adaptive immune response. T cells develop in the thymus, producing the repertoire of effector cells that provides protection from the vast array of foreign infections. Each T cell maintains specificity for antigen as a consequence of rearrangement of the TCRα and β chains and therefore the main function of T cells is to propagate a specific immune response targeting detected antigens. CD4 T cells produce cytokines to help activate other immune cells, such as CD8 T cells and B cells. CD4 T cells can differentiate into a population of memory cells that maintain a quiescent but highly responsive state to protect the host upon reinfection. CD8 T cells have cytolytic properties to directly kill infected cells.

Unlike B cells, which can undergo somatic hypermutation to generate B cell receptors of increased affinity, the TCR specificity and affinity for peptides is determined in the thymus by selection during T cell development. The TCR loci recombine V-(D)-J segments to sequentially generate the β and α chains of the TCR. Productive rearrangement of both chains leads to selection of T cells that bind self-peptides presented on MHC class I or II. The TCR affinity for pMHC regulates outcomes of T cell selection in the thymus and activation of T cells in the periphery (1-4). The affinity ($K_D$) of the TCR:pMHC complex is regulated by the dissociation rate ($k_{off}$) and association rate ($k_{on}$). Agonist peptides induce full T cell activation through strong interactions with the TCR (3, 5). In the thymus, these highly responsive T cells can be deleted by negative selection. Weaker TCR:pMHC interactions can result in partial T cell activation (6) or anergy (7, 8), though positively selecting TCR:endogenous pMHC interactions are also of very low affinity (9).

**Structural basis of TCR specificity and flexibility for recognition of pMHC**

TCR:pMHC complex formation needs to overcome a high activation threshold leading to T cell activation (1, 10-13). Subtle conformational changes are necessary to ensure a stable TCR:pMHC complex and productive signaling through the TCR (14-17). Therefore, this activation threshold is a result of the energetics of TCR:pMHC complex formation. It has been suggested that TCR:pMHC binding is entropically unfavorable while being enthalpically favorable as order is increased (12, 18). Recent data has altered this thinking, favoring instead an activation threshold based on the affinity of the interaction, where summation of the energy from individual amino acid interactions results in varying levels of T cell activation (19). The TCR:pMHC binding footprint is a specific but flexible structure (20) where CDRs 1, 2, and 3 of the TCR form contacts with the pMHC complex. TCRs have specificity for pMHC but also have the ability to recognize many different but closely related peptides. Inherent TCR flexibility is an effective mechanism for generating a sufficient T cell repertoire to target infections and tumors but can go awry generating autoimmunity (10, 21). Relatively large conformational changes have been described for the CDR3 regions, potentially resulting in stable peptide engagement (17, 22). However, it seems clear that another factor must be initiating the association and inducing the CDR3 conformational changes.

TCR specificity for pMHC is encoded in the variable CDR loops, which form the binding footprint for TCR to contact the pMHC complex (23, 24). TCR specificity for MHC is maintained by interactions with CDRs 1 and 2 (25, 26). The germline encoded interaction between a TCR and an MHC is best defined for T cells using Vβ8.2 in which

a set of conserved of interactions exists between the TCR CDR1β and two tyrosine residues on the MHCβ chain (26-28). While CDRs 1 and 2 are highly conserved, introduction of mutations in these CDR loops can result in generation of high affinity TCRs (29, 30), potentially as a consequence of an optimal binding conformation or enhanced TCR:pMHC stability (16, 20, 25, 31, 32). The CDR1α region can stabilize the TCR and contribute energetically to the overall complex through contact with the MHC or by directly influencing the CDR3α contact with peptide (22, 32, 33). In the general diagonal orientation of the TCR on pMHC, the CDR3 loops position across the peptide binding groove providing direct interactions with specific amino acid side chains (17, 22, 34, 35). Since the CDR3 loops interact with the peptide, conferring the cross-reactive property of T cells (36), they have been the main focus in determining what makes a T cell potentially autoreactive (37, 38). However, mutations in the CDR1 and 2 loops can generate a higher affinity TCR (29) that are potentially autorreactive.

**Components of TCR:pMHC association that determine T cell activation**

Through thermodynamic and kinetic studies, TCRs have generally been described as having slow association rates and fast dissociation rates (17, 39) compared to antibodies, leading to short windows for productive activation and signaling outcomes post TCR engagement. Some studies have found correlations between dissociation rate ($k_{off}$) measurements and T cell activation (39-43), though activation cannot be reliably predicted based on $k_{off}$ alone (1, 12). Since structural changes occur when the TCR engages pMHC (1, 16, 17), the initial TCR:pMHC association is somewhat temperature dependent and thermodynamic measurements, such as heat capacity, can correlate with T

cell activity (12, 44, 45), especially when combined with $k_{off}$. Because of the number of outliers with each model, there is no consensus for one parameter being a predictor of a peptide's ability to stimulate a TCR (46).

A few studies have suggested a role for $k_{on}$. TCR mutants engineered *in vitro* for higher affinity resulted from a dominant association rate ($k_{on}$) (1, 16). Recently, it was shown that a stimulatory pMHC with a very fast $k_{off}$ could compensate with a fast $k_{on}$ resulting in sufficient interaction between the TCR and pMHC for full activation (47, 48). Mutations that increase TCR $k_{on}$ also stabilize the TCR structure (16). T cells with increased $k_{on}$ and affinity would reflect a structure optimized to bind pMHC. In support of this theory, studies have implicated faster $k_{on}$ in better IFNγ-IFNγR interaction (49) and increased autoreactivity leading to spontaneous EAE pathogenesis (10). Faster $k_{on}$ would mimic the effect of slower $k_{off}$, resulting in the same kinetic discrimination for T cell activation (2, 3).

**Models of productive T cell activation**

There are multiple models to explain how the association of TCR with specific pMHC complexes results in varying levels of T cell activation. Some evidence suggests the level of T cell activation may be a result of the inherent affinity of the TCR:pMHC complex, with increasing affinity leading to formation of more TCR:pMHC complexes and therefore stronger proliferation and cytokine production (46, 50). A large number of clusters of TCR:pMHC would result in sufficient phosphorylation of kinases proximal to the TCR to fully activate a T cell (51). Alternatively, a similar result can be achieved with multiple interactions between the TCR and either the same or neighboring pMHC (2, 43).

Serial triggering of a TCR leads to accumulation of signals the sum of which can overcome an activation threshold or increase the maximal response (4, 52). The frequency of rebinding can be driven by $k_{on}$ or $k_{off}$. In both the affinity and serial triggering models, changes in the $k_{off}$ or $k_{on}$ would alter the outcome of activation, potentially resulting in partial activation of a T cell. Full T cell activation requires a sufficient length of contact between the TCR and pMHC to phosphorylate downstream signaling molecules (53-55). The density of TCR on a T cell or presented pMHC contributes to the overall contact time. Dual TCR T cells express lower levels of specific TCR and have decreased sensitivity and reduced responses to pMHC as a result (56). The contact duration or confinement time is proportional to the overall affinity and changes in $k_{on}$ and $k_{off}$ would alter the longevity of the TCR:pMHC complex (47, 48).The overall duration of TCR:pMHC takes into account the ability of receptors to rebind in addition to affinity, measuring the effective half-life for T cell activation. A high local concentration of TCR and pMHC enhances the likelihood of forming multiple productive or sustained interactions (57-59). In fact, a stronger correlation was observed between antigen potency and maximal efficacy when confinement time was taken into consideration with $k_{off}$ or $K_D$ and this relationship may have been more dependent on $k_{on}$ (43).

Two possible structural mechanisms for TCR:pMHC interaction kinetics have been described. The first model is an induced-fit model where a ligand-induced conformational change results in stabilization of the initial complex and determines the association rate (1, 60). The rate can also be a function of the ligand's structure, confirming how increasing affinity is possible. In this scenario, cross-reactive peptide recognition is maintained by TCR flexibility, though it is limited by selection. The

second model predicts the existence of multiple free-site conformers, which account for the TCR flexibility (16). The overall association rate would be controlled by the transition between these conformers of the TCR binding site and would explain crossreactivity of the TCR. Increased $k_{on}$ would reflect preferential conformations for TCR:pMHC binding.

**Caveats with previous studies of $k_{on}$**

Previous studies have been unable to differentiate between the effect of increased $k_{on}$ and decreased $k_{off}$ as TCR modifications have resulted in changes to both kinetic parameters. Studies by Aleksic, et al. and Govern, et al. (47, 48) clearly revealed that changes in $k_{on}$ can affect the ability of a peptide to stimulate a T cell, but based their conclusions on TCR:pMHC combinations with changes in both $k_{on}$ and $k_{off}$. Therefore, it remains important to understand the individual contribution $k_{on}$ makes in determining T cell selection and activation. Other studies have found no correlation between $k_{on}$ and increased affinity (40, 61) but these systems involved either large conformational changes (40) or did not measure any affinity maturation (61) and therefore would not observe the proposed affect.

**Stimulatory ability of different peptides**

The TCR recognizes structural features of amino acid side chains of specific peptides bound to MHC molecules (35). The sum of binding energetics between the TCR and pMHC dictate the overall affinity of the complex and determine how a T cell will respond to a specific peptide presented on MHC in both the thymus and periphery (19).

There are critical residues on these peptides for generating TCR recognition (62), but some modifications can maintain peptide potency. In addition to identification of naturally occurring stimulatory peptides, altered peptide ligands (APL), modified versions of agonist peptides, have been used to measure TCR flexibility and differential T cell activation. APLs are synthetically generated peptides with substitutions in TCR or MHC contact residues that potentially enhance or inhibit the formation of the TCR:pMHC complex. A peptide that induces full activation, both cytokine production and proliferation, is deemed an agonist. While multiple agonist ligands can be recognized by a single TCR, these peptides may have little sequence or structural homology (63). A second tier of peptides consists of partial agonists that activate T cells to varying degrees. Partial agonists may induce lower levels of cytokine production or proliferation but also can result in entirely distinct signaling patterns from cognate antigen (6, 42, 64). Peptides with a lower potency than partial agonists can inhibit T cell activation in response to agonists (65). These antagonists are unable to stimulate T cell function but may be important for thymic selection of T cells.

**TCR:pMHC affinity regulates T cell development**

T cell development results in death by neglect, death by negative selection, or life by positive selection (66). There is an affinity continuum of a TCR for endogenous pMHC that regulates selection of T cells in the thymus (67). For T cells to be selected, the TCR must have sufficient affinity for endogenous pMHC above the threshold for positive selection but below the threshold for negative selection (9, 68, 69). T cells on the low end of the affinity spectrum have insufficient recognition of pMHC and die from neglect (70).

An entire population of T cells must be selected by a potentially small number of different self-peptides. In mice expressing a single pMHC in the thymus, a large and diverse repertoire of T cells develops (71). These studies suggest preselection T cells may favor contact with the MHC molecule but are selected for peptide specificity during negative selection (23, 72). This specificity is retained in peripheral activation, a key feature of T cell reactivity.

**Low affinity TCR:pMHC interaction leads to positive selection**

Positively selecting peptides are highly specific and do not reflect the structural features of agonists (70, 73-75). Positive selection has an analog threshold due to partial or low levels of T cell activation (76). Positive selection has been induced using low affinity APLs, which mimic the affinity of self-peptides in the thymus (68, 73, 77). Naturally occurring selecting peptides have being identified for $CD8^+$ (9, 75) and $CD4^+$ T cells (74). These peptides are not agonist peptides for T cell activation and proliferation in the periphery but instead are lower affinity peptides that usually function as weak agonists or antagonists. The role of peptide strength in selection was assessed *in vivo* by generation of mice expressing chimeric APL Hb–HEL transgenes on H-$2^k$. Using APLs of various strengths, Williams et al. (78) dissected the ability of strong agonists, weak agonists, and null peptides to induce negative and positive selection. Antagonists, a null peptide, and weak agonists induced positive selection at low concentrations and negative selection at higher concentrations. Similar findings have been reported in other studies (9, 79). It was also thought that the amount of peptide and MHC on the surface, and consequently the amount of TCR, would be a determinant of positive selection (80). Kersh et al. (79)

assessed the levels of pMHC required for selection. By reducing the I-$E^k$ expression using crosses of H-$2^k$ mice to H-$2^b$ haplotype, levels of specific TCR expression in the periphery decreased. Therefore, specific levels of pMHC are required to provide sufficient niches for efficient positive selection and transgenic TCR expression. As the T cells examined expressed multiple α chains, it could be that selection worked through one TCR efficient for selection and a second, self-restricted TCR could be activated in the periphery post selection, leading to autoimmunity.

Additionally, TCR coreceptors might regulate positive selection. Using a positively selecting ligand, Jameson et al. (70) found that CD8 levels were decreased on selected T cells. By blocking CD8, they altered T cell clones' abilities to respond to peptides, resulting in weak agonists functioning as antagonists. The coreceptor modulates the ability of a T cell to respond to peptide and therefore down modulation of CD8 could dampen reactivity to selecting self-peptides, as proposed in the "quantitative instructive" model (66). In the absence of CD4, positive selection of T cells is maintained by addition of antagonist APLs, which would induce negative selection in the presence of CD4 (81). Lack of CD4 did not skew the T cell repertoire towards CD8 but did indicate that higher affinity TCR:pMHC interactions are required for T cell development in the absence of coreceptors. Positive selection efficiency may be a result of other signaling molecules immediately downstream of the TCR, including CD3 subunits. CD3δ knockout mice have a developmental block at the double positive stage, prior to positive selection (82). Knocking-out the CD3ζ chain led to defective positive and negative selection, indicating that signal amplification through the TCR controls selection (83). A recent paper from our lab has established that decreased signaling through the TCR in PKCθ $^{-/-}$ mice also

led to inefficient positive selection (84). Therefore, peripheral T cell populations are selected by lower signal strength through the TCR in response to self-peptide, confirming the continuum of peptide affinity versus selection.

**Negative selection of high affinity TCRs**

High affinity recognition of self-peptide MHC can result in negative selection. High affinity TCR:pMHC interactions have a longer contact time leading to increased signaling through the TCR (78). By increasing the affinity of the TCR for self pMHC complexes, peptides which were low affinity, inducing positive selection, would have high enough affinity to overcome the threshold for negative selection. TCRs that can respond to multiple peptides are equally more likely to be eliminated by negative selection (85, 86). Negative selection is a digital response due to the accumulation of specific signals downstream of the TCR (87), resulting in apoptosis of high affinity T cells to generate central tolerance (77, 78). Two potential models can explain development of a signal strong enough to induce negative selection. First, the TCR may have a high affinity for a selecting pMHC in the thymus. Second, accumulated signals as a result of multiple interactions with different pMHC complexes can lead to negative selection.

Negative selection ensures central tolerance by elimination of self-reactive T cells from the repertoire, preventing autoimmunity upon T cell egress to peripheral lymphatic tissues. While positive selection occurs in the thymus medulla and results in pro survival signals, negative selection occurs in response to contact with cortical epithelial cells and results in apoptotic signals (88, 89). Initial studies of negative selection and central

tolerance were conducted by examining transplantation (90). Thymic grafts suggested that the thymus controlled the fate of T cell development, inducing tolerance to antigen due to restriction of T cell specificity. Kappler and Marack definitively proved that negative selection occurs at the transition from the double positive thymocyte state to the naive single positive thymocyte through elimination of specific subsets of T cells by specific self antigens (90, 91).

However, the efficiency of negative selection is variable and some autoreactive T cells can enter the periphery, potentially leading to disease development. High affinity TCRs that escape negative selection are potentially selected using different binding conformations from those used for recognition of antigen in the periphery (92). It is suggested that low levels of some antigens in the thymus can result in elimination of only the highest affinity T cells, allowing lower affinity T cells to escape selection. As selecting antigens are limited in the thymus, complete elimination of high affinity TCRs can be achieved in transgenic mice with small thymocyte populations (93, 94).

**Regulation of T cell activation by TCR:pMHC**

The functional ability of T cells is a reflection of stimulation through the TCR and costimulatory molecules. Complete T cell activation is the result of productive signaling through the TCR resulting in full phosphorylation of the TCR/CD3 complex and activation of ZAP-70. The kinetics of TCR:pMHC binding regulate whether full T cell activation occurs and the level of phosphorylation (95). Fast dissociation would result in incomplete activation (2, 3) and could be a mechanism of antagonism. Some ligands are able to activate, partially activate, or inhibit activation of a T cell (64). There are

measurable differences in downstream signaling factors from each of these ligand classes. TCR clustering can enhance signaling either by producing longer TCR:pMHC contacts or by increasing the rate of serial ligation and triggering (4, 96). The actin cytoskeleton of a T cell arranges to form and maintain contact with an APC necessary for sustained signaling and formation of new or rebinding TCR:pMHC complexes (97). A high density of pMHC may be required to activate rather than suppress T cell response (98). However, the quality of the peptide has a stronger effect on the response of a T cell. Low levels of strong agonist peptides are more able to stimulate IL-2 production than high levels of weak agonist *in vivo* (99), though agonists can induce anergy if very few pMHC compexes are engaged by a TCR (98). Affinity matured human TCRs lose sensitivity to low density of agonists but are able to respond to weak agonists (100). T cells with affinity at the high end of the normal spectrum maintain high sensitivity and recognize low affinity APLs (100).

Formation of microclusters of TCR:pMHC quickly after contact generates an environment for signaling downstream of the TCR (101). These microclusters are continuously being generated to sustain signaling (101) but can fuse into larger structures with reduced signaling capacity (102). When the adhesion molecule ICAM-1 binds LFA-1, recruitment of costimulatory and signaling intermediates to the site of TCR:pMHC contact can alternatively result in formation of the highly organized immune synapse (103, 104). The synapse is an adaptive controller of immune responses depending on the strength of the TCR:pMHC interaction, enhancing weak signals and degrading strong responses. The CD3 and CD4 coreceptors augment weak TCR signaling (105-107). Accumulation of CD3, CD4 and costimulatory molecules, such as CD28, leads to

amplification of initial signals through the TCR leading to the overall determination of T cell activation and function.

**Ca2+ signaling**

Intracellular signaling molecules differ in level and state according to levels of initial TCR signaling (108). One of the first biochemical responses upon TCR signaling is calcium ($Ca^{2+}$) influx. Variation in activation and differentiation state of T cells produces unique $Ca^{2+}$ flux signatures that can be measured by imaging with $Ca^{2+}$ indicator dyes. Strong agonist peptides induce $Ca^{2+}$ influx with a high initial peak followed by increased sustained intracellular $Ca^{2+}$ levels (64). Weaker agonist peptides will produce lesser initial influxes and lower sustained levels, though still result in activation. $Ca^{2+}$ flux changes have also been seen due to peptide concentration (109) and APL strength (110), strengthening the link between TCR:pMHC affinity and $Ca^{2+}$ signaling. Complete T cell activation is achieved based on regulation of $Ca^{2+}$ store release and influx by TCR signal strength. This signal can further be regulated based on timing of sustained signaling through synapse formation and receptor downregulation.

**IL-2 production**

IL-2 is critical for development and proliferation of T cells. The level of IL-2 production by activated T cells depends on costimulation (111, 112). Upon activation, a T cell expresses a high affinity version of the IL-2 receptor making it more sensitive to the presence of IL-2. When a T cell is anergized, IL-2 secretion is suppressed whereas release of other cytokines may be maintained (113). Addition of IL-2 to anergized cells

overcomes the inhibitory signals, leading to T cell proliferation and further production of cytokines. Interestingly, IL-2 promotes the generation of high affinity regulatory T cells ($T_{regs}$) and therefore can function as an enhancer and inhibitor of T cell response (114).

**Limiting and inhibiting T cell activation**

There is a delicate balance, however, between heightened activation and over responsiveness to antigen. A hyperresponsive T cell can lead to inappropriate recognition of self-peptides resulting in autoimmune disease. Mechanisms have been built in to T cell machinery that finely regulate activation. In addition to stimulation through the TCR and coreceptors CD4/CD8 and CD3, costimulatory molecules on the surface of the TCR bind ligands on the APC activating new signaling cascades. Engagement of B7-1 and B7-2 on an APC by CD28 is thought to be important in driving T cell proliferation, cytokine production, and survival through regulation of Bcl-XL (112, 115, 116). CD28 has found to induce stabilization of IL-2 mRNA, leading to sustained T cell proliferation and responsiveness (112). Competing with CD28 for access to B7-1 and B7-2 is CTLA-4, primarily described as an inhibitor of T cell activation. CTLA-4 can block phosphorylation of Zap-70 suppressing proximal signals through the TCR complex (117). While CTLA-4 may contribute to a hypoproliferative T cell response by blocking IL-2 production, it is not required for the induction of anergy as T cells deficient in CTLA-4 will be hyperproliferative in response to chronic exposure to antigen and then enter into a state of anergy (118). CTLA-4 and PD-1 are both upregulated on T cells following activation through the TCR:pMHC complex. PD-1 also functions to limit T cell responsiveness but increased IL-2 overcomes PD-1's suppressive effect through

activation of STAT5 (111). While many pathways of activation and suppression exist in a T cell, the balance of these signals and the influence of the surrounding milleu dictate the level of T cell response.

**How T cell selection influences activation, autoimmunity, and tolerance**

A complex set of distinct signals regulates positive and negative selection (76, 119), tuning T cell responsiveness in the periphery. Sustained signaling through ERK leads to positive selection of thymocytes whereas transient signaling results in negative selection (120, 121). Negative selection is an incomplete process and some high affinity T cells escape to the periphery where they can cause autoimmune disease (122). To prevent autoimmunity, potentially autorreactive T cells are either rendered unresponsive to antigenic stimulation (123) or deleted in the periphery to maintain peripheral tolerance (78). Because of the dual role of T cell affinity in selection and activation, the propensity for T cells to undergo tolerance may be set in the thymus by the affinity of the expressed TCR for self pMHC (124).

Anergy, a state of hyporesponsiveness characterized by low IL-2 production and inhibited proliferation (123), has been induced in naive T cells through lack of costimulation (125, 126), exposure to APLs (6, 8, 77), sustained exposure to antigen (127), or low stimulation through the TCR as a result of either low affinity interactions (86, 128, 129) or unstable pMHC complexes (128). Activation following suboptimal stimulation, such as in the absence of costimulation or with high immunosuppressive signals, results in a phenotype akin to anergy. Anergized T cells downregulate TCR and costimulatory receptors to maintain the hyporeactive state (130). Rechallenge with an

agonist after anergy induction by APL stimulation leads to an inability to proliferate but restored IL-2 production both *in vitro* and *in vivo* (124). Weak agonist TCR:pMHC interactions, such as is measured with some APLs, often result in incomplete T cell activation and induction of anergy(5, 6, 8, 110, 131-133). However these mid affinity APLs may maximize T cell function *in vivo* where a high affinity interaction can lead to an attenuated T cell response by altering intracellular signaling (134).

**Hb as a model antigen used in the presented studies**

Hemoglobin is a self-protein found intracellularly or bound to haptoglobin, not free in circulation. Hb/$E^k$ complexes have been found on all APCs, including in the thymus (135). In the mouse, the Hb protein exists in two naturally occurring allelic variants, $Hb^d$ and $Hb^s$, such that T cells developing normally in $Hb^s$ strains can be reactive to cells from $Hb^d$ mice. The Hb system is ideal for examining T cell selection and activation consequences as T cells can be exposed to Hb peptide as a foreign or endogenous antigen.

**The n3.L2 system**

A series of T cell clones and hybridomas were originally generated against the β chain of the $Hb^d$ allelic variant and restricted to H-$2^k$(135, 136) with dominant reactivity to the Hb(64-76) peptide (GKKVITAFNEGLK). One T cell clone that has been used extensively in studies of the Hb model antigen was designated as 3.L2. The 3.L2 T cell receptor is composed of rearranged Vα18 and Vβ8.3 chains. 3.L2 specifically recognizes the $Hb^d$(64-76) peptide presented on I-$E^k$ (62) and is not reactive to the $Hb^s$ variant. 3.L2

was identified as a Th1 clone and its specificity has been examined with a panel of $Hb^{d}$(64-76) altered peptide ligands.

Early studies with Hb(64-76) reactive TCRs identified key peptide amino acid residues that were TCR or MHC contact residues. The TCRs were specific for the pMHC complex as mutagenesis of the primary contact residue, N72, and secondary TCR contact residues resulted in decreased proliferation (62). Some amino acid substitutions in the peptide could maintain T cell activation, identifying a range of permissible alterations of secondary TCR contact residues (63). Therefore, while the naturally occurring TCR was specific for the Hb(64-76) peptide on I-$E^{k}$, the TCR exhibited flexibility and could productively recognize altered peptides. To test the breadth of T cell flexibility, a panel of altered peptide ligands (APLs) was synthesized where select amino acids were substituted into the P2, P3, P5 or P8 peptide positions, which contact the TCR. These APLs were used to identify the phenomenon of TCR antagonism and characterize T cell recognition of ligands of varying potency (8, 42, 65).

The cloned 3.L2 TCR was used to generate a TCR transgenic mouse (79). When the original 3.L2 TCR transgenic mouse was crossed to a $Rag1^{-/-}$ background, transgenic CD4 T cells failed to develop. It was identified that a mutation had been introduced into the transgenes and therefore the mouse was regenerated and named n3.L2. n3.L2 T cells developed in the presence of H-$2^{k}$ on a C57BL/6J $Rag1^{-/-}$ background. The presence of n3.L2 T cells was measured by a monoclonal antibody specific for the n3.L2 TCR clonotype, CAb. In the H-$2^{k/k}$ mice, approximately 6% of thymocytes were $CD4^{+}$ T cells that expressed the n3.L2 receptor, though the level of positive selection was dependent on I-$E^{k}$ expression levels, as reducing the amount of I-$E^{k}$ in the thymus reduced the number

of $CAb^+$ T cells (79). In the peripehery, the majority of $CD4^+$ T cells expressed the transgenic receptor with a second endogenous TCR. While dual TCR expression occurred on $CD4^+$ T cells, the n3.L2 transgenic TCR was the dominant TCR undergoing positive selection. Therefore, this system provides a method to examine positive and negative selection of a $CD4^+$ skewed TCR of known affinity.

The n3.L2 model antigen system has been extensively used to understand T cell biology. From the initial studies of selection, it has been used to generate and characterize a series of Hb(64-76) altered peptide ligands (APLs) (35, 42) and describe the immunological synapse (103). Transgenic mice expressing APLs attached to membrane-bound HEL were generated and crossed to the n3.L2 transgenic mouse to measure selection by APLs (78). The breadth of n3.L2 flexibility was tested in response to the panel of Hb(64-76) APLs by determining the $EC_{50}$ of an IL-2 production assay. Correlations between APL stimulatory ability (agonist, antagonist, or null) and TCR binding kinetics were determined, permitting the first association between TCR:pMHC association and selection outcome *in vivo*.

**Generation of higher affinity n3.L2 mutants**

Extending upon these studies of n3.L2, a series of n3.L2 TCR mutants was generated to create high affinity receptors specific for the Hb(64-76) peptide (137, 138). Using the n3.L2 TCR sequence, a single chain TCR construct was generated. This scTCR was expressed on a yeast display system and used as the template for directed PCR mutagenesis to generate stable TCR mutants (139). Mutants with increased stability were detected on the surface of the yeast by labeling with CAb, a clonotypic antibody specific

for the n3.L2 TCR. After the first round of mutagenesis to generate a stably expressed n3.L2 TCR, two clones were identified with mutations in the TCRα and β chains. Since these two clones had moderately increased labeling by CAb, they were used as the templates for a second round of mutagenesis followed by selection with CAb. One of these clones that had the highest labeling by CAb was named M2. M2 expressed two mutations in CDR1α in addition to the stabilization mutations from the first round of mutagenesis. M2 was used as the template for generation of a library of affinity matured n3.L2 mutants selected by binding to the Hb/I-$E^k$ Ig dimer. After multiple rounds of mutagenesis, a panel of n3.L2 mutants was generated with mutations in the CDR1α and CDR3α and β regions. M5 and M15 contain the M2 CDR1α mutations in addition to mutations in CDR3s. M4 and M14 have reverted forms of CDR1α, matching the wildtype n3.L2 TCR, but have the same CDR3 mutations as M5 and M15, respectively. This full panel permits the examination of each set of mutations separately and in combination to determine how alterations in one CDR loop affect TCR affinity and peptide specificity. Interestingly, the majority of changes in TCR reactivity and affinity that have been reported using various T cell sytems focus on differences in the CDR3 loops. The unique changes in CDR1 resulting in the M2 TCR set up a system to specifically examine changes in the TCR structure that do not specifically contact the peptide surface. Surface plasmon resonance (SPR) analysis of scTCR constructs of all the mutants revealed a range of increased affinity for binding immobilized Hb/I-$E^k$. M2 had an affinity of 4.5μM. M4 and M5 had approximately 10-fold stronger affinity (580nM and 159nM, respectively). M15 was a full 800-fold increase over the wildtype n3.L2 affinity for Hb/I-$E^k$, with a 25nM affinity.

**Conclusions from previous studies using M4 and M15 mutants**

After generation of the n3.L2 high affinity mutants, M4 and M15 TCRs were expressed in hybridomas and used to further characterize TCR peptide specificity. M4 and M15 did not have increased sensitivity to wildtype Hb(64-76) (137, 140). A full panel of Hb(64-76) APLs was then developed where each of the standard amino acids was singly substituted in to TCR contact sites, P2, P3, P5 and P8, on the Hb(64-76) peptide. n3.L2, M4, and M15 were screened against the entire Hb(64-76) APL panel to examine specificity and degeneracy of peptide recognition. n3.L2 responded to a limited pool of APLs, maintaining remarkable specificity. Because of increased affinity, M4 and M15 exhibited broader recognition of APLs, with M15 recognizing the majority of APLs at each position including weak n3.L2 ligands (138). M15, which had mutations in CDR3β that were not present for M4, reacted to many more APLs, suggesting that while specificity is maintained by TCR contact residues, alterations in the CDR3 regions can drastically change peptide specificity. Thus, increased TCR affinity for pMHC led to a broader spectrum of allowable amino acids at TCR contact residues.

While providing insight into the sensitivity of a high affinity TCR for pMHC, these studies were only conducted *in vitro* and failed to answer questions about how kinetics of TCR:pMHC regulate the response of a naturally selected T cell. Additionally, the increased affinities of M4 and M15 were due to changes in both the $k_{on}$ and $k_{off}$. Therefore, the question of $k_{on}$'s contribution in selection and activation of T cells remains.

**M2 TCR: a system to study the effect of $k_{on}$ *in vitro* and *in vivo***

The M2 TCR variant differed from the wildtype n3.L2 TCR by two amino acid changes in the CDR1α region, a lysine to glutamic acid at residue 25 and a threonine to serine mutation at residue 28. These two mutations resulted in a 3.7 fold higher affinity due specifically to a faster $k_{on}$. Therefore, M2 provides a unique system to investigate how alterations in TCR $k_{on}$ affect T cell biology. Neither the Glu25 nor Ser28 in the CDR1α loop directly contact the pMHC (based on a crystal structure of M15:Hb(64-76)/I-$E^k$ by T. Brett and D. Fremont) and therefore must be affecting the TCR affinity in another way. Glu25 is a charge reversal mutation whose side-chain is completely solvent exposed and distant from the pMHC interface. In contrast, Ser28 is buried within the Vα domain with its hydroxyl group forming a hydrogen bond to the backbone of Thr26 of the α chain. Importantly, the two CDR1α residues flanking Ser28, Try27α and Thr29α, directly contact the pMHC. Thus, while the Ser28 mutation does not directly contact I-$E^k$ or Hb, it nonethless could enhance binding by providing an advantageous conformation that would rapidly associate with the pMHC.

Like changes in $k_{off}$, $k_{on}$ could regulate activation and selection of T cells potentially by altering the overall dwell time of the TCR with endogenous and foreign pMHC. As the affect of $k_{on}$ has not previously been isolated, comparison of n3.L2 and M2 is a novel system to examine how the $k_{on}$ of the TCR binding pMHC regulates T cell selection and activation. Since the measured affinity of M2 for Hb(64-76)/I-$E^k$ was within the range of naturally occurring T cells (1-50μM), we predicted that M2 specific T cells would develop in a B6.K mouse, in contrast to the highest affinity M15 TCR which would be negatively selected. Generation of the M2 TCR transgenic mouse allows

studies of specificity to be extended to a naturally developed T cell. The mouse also provides a way to study the selection of CD4 T cells expressing the M2 TCR. By comparing n3.L2 and M2 T cells, we can now determine how $k_{on}$ alters development and activation of T cells *in vitro* and *in vivo*.

# CHAPTER 2

## CD4 T cell response to altered peptide ligand recognition correlates with kinetics of TCR:pMHC association

## Introduction

T cells are the main effectors of the adaptive immune system. Through recombination of V-(D)-J segments up to $10^9$ T cells with different specificities can be produced in the thymus. The repertoire of T cells recognizes a wide variety of foreign peptides, though all T cells retain recognition of MHC (141, 142). Upon binding a cognate pMHC complex, a T cell will undergo a process of activation, starting with phosphorylation of molecules associated with the TCR and resulting in cytokine production, proliferation, and initiation of T cell help to other cells or cytolysis of infected target cells. TCR recognition of pMHC presented on APCs is a complex process, involving conformational changes to ensure optimal contact between the TCR and pMHC (14-17) and recruitment of costimulatory molecules to ensure full T cell activation (105-107, 143). There is a high degree of specificity and sensitivity for TCR binding pMHC, even with micromolar affinity. The TCR has inherent specificity for an agonist peptide but retains flexibility allowing sufficient interaction with slight variants of the agonist (20). This flexibility is critical during T cell development in the thymus and ensures recognition of mutated foreign antigens present during an infection. While flexible recognition of pMHC is an advantage in mounting an immune response against infection or tumor escape variants, highly promiscuous T cells can inappropriately recognize self-peptides and cause autoimmune disease (10, 21). Therefore, it remains important to understand the process by which a T cell discriminates between peptides to generate a productive, and appropriate, immune response.

TCR specificity for pMHC is encoded in the set of 6 complement determining regions. These CDR loops contact the pMHC interface generating the direct interactions between residues on the TCR and peptide side chains and residues on the MHC helices (144). It was discovered that subtle changes in the peptide do not abolish T cell activation (62). Instead the TCR is flexible enough to recognize these altered peptide ligands (APLs), though the strength of APL recognition regulates the level of T cell response. The energetics of bonds between the pMHC and the TCR CDR loops set a threshold for T cell activation (19). Therefore, APLs that still make sufficient contact with the TCR can overcome the activation barrier generating varying levels of T cell activation. It should be noted that not all amino acid changes result in APLs that are able to activate a T cell as some APLs, named null peptides, do not elicit a T cell response.

APLs function in a distinct manner from wildtype ligands and have been shown to produce a variety of T cell activation phenotypes. APLs have induced IL-4 production without proliferation, altered the cytokine profile of T cells, functioned as antagonists to agonist activation, and induced anergy. APLs have been shown to induce a different pattern of signals downstream of the TCR as a consequence of partial T cell activation (42, 145). This state of partial activation may not be merely a reduced level of signaling or lack of costimulation but an entirely different activation state. As a consequence of partial activation, T cells stimulated by an APL can undergo anergy, a state of reduced or no proliferation and cytokine production (8, 65). Unlike anergy induction upon exposure to agonists, such as in a chronic infection, anergy from exposure to APLs cannot be overcome by costimulatory signals, further proof of a different rather than reduced signaling profile.

During thymic selection, T cells encounter a large number of peptide ligands that may be structurally different from specific antigens encountered in the periphery. To undergo full development, the T cell must recognize suboptimal ligands whereas stronger signals result in death by negative selection (9, 68, 69). By retaining TCR flexibility, a few peptides in the thymus can generate the diverse repertoire of T cells required to recognize a vast array of foreign antigens (71). APLs have been used to induce positive selection of transgenic T cells *in vitro* and *in vivo* (68, 73, 77, 78). The weakly stimulatory peptides used suggest APLs that can select peptides are of extremely low affinity. T cells selected in this method are still able to respond to agonists in the periphery. APLs have therefore been used as a method of "vaccination" against viruses, tumors, and autoimmunity by fine-tuning the specificity and affinity of T cells that develop (146-148).

Attempts have been made to understand the structural regulation of activation by APLs. It is now accepted that the state of T cell activation by an APL depends to some degree on the affinity of the TCR for the APL/MHC complex (1-4). Full activation of a T cell requires sufficient contact time between the TCR and pMHC (47, 48). Partial activation of T cells by APLs can be the result of fast dissociation rates or insufficient dwell time, which includes rebinding events, for productive signaling through the TCR (42). APLs that induce positive selection are of very weak affinity as they are unable to induce IL-2 production or proliferation in peripheral T cells (9, 78). Therefore, the spectrum of APL functions is due to the affinity of the TCR for the APL/MHC.

High affinity TCRs may have increased flexibility in recognizing peptides. Previous studies using a TCR mutant of the n3.L2 receptor showed that a high affinity

TCR is able to respond to a large number of APLs but retains specificity for cognate antigen (137). This dichotomy suggests further regulation of activation rather than just overall affinity of the complex. To measure how subtle changes in the TCR can alter recognition of APLs, we used n3.L2 and a mutant variant, M2, to examine the kinetic differences leading to T cell activation. Hybridomas expressing the M2 TCR responded to a larger number of Hb(64-76) APLs and produced more IL-2 upon stimulation by agonists than n3.L2 hybridomas. The M2 response was not due to increased affinity for all APLs. Instead, peptide specificity was maintained. For instance, G69 was a stronger agonist for n3.L2. A69 was able to stimulate more CD69 upregulation on n3.L2 thymocytes than M2 thymocytes. The structural differences between n3.L2 and M2 alter the generation of favorable bonds with the peptide, confirming specificity in recognition of APLs. While higher affinity TCR:APL/MHC complexes led to increased IL-2 production, the $K_D$ did not accurately predict the level of activation. Instead, maximal IL-2 strongly correlated with $k_{off}$, similar to what has previously been reported (43, 48).

## Materials and Methods

*Generation of n3.L2 and M2 hybridomas*

n3.L2 and M2 TCRα and β chains were cloned into a p2A retroviral vector with an IRES-GFP tag (pMIIG) developed by the Vignali lab (149), which places the α and β chains as a single polypeptide linked by the p2A peptide. No stability mutations used in the yeast display were added into the sequence. The p2A peptide is cleaved posttranslationally, ensuring equal expression of the α and β chains and resulting in

efficient expression of transduced αβ TCRs. Viral particles were packaged in the PlatE cell line spinfected with 30μg retrovirus. Purified retrovirus containing supernatants from PlatE cells were used to infect the 58 $\alpha^-\beta^-$ $CD4^+$ hybridoma cell line. M2 and n3.L2 expressing hybridomas were generated simultaneously, sorted for comparable high GFP expression and equal expression of the n3.L2 and M2 TCRs. Cells were sorted a second time to generate a population with stable TCR expression. Equivalent expression levels of CD3, CD4, and TCR between n3.L2 and M2 were confirmed by flow cytometry. Surface TCR levels were assessed with CAb, Vβ8.3, and H57. Hybridomas were cultured in RPMI + 10% FCS + 1% β-2-mercaptoethanol + 1% Glutamax + 0.5% gentamycin.

*T cell hybridoma IL-2 production assay*

To assess T cell hybridoma responses, $5x10^5$ hybridomas were cultured overnight at 37°C 5% $CO_2$ in wells of a 96-well plate with $2x10^4$ CH27 B cell APCs and varying concentrations of the Hb(64-76) peptide from 0.0001-100μM. Peptides were synthesized in our laboratory and purified by HPLC prior to use. 18-20 hours after culture, supernatants were assayed using an IL-2 ELISA. Briefly, IL-2 was captured using an anti-IL-2 antibody (BioXCell) and detected with a second, biotinylated anti-IL-2 antibody (BioLegend). Biotin-labeled IL-2 was detected by a streptavidin conjugated horseradish peroxidase antibody (Southern Biotech) followed by TMB substrate for accurate detection of 5-500 pg/mL of IL-2 (1-step Ultra TMB ELISA, Thermo Scientific). After stopping the reaction with 2M sulfuric acid, absorbance was read at 450nm. Absorbance levels were converted into amount of IL-2 based on a regression analysis of IL-2 standards using GraphPad Prism (GraphPad Software). For the APL

studies, the amount of peptide required for 50% maximal IL-2 production ($EC_{50}$) was calculated to determine relative levels of activation. For other experiments, the maximal IL-2 production and minimum stimulatory dose were compared.

*Surface Plasmon Resonance*

We used established lab protocols to measure binding affinities for n3.L2 and M2 single chain TCR (scTCR) to Hb(64-76)/I-$E^k$ (137). Hb(64-76)-loaded I-$E^k$ Ig dimers were directly coupled to a CM5 sensor chip by amine coupling. I-$E^k$ dimers were produced in Drosophila S2 cells, as previously described (74, 150). Previously, refolded Hb(64-76)/I-$E^k$ was generated from *E. coli* inclusion bodies for use in SPR studies. Both ligands were tested in this system and the affinity measurements were the same using either the refolded monomer or Ig dimer and maintained a 1:1 TCR:MHC binding ratio ((140), data not shown). Data presented are based on measurements obtained using only peptide loaded I-$E^k$ dimers. Refolded, soluble single chain n3.L2 or M2 TCR (Vα-linker-Vβ) (149) was purified by FPLC, concentrated in PBS, and injected over the bound I-$E^k$ at a rate of 30μL/min. scTCR was injected in duplicate at increasing concentrations from 0-100μM at 25°C. MCC loaded I-$E^k$ was used as a negative control for binding. MCC sensograms were subtracted from experimental sensograms to eliminate nonspecific binding artifacts. Measurements were performed using a Biacore 2000. BiaEval version 4.1 software (Biacore AB) was used to generate 1:1 Langmuir best fit approximation of sensograms to determine $K_D$, $k_{off}$ and $k_{on}$. The Langmuir model was adjusted until a $Chi^2$ value below 50 was obtained, indicating the best approximation of data. Kinetic measurements are compiled from 5 independent experiments using separate CM5 chips.

$K_D$ and $k_{off}$ values were confirmed by Scatchard analysis using GraphPad Prism (GraphPad Software). Statistical significance was measured by Student's t test for differences between n3.L2 and M2 parameters.

*CD69 upregulation*

Pre-selection double positive (DP) thymocytes were isolated from thymi of TCR transgenic mice aged 4-6 weeks by depletion of DN and already selected cells with anti-CD25-biotin (Biolegend, clone PC61), anti-CD44-biotin (Biolegend, clone IM7) and anti-CD53 (Biolegend, clone OX-79) antibodies. For anti-CD53, primary antibody labeling with unlabeled anti-CD53 was followed by addition of goat anti-rat IgM-biotin (Jackson Immuno Research) antibody. After incubation with the biotinylated antibody cocktail, Miltenyi anti-biotin microbeads were added and DP cells were isolated by negative selection on a Miltenyi AutoMACS. $1x10^5$ isolated cells were cultured with either $5x10^5$ Hb(64-76)-pulsed irradiated B6.K splenocytes or wells precoated for 2 days with 5μg/mL anti-CD28 (Biolegend, LEAF purified, clone 37.51) and increasing amounts of anti-CD3 (Biolegend, LEAF purified, clone 2C11) antibodies. After 18 hours of incubation at 37°C 5% $CO_2$, cultures were measured for CD69 upregulation by flow cytometry. Cultures were gated on live lymphocytes, followed by gating on $CD4^+$ $CD8^+$ DP thymocytes, and assessed for percent $CD69^+$.

## Results

*Generation of an n3.L2 mutant with only an increased $k_{on}$*

The n3.L2 TCR is specific for the $Hb^d$(64-76) peptide presented on the I-$E^k$ MHC class II molecule (62). Previously, the n3.L2 receptor was mutagenized using a yeast display system (139). Mutants were isolated by increased surface levels on yeast, indicating enhanced TCR stability. One mutant, M2, contained two point mutations in the CDR1α chain (K25E and T28S) in addition to mutations leading to stable expression of the TCR. Although it had not been selected for higher affinity binding to Hb(64-76)/I-$E^k$, M2 was shown to have several fold improved affinity over the n3.L2 TCR (137). Soluble single chain TCR molecules (Vα-linker-Vβ; scTCR) were generated for the n3.L2 and M2 T cell receptors (149), containing several additional stabilizing mutations in framework regions (151). These scTCR stabilizing mutations were needed to produce the soluble scTCR, but not for expression of the mutants in T cell (140). The scTCRs were used previously to measure binding affinity of the series of mutants to Hb(64-76)/I-$E^k$ by surface plasmon resonance. To confirm and extend these studies, we performed similar surface plasmon resonance studies. n3.L2 had an affinity of 16.6μM for Hb(64-76)/I-$E^k$ (Table 2.1). M2 had a 3.7 fold higher affinity for Hb(64-76)/I-$E^k$ (4.3μM) due to an equivalent change in $k_{on}$, without a significant change in $k_{off}$ (Figure 2.1A, Table 2.1). Sensograms of increasing concentrations of scTCR up to 100μM were modeled for a 1:1 binding ratio to determine kinetic measurements of n3.L2 and M2 scTCR binding to Hb(64-76)/I-$E^k$ dimers (Figure 2.1B). The $K_D$ values were confirmed by Scatchard analysis (Figure 2.1C). These kinetic values were consistent with what was originally

reported for n3.L2 and M2 (137). Therefore, the M2 TCR has an increased affinity for Hb(64-76)/I-$E^k$ due solely to a faster $k_{on}$.

*n3.L2 and M2 hybridomas had the same sensitivity and maximal IL-2 production in response to Hb(64-76)/I-$E^k$*

The M2 TCR had not been previously tested functionally. Because the M2 mutations altered the affinity of the TCR for pMHC, we predicted M2 T cells would differ in their response (sensitivity or specificity) to the Hb(64-76) peptide in comparison with n3.L2 T cells. To measure the sensitivity of n3.L2 and M2 TCRs to Hb(64-76)/I-$E^k$, we generated a set of T cell hybridomas using a retroviral system designed by the Vignalli lab (149). Sorted n3.L2 and M2 hybridomas expressed equivalent levels of the n3.L2 or M2 TCR and CD4 (Figure 2.2). Hybridomas were stimulated by CH27 cells pulsed with varying doses of purified Hb(64-76) peptide. n3.L2 and M2 response to agonist stimulation was measured by IL-2 production. The response curves for the n3.L2 and M2 hybridomas were the same, with the same maximal response and sensitivity to the Hb(64-76) peptide (Figure 2.3). A similar result was obtained for a related, higher affinity TCR, M15 (137). Therefore, the M2 TCR is fully functional and equivalent to the n3.L2 TCR in its ability to recognize and be stimulated by Hb(64-76)/I-$E^k$ independent of effects from development.

*n3.L2 and M2 T cells differ in response to Hb(64-76) APLs*

Since the affinity difference did not alter recognition of the Hb(64-76) peptide, we examined TCR specificity for peptide by testing the ability of Hb APLs to stimulate the

n3.L2 and M2 hybridomas. A panel of 76 peptides was generated by singly substituting each amino acid at the 4 TCR contact residues and tested for the ability to stimulate IL-2 production. This panel was previously used to characterize the reactivity of the M4 and M15 mutants of the n3.L2 TCR. However, both of those mutants contained CDR3 mutations, which most likely contribute to the broad reactivity measured (137). APLs were ranked for their ability to stimulate IL-2 production relative to the WT Hb(64-76) peptide according to $EC_{50}$ values. A 4-log range of APL reactivity was measured, from null peptides to weak and strong agonists. Of the 76 APLs, 13 APLs stimulated IL-2 production by the n3.L2 hybridomas (Figure 2.4), whereas, 25 of the 76 peptides were agonists for M2 hybridomas. M2 recognized changes at each of the 4 TCR contact residues. M2's broader response to APLs suggests the structural changes that led to the faster $k_{on}$ and increased affinity of M2 for wildtype Hb(64-76) peptide also raised the affinity of a number of APLs over the threshold for agonist stimulation. Thus, the increase in $k_{on}$ of the M2 T cells has a functional affect in that it broadens the number of APLs which are stimulatory.

Additionally, M2 hybridomas were more sensitive to some APLs that were agonistic for n3.L2 and M2 hybridomas, with a lower $EC_{50}$ value for IL-2 production (Figure 2.5). For example, the M69 APL stimulated both n3.L2 and M2 hybridomas (Figure 2.5A). The $EC_{50}$ for M2 was 5μM with a maximal IL-2 production at 350 pg/mL. M69 was able to stimulate n3.L2 hybridomas at concentrations as low as 3.1μM but did not produce maximal IL-2 at 100μM, the highest concentration testable. A similar difference was seen with the D70 APL. M2 hybridomas produced more IL-2 in response to D70 but the sensitivity of the two hybridomas was similar (Figure 2.5B). T72 (Figure

2.5C) and V75 (Figure 2.5D) were null peptides for the n3.L2 hybridomas. Interestingly, both stimulated IL-2 production by M2 hybridomas. T72 went from a null peptide for n3.L2 to a strong agonist for M2, only 10-fold less stimulatory than wildtype Hb(64-76), while V75 was only a weak agonist. While M2 was a stronger responder in most cases, no pattern emerged in terms of structure to predict which APLs would be activating. It seemed likely that changes in the affinity were regulating the APL response.

*$k_{off}$ of TCR:APL/I-$E^k$ interaction correlates with maximal IL-2 production*

Since IL-2 production, including maximal IL-2 production, is dependent upon the kinetics of TCR contacting the specific pMHC complex, we used surface plasmon resonance to measure the binding affinity of n3.L2 and M2 scTCRs to I-$E^k$ dimers loaded with specific APLs. Purified single chain n3.L2 and M2 TCRs were injected over flow cells with amine coupled APL/I-$E^k$ Ig dimers. As predicted, the higher the affinity, the stronger the IL-2 production. However, the overall affinity of TCR:pMHC did not completely reflect the level of IL-2 production by the n3.L2 and M2 hybridomas. N3.L2 had an affinity of 16μM for wildtype Hb(64-76)/I-$E^k$ and M2 had an affinity of 4.4μM though IL-2 production was nearly identical.

The lowest affinity measured was for n3.L2 interacting with H70/I-$E^k$ (Figure 2.6, Figure 2.7, Table 2.2). H70 failed to induce IL-2 production by the n3.L2 hybridomas. Accordingly, n3.L2 bound H70/I-$E^k$ with an affinity of 158μM. M2 hybridomas produced IL-2 at an $EC_{50}$ lower than for wildtype Hb(64-76) the result of a 37μM affinity. Interestingly, the difference in affinity and activity was the result of changes in $k_{on}$ and, more dramatically, in $k_{off}$. M2 had a faster $k_{on}$ in binding H70, which could

account for the increased sensitivity, overcoming a fast $k_{off}$, as has been reported for other systems(47, 48).

V69 was an agonist for both n3.L2 and M2 hybridomas (Figure 2.4). Agonistic activity was the same as wildtype Hb(64-76) for M2 but was 10-fold weaker for stimulating n3.L2. Correspondingly, M2 bound V69 with an affinity of 17μM similar to that measured for the wildtype peptide and stronger than the 54μM for n3.L2:V69/I-$E^k$ (Figure 2.6, Table 2.2). The affinity change in this case was driven by changes solely in the $k_{off}$. The affinity measured for n3.L2:V69/I-$E^k$ is weaker than expected given the IL-2 response.

The affinity of n3.L2 and M2 for E70 did not correlate with affinity (Figure 2.6, Figure 2.8, Table 2.2). E70 stimulated weak IL-2 production from n3.L2 hybridomas, requiring 100-fold more peptide than wildtype Hb(64-76). M2 hybridomas were 10-fold more sensitive to E70 than n3.L2 hybridomas. However, the affinity of M2 for E70/I-$E^k$ was 2 times weaker than n3.L2 binding E70. Interestingly, M2 had a slower $k_{off}$ and significantly higher $E_{max}$ for IL-2 production. E70 may lend credence to the dependence of $E_{max}$ on $k_{off}$ (43). Additionally, a correlation was only measured between the $E_{max}$ and $k_{off}$ using our combined kinetic and APL response data, confirming the relationship.

Interestingly, the G69 APL was a stronger agonist for n3.L2 than for M2. M2 had an $EC_{50}$ value 10-fold lower than n3.L2 for IL-2 production in response to G69. N3.L2 had a stronger affinity than M2 for G69 (Figure 2.6, Figure 2.9, Table 2.2). The affinity difference was driven by $k_{on}$, since the $k_{off}$ remained the same for the n3.L2 and M2 complexes with G69/I-$E^k$. By having a slower $k_{on}$ for TCR:pMHC, the M2 hybridomas produced significantly less IL-2 than the n3.L2 hybridomas, even with 100μM peptide.

This result suggests that in addition to $k_{off}$, $k_{on}$ may regulate $E_{max}$ for IL-2 production. Overall, the APL studies highlight the importance of kinetics in determining the activation outcome of TCR:pMHC. As has been seen with other systems, the Hb APLs are able to induce IL-2 production to varying levels given a TCR affinity above the threshold for recognizing presented APLs. Fine tuning by both $k_{on}$ and $k_{off}$ of complex formation set the sensitivity of TCRs to stimulation and maximal IL-2 production levels.

*A larger percentage of M2 DP thymocytes upregulate CD69 in response to wildtype Hb(64-76) and APLs that failed to stimulate IL-2 production by peripheral T cells*

A majority (51/76) of the APLs were null peptides for both n3.L2 and M2 hybridomas. However, the peptides involved in positive selection of thymocytes are of low enough affinity that they cannot stimulate IL-2 production by peripheral T cells (9, 78). As thymocytes are more sensitive to stimulatory signals, we tested the ability of APLs to induce CD69 upregulation on DP thymocytes. CD69 is upregulated on DP thymocytes that have received a positive selection signal, though this is quickly downregulated in the thymus (152). Isolated DP thymocytes from n3.L2 and M2 TCR transgenic mice were cultured with irradiated B6.K splenocytes pulsed with wildtype Hb(64-76) or APLs. (The M2 TCR transgenic mouse is described in detail in Chapter 3. This was not included here to maintain the flow of each storyline.) After 18 hours, cultures were analyzed by flow cytometry for CD69 upregulation. n3.L2 and M2 DP thymocytes had the same ability to upregulate CD69 in response to anti-CD3 + anti-CD28 stimulation, indicating no inherent cellular difference in signaling downstream of the TCR (Figure 2.10A).

We next tested antigen specific CD69 upregulation, which reflects recognition of endogenous pMHC during selection. A greater proportion of M2 DP thymocytes were CD69 positive 18 hours after stimulation with Hb(64-76) peptide in comparison to n3.L2 DP thymocytes (Figure 2.10B). Therefore the increased sensitivity of thymocytes uncovered a difference in sensitivity to the Hb(64-76) peptide that may be detuned as a consequence of the decreased sensitivity of peripheral thymocytes. These results suggest the increased affinity of the M2 TCR for Hb(64-76)-I-$E^k$ resulted in stronger signaling through the TCR.

A larger percentage of M2 DP thymocytes upregulated CD69 in comparison to n3.L2 DP thymocytes in response to the majority of the APLs tested (Figure 2.11), including those deemed null peptides from peripheral T cell stimulation (Figure 2.4). Therefore the affinity of M2 for APLs that failed to stimulate peripheral cells may be stronger than n3.L2 in the thymus, potentially as a result of increased affinity for MHCII. Like in the periphery, the M2 mutations set the binding energetics close to the threshold for selection permitting recognition of a broader range of APLs. Interestingly, the A69 APL induced greater CD69 upregulation on the n3.L2 thymocytes. Like G69 in the periphery, the n3.L2 CDR1$\alpha$ residues must permit favorable interactions with the A69 residue which are altered with the M2 CDR1$\alpha$. The permissible amino acid changes are dictated by the structure of the TCR, maintaining TCR specificity even with enhanced affinity.

## Discussion

The M2 TCR has a stronger affinity for Hb(64-76)/IE$^k$ than the wildtype n3.L2. The same changes in the CDR1α loop that lead to an increased $k_{on}$ for the TCR:pMHC interaction set the binding energetics of M2 with peptide loaded I-E$^k$ near the threshold for T cell activation. As such, M2 expressing hybridomas are more sensitive to and produce higher levels of IL-2 in response to Hb(64-76) APLs. A larger number of the APLs were able to activate M2 hybridomas than n3.L2 hybridomas. Interestingly, while the overall sensitivity did not correlate with affinity or kinetics, the maximal IL-2 level ($E_{max}$) correlated with the $k_{off}$ of the TCR:APL/I-E$^k$ complex. This confirms results previously published by Dushek et al. (43). Thymocytes isolated from M2 and n3.L2 TCR transgenic mice were more sensitive to APLs, upregulating CD69 in response to APLs that were null for stimulating hybridomas. Again, M2 DP thymocytes responded to a larger number of APLs, suggesting the same principles at work for peripheral T cells also regulate thymocyte responses. Interestingly, in both the hybridoma and DP thymocyte responses, APLs were identified that better stimulated cells expressing the n3.L2 receptor. This suggests that while the M2 TCR may have a stronger affinity for pMHC complexes in general, the orientation of residues in the CDR1α loop restricts productive association with the P2 site of the peptide. Therefore, the M2 TCR still retains specificity instead of responding more strongly to all peptide mimics.

While the overall affinity and $k_{on}$ did not seem to correlate with the presented kinetic and activation measurements, the system studied here may be too simplified. In addition to TCR affinity, the CD4 coreceptor and costimulatory receptors on the T cell

surface may fine-tune T cell activation (105-107). We did not include these molecules in our analysis of activation or kinetics. By including CD4 in kinetic measurements a stronger correlation with $K_D$ may be observed, though some high affinity TCRs are CD4 independent (81). The values presented in this analysis are significantly weaker than previously published data sets (12, 47, 48). Confinement time is not predicted to be a restriction due to the small magnitude of kinetic values for our system, though it may exacerbate the difference between M2 and n3.L2 interactions with Hb(64-76)/I-$E^k$ (personal communication with C. Govern). This factor was found to reliably correlate to 1G4 binding with pMHC mutants by Aleksic et al. (48). They hypothesized that while some interactions are dominated by $k_{off}$, as previously reported, changes in $k_{off}$ can mask the contribution of $k_{on}$. Instead, TCR and pMHC complexes with increased $k_{on}$ can be retained in proximity far longer than predicted by diffusion and $k_{off}$. Complete T cell activation can then occur by multiple rebinding events with a pMHC molecule. To completely examine the role of $k_{on}$ in regulating TCR response, data sets need to be expanded. In our examination of the kinetics of our two TCRs binding APLs only one additional interaction was influenced by changes in $k_{on}$ rather than $k_{off}$. Interestingly, this interaction seemed to depend more on the structure of the TCR, as G69 seems to more productively associate with n3.L2 rather than M2. Therefore, $k_{on}$ may indicate conformational shifts are required for full T cell activation, as suggested by the induced-fit hypothesis (1, 60).

The kinetic measurements discussed in our system were performed using 3D binding on restricted ligand surfaces. Huang et al. (153) recently suggested that 2D kinetics more accurately predict *in vivo* affinity than 3D, such as SPR values. The 2D $k_{on}$

and $k_{off}$ values are drastically different than 3D and also are more sensitive to kinetic differences for peptides. 2D may more accurately predict the stimulatory ability of peptides (25). The 2D system takes into account adhesion to multiple ligands clustered in a cell membrane. Using adhesion and thermal fluctuation assays, Huang et al. suggest that CD8 T cells rapidly contact multiple pMHCs, the rate of which is mainly driven by $k_{on}$ compensating for a fast $k_{off}$. This study suggests that the differences observed in our system might be magnified *in vivo* and potentially gives us another way to model our kinetic interactions. In another system, it was identified that $k_{on}$ variation is increased *in vivo* (41), lending further credit to the potential role of $k_{on}$.

The response of a T cell to APLs mimics the ability to recognize variations in endogenous peptides during thymic selection. M2 thymocytes were more sensitive to APLs, upregulating CD69 on a larger percentage of cells, even APLs that were unable to induce IL-2 production by hybridomas. The increased recognition of APLs may reflect an ability to recognize a larger pool of self-peptides in the thymus, suggesting increased levels of selection of M2 thymocytes. However, positive selection requires low affinity interactions (9, 68, 73, 75-77). By increasing the affinity of the M2 TCR for I-$E^k$, peptides that select the n3.L2 TCR may bind M2 with too high affinity leading to negative selection. When the n3.L2 mouse was crossed to express the A72 APL endogenously, a small population of n3.L2 T cells were deleted by negative selection (154). APLs of the A10 T cell depleted DP thymocytes at doses that were antagonistic to peripheral T cells (155). These studies suggest that a TCR with slightly higher affinity for APLs may in fact develop as a hyporesponsive T cell, unable to mount an effective immune response.

Selection in the thymus then sets the responsiveness of T cells in the periphery by promoting the development of mid affinity TCRs. Signaling downstream of the TCR depends on the strength of the interaction with antigen in the periphery. A longer half-life and dwell time for a TCR:pMHC complex enhances phosphorylation of CD3ζ and Zap-70 (42), increases $Ca^{2+}$ influx, and supports T cell proliferation. The affinity of TCR:pMHC association may regulate the timing of downstream signaling cascades by altering strength of TCR proximal signaling (51). However, a stronger affinity does not always correlate with better effector function. Many efforts have attempted to use APLs to boost an immune response to clear chronic viral infections or tumors (147). Exposure of a T cell to a high potency agonist *in vivo* results in an attenuated response, presumably as the result of some negative feedback though not necessarily through CTLA-4 (134). This hyporesponsive state may be due to changes in the TCR binding presented antagonist peptides (8, 35). A T cell may need to retain antigen specificity to effectively enhance an immune response or target cells for lysis (156). Detuning or increasing the affinity by use of the TCR coreceptor may be an effective way to maintain T cell specificity and reactivity. In two separate systems, mid/low-affinity CD8 T cells lysed tumor cells, potentially with enhancement by the CD8 coreceptor, whereas high-avidity CD8 T cells failed to clear tumors and did not respond to agonist *ex vivo* (156, 157).

T cell affinity must be regulated, to be not too strong and not too weak, to effectively activate upon recognition of specific antigens and mount an immune response. Evidence has determined that the 3D affinity of a TCR for pMHC does not entirely predict its response. While $k_{off}$ may reflect the maximal response, other parameters moderate T cell activation *in vivo*. Perhaps future studies utilizing systems like M2 versus

n3.L2 *in vivo* will provide more concrete ways to predict the potency of antigen in stimulating a T cell and if that is due to a TCR:pMHC interaction that is just right.

**Figure 2.1 Kinetics of n3.L2 and M2 scTCRs binding Hb(64-76)/I-$E^k$ Ig dimers**

**A.** Kinetics of n3.L2 and M2 were measured by surface plasmon resonance using scTCRs binding to Hb(64-76)/I-$E^k$ dimers. Values in arrows indicate fold change above n3.L2 for $k_{on}$ measurements. Measurements are averages of 5 independent experiments on separate CM5 chips. Statistical differences were determined using Student's t test. **B.** scTCR was injected over flow cells coupled with Hb(64-76)/I-$E^k$ dimer. Representative sensograms are shown for scTCR injections at the indicated concentrations. Kinetic constants were calculated by fitting sensograms to a 1:1 Langmuir binding model. **C.** Equilibrium responses at each scTCR concentration were used to generate Scatchard plots of n3.L2 and M2 to confirm values predicted from 1:1 modeling. The response was highly linear, with $r^2$ values of 0.8, indicating a 1:1 binding ratio between the TCR and each arm of the I-$E^k$ Ig dimer.

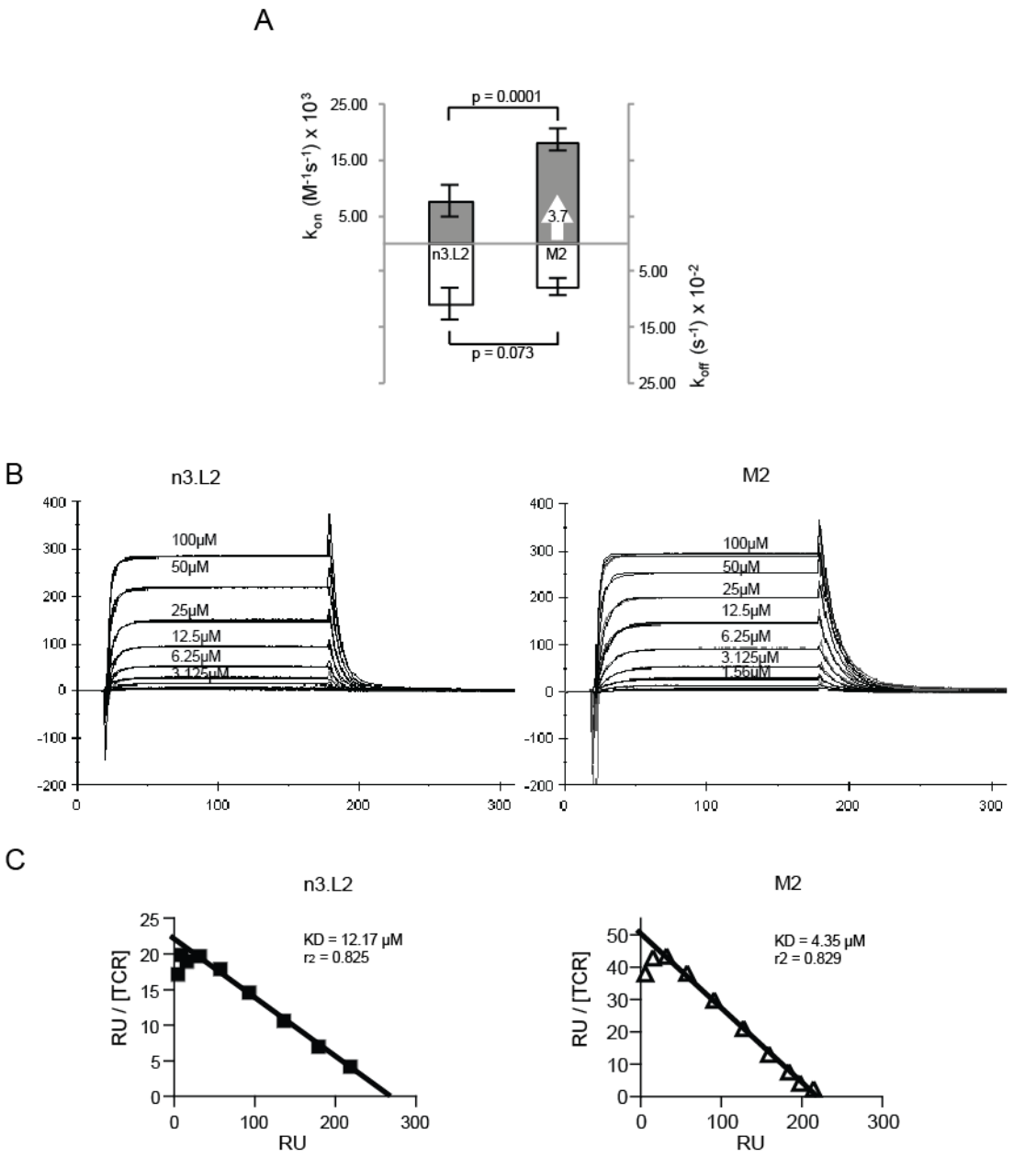


Figure 2.1. Kinetics of n3.L2 and M2 scTCRs binding Hb(64-76)/I-Ek Ig dimers

**Figure 2.2 Characterization of n3.L2 and M2 hybridomas**

Hybridomas were sorted for the top 10% $GFP^+$ to generate a population of retrovirally infected $58\alpha^-\beta^-$ cells expressing either the n3.L2 or M2 TCR. Surface levels of CD4 and TCR were measured by flow cytometry. n3.L2 (black) and M2 (filled) histogram overlays for CD4, Vβ8.3, and the TCR clonotypic antibody, CAb.

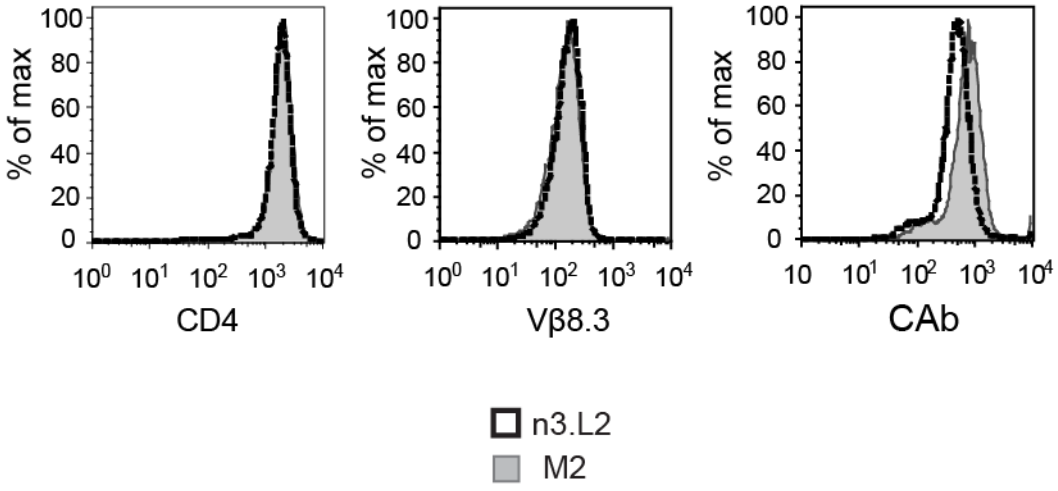


Figure 2.2. Characterization of n3.L2 and M2 hybridomas

**Figure 2.3 Response of n3.L2 and M2 hybridomas to WT Hb(64-76)**

IL-2 production by n3.L2 (blue square) and M2 (green triangle) hybridomas in response to wild-type Hb(64-76). Hybridomas were cultured in triplicate for 18-20 hours with peptide loaded CH27 APCs. Mean + SEM is presented for triplicates at each concentration in the dose curve, which is representative of 6 independent experiments.

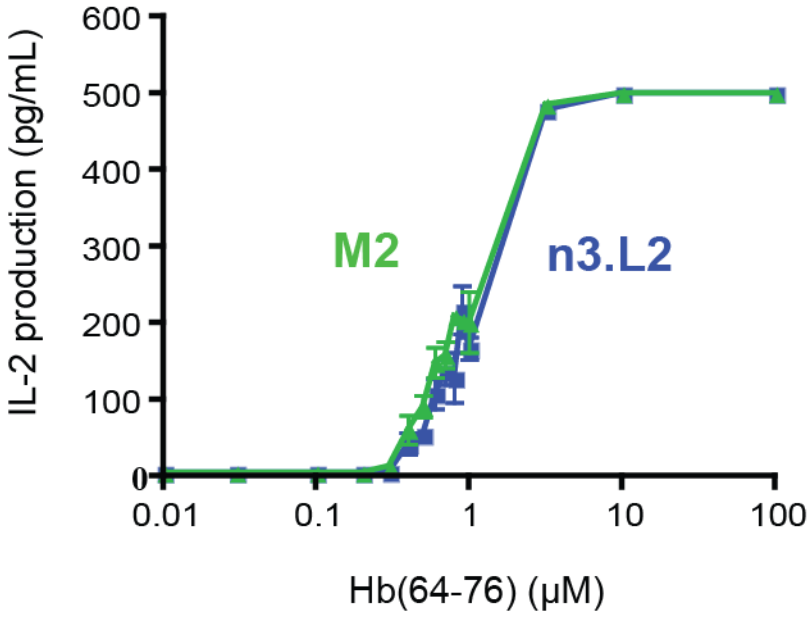


Figure 2.3. Response of n3.L2 and M2 hybridomas to WT Hb(64-76)

**Figure 2.4 Response of M2 and n3.L2 hybridomas to Hb(64-76) APLs**

Response of n3.L2 and M2 hybridomas to Hb(64-76) APLs. All 20 amino acids were substituted individually into each of the 4 TCR contact positions in the Hb(64-76) peptide (P2, P3, P5 and P8). Wildtype Hb(64-76) residues are noted under the label for each position. APLs that induced IL-2 production are shaded according to their stimulatory ability relative to the wildtype Hb(64-76) peptide. 13/76 APLs were agonists for n.3L2. 25/76 APLs were agonists for M2 hybridomas. Each APL was tested in triplicate up to 100μM in at least 3 independent experiments.

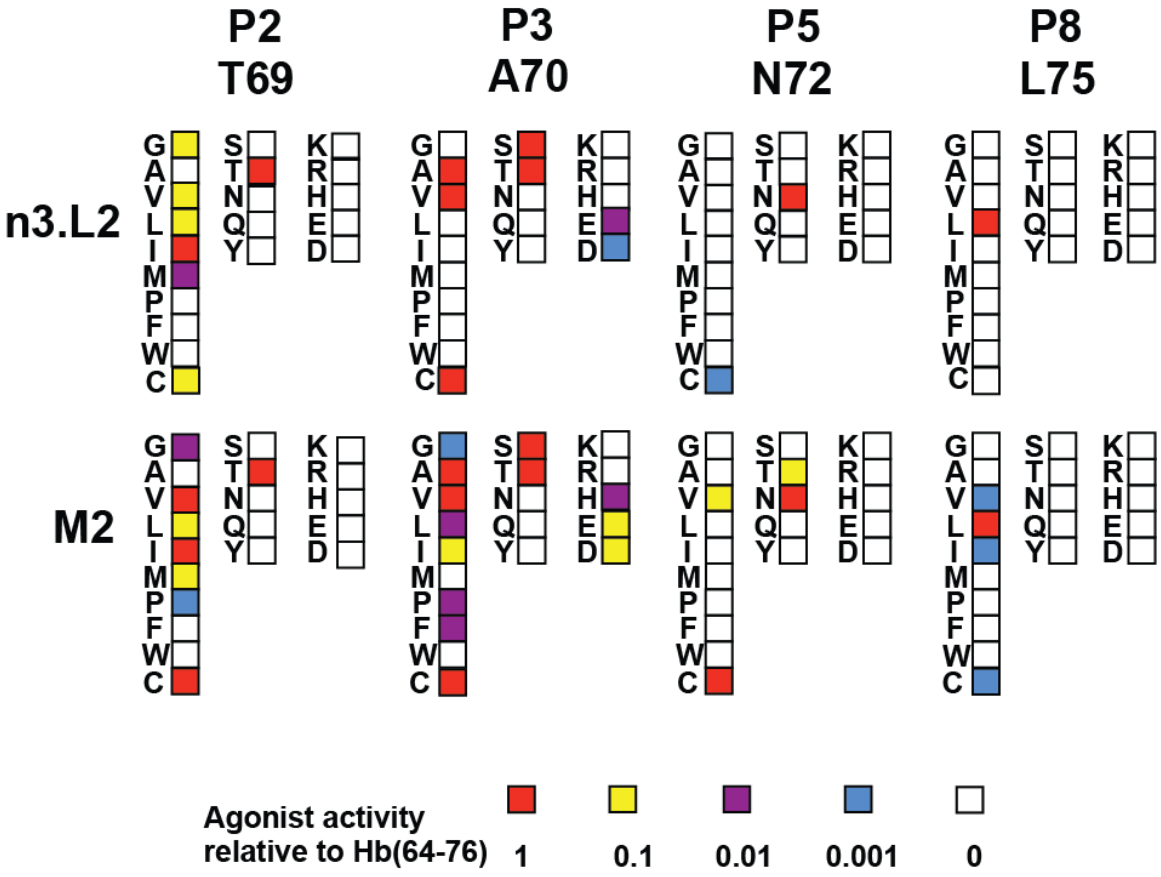


Figure 2.4. Response of M2 and n3.L2 hybridomas to Hb(64-76) APLs

**Figure 2.5 IL-2 response by n3.L2 and M2 hybridomas to APLs**

**A-D.** Stimulation of IL-2 production by n3.L2 (blue square) and M2 (green triangle) hybridomas with example APLs from each TCR binding position. Mean + SEM is presented for the full dose curve which is representative of 4 independent experiments. **A.** Stimulation with M69. **B.** Stimulation with D70. **C.** Stimulation with T72. **D.** Stimulation with V75 and wildtype Hb(64-76) for comparison.

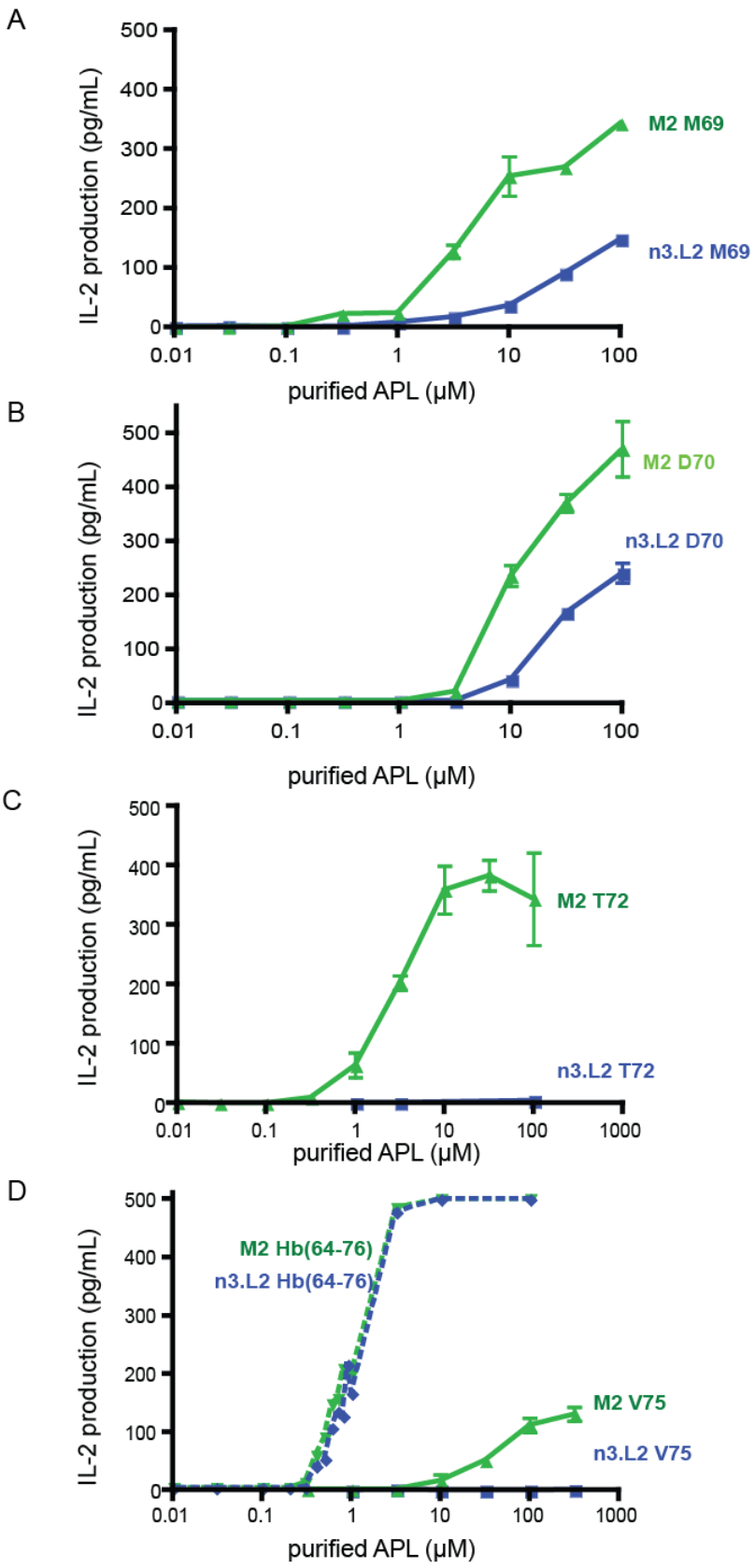


Figure 2.5 IL-2 response by n3.L2 and M2 hybridomas to APLs

**Figure 2.6 Relative kinetic measurements binding to APLs**

Visual representation of kinetic measurements determined by surface plasmon resonance for n3.L2 and M2 scTCRs binding to APL loaded I-$E^k$ dimers. Presented are mean + SD for 1-5 separate experiments on new CM5 chips. Values above the x-axis are measured $k_{on}$, below are $k_{off}$.

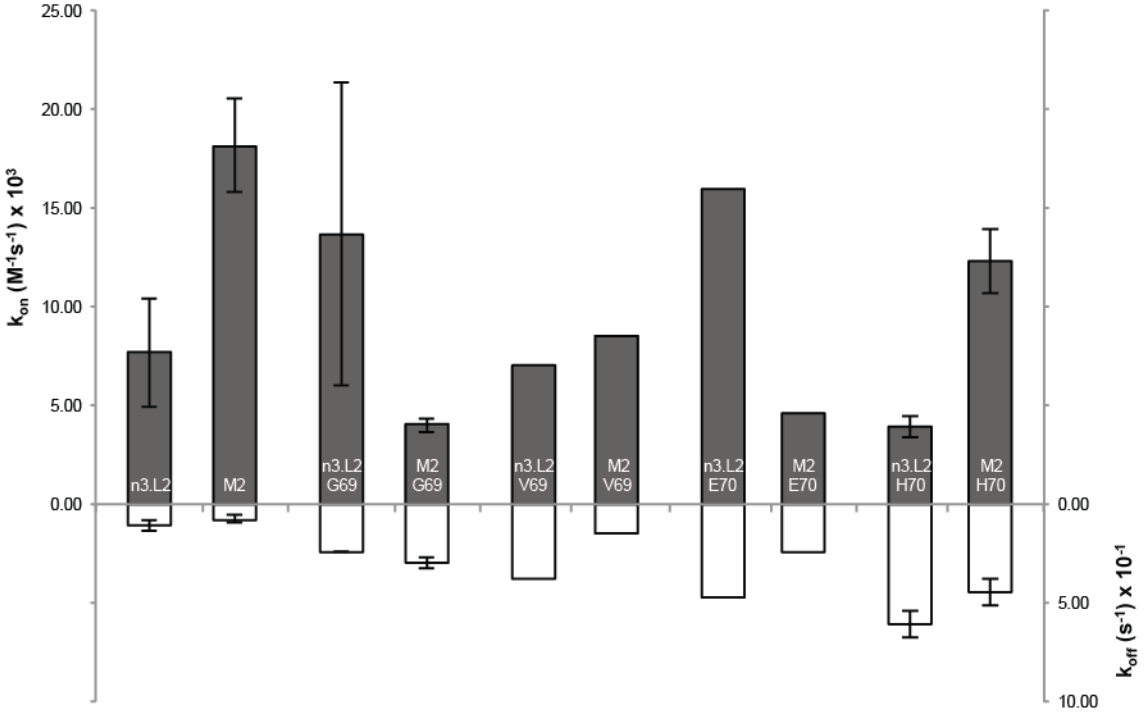


Figure 2.6. Relative kinetic measurements binding to APLs

**Figure 2.7 Kinetics and response to APL H70**

Representative IL-2 response of n3.L2 and M2 hybridomas to doses of H70 APL up to 314μM. Each dose was measured in triplicate in at least 3 independent experiments. Kinetics of n3.L2 and M2 scTCRs binding to H70/I-$E^k$ dimers by surface plasmon resonance. Presented are mean + SD for 2 separate experiments on new CM5 chips.

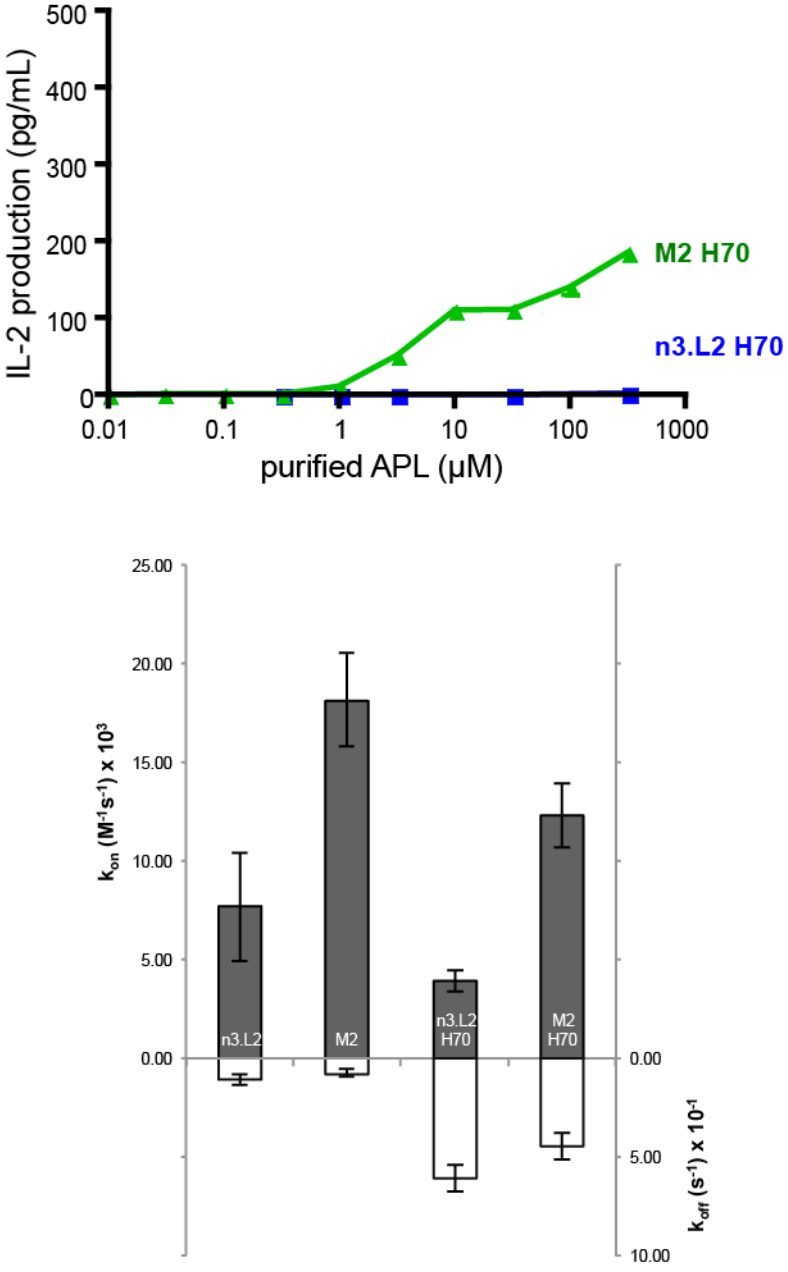


Figure 2.7. Kinetics and response to APL H70.

**Figure 2.8 Kinetics and response to APL E70**

Representative IL-2 response of n3.L2 and M2 hybridomas to doses of E70 APL up to 100μM. Each dose was measured in triplicate in at least 3 independent experiments. Kinetics of n3.L2 and M2 scTCRs binding to E70/I-$E^k$ dimers by surface plasmon resonance. Presented are mean values for 1 experiment performed in duplicate.

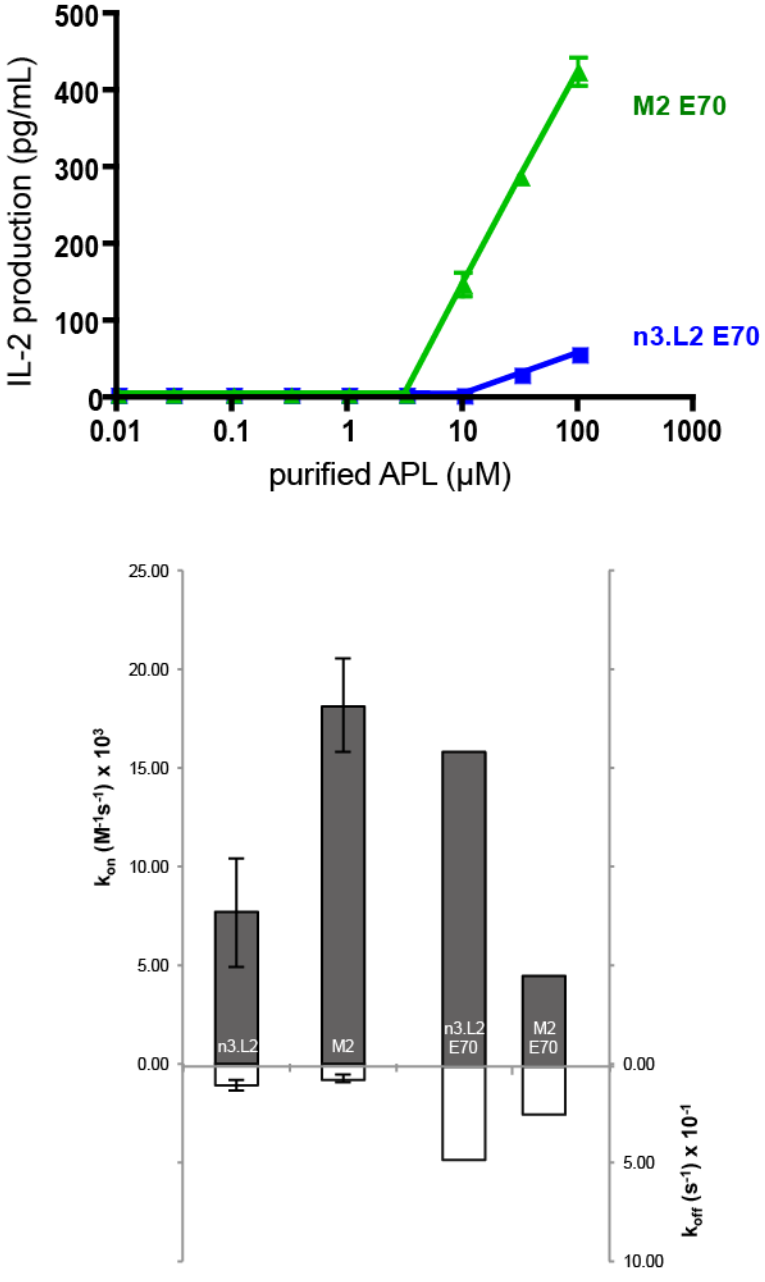


Figure 2.8. Kinetics and response to APL E70

**Figure 2.9 Kinetics and response to APL G69**

Representative IL-2 response of n3.L2 and M2 hybridomas to doses of G69 APL up to 314μM. Each dose was measured in triplicate in at least 3 independent experiments. Kinetics of n3.L2 and M2 scTCRs binding to G69/I-$E^k$ dimers by surface plasmon resonance. Presented are mean + SD for 2 separate experiments on new CM5 chips.

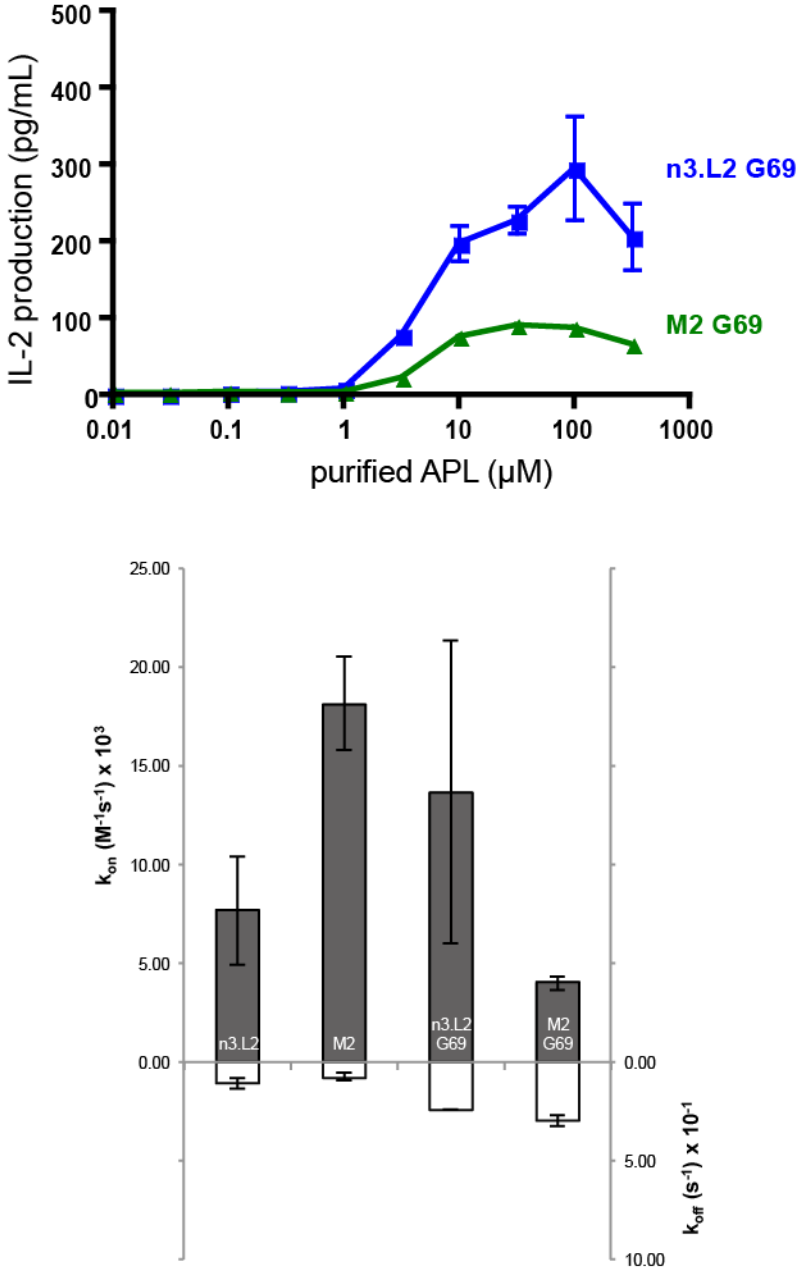


Figure 2.9. Kinetics and response to APL G69

**Figure 2.10 CD69 upregulation in response to Hb(64-76) and anti-CD3 + anti-CD28**

DP thymocytes were isolated from n3.L2 (blue squares) or M2 (green triangles) thymi and cultured for 18 hours with Hb(64-76) pulsed APCs (**A**) or plate bound anti-CD3 + anti-CD28 (**B**). CD69 upregulation was measured by flow cytometry. Populations were gated on DP thymocytes and percent CD69 was recorded. Presented are mean and SEM of 4 independent experiments for anti-CD3 + anti-CD28 (A) and 8 independent experiments for Hb(64-76) (B). p values determined by $X^2$ to test higher CD69 levels in the M2 population.

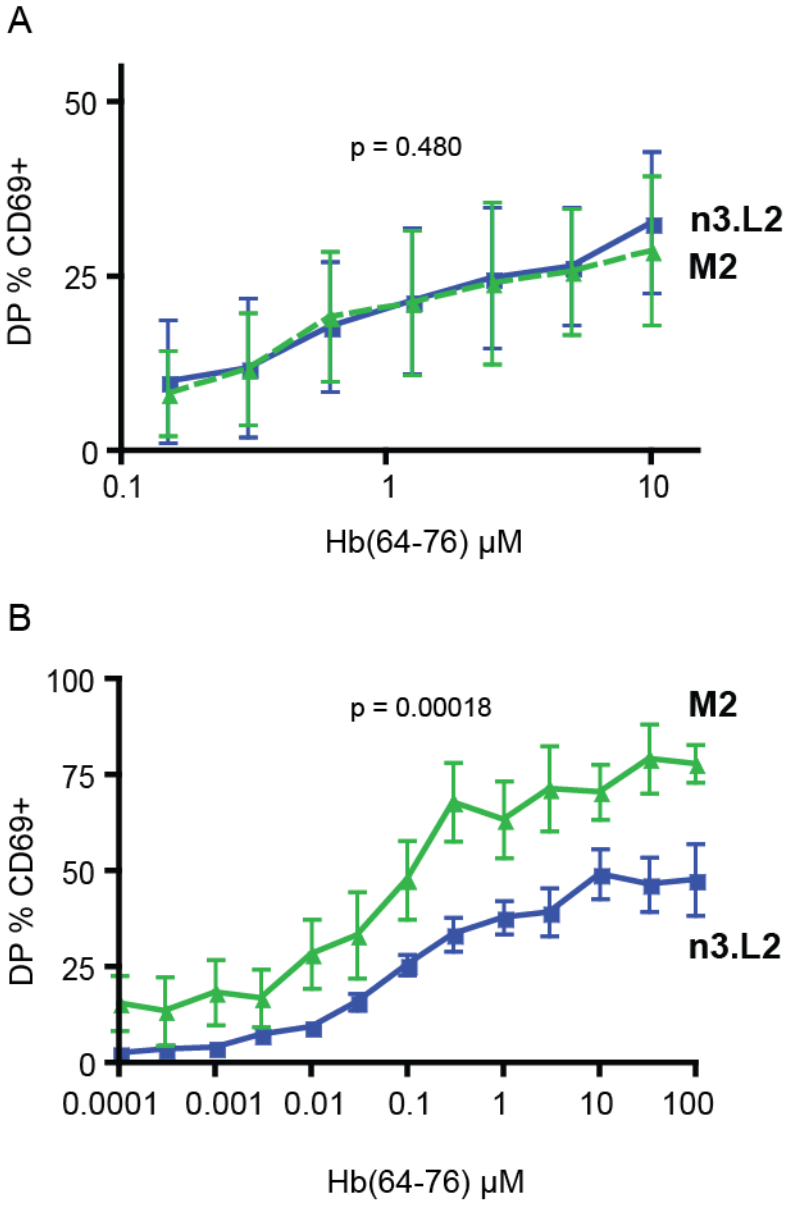


Figure 2.10. CD69 upregulation in response to Hb(64-76) and anti-CD3 + anti-CD28

**Figure 2.11 CD69 upregulation by DP thymocytes in response to APLs**

DP thymocytes were isolated from n3.L2 (blue squares) or M2 (green triangles) thymi and cultured for 18 hours with APL pulsed APCs at multiple doses (left) or a single dose of 0.3μM (right) in duplicate. CD69 upregulation was measured by flow cytometry. Populations were gated on DP thymocytes and percent $CD69^{+}$ was recorded. Presented are mean and SEM for at least 2 independent experiments at each dose.

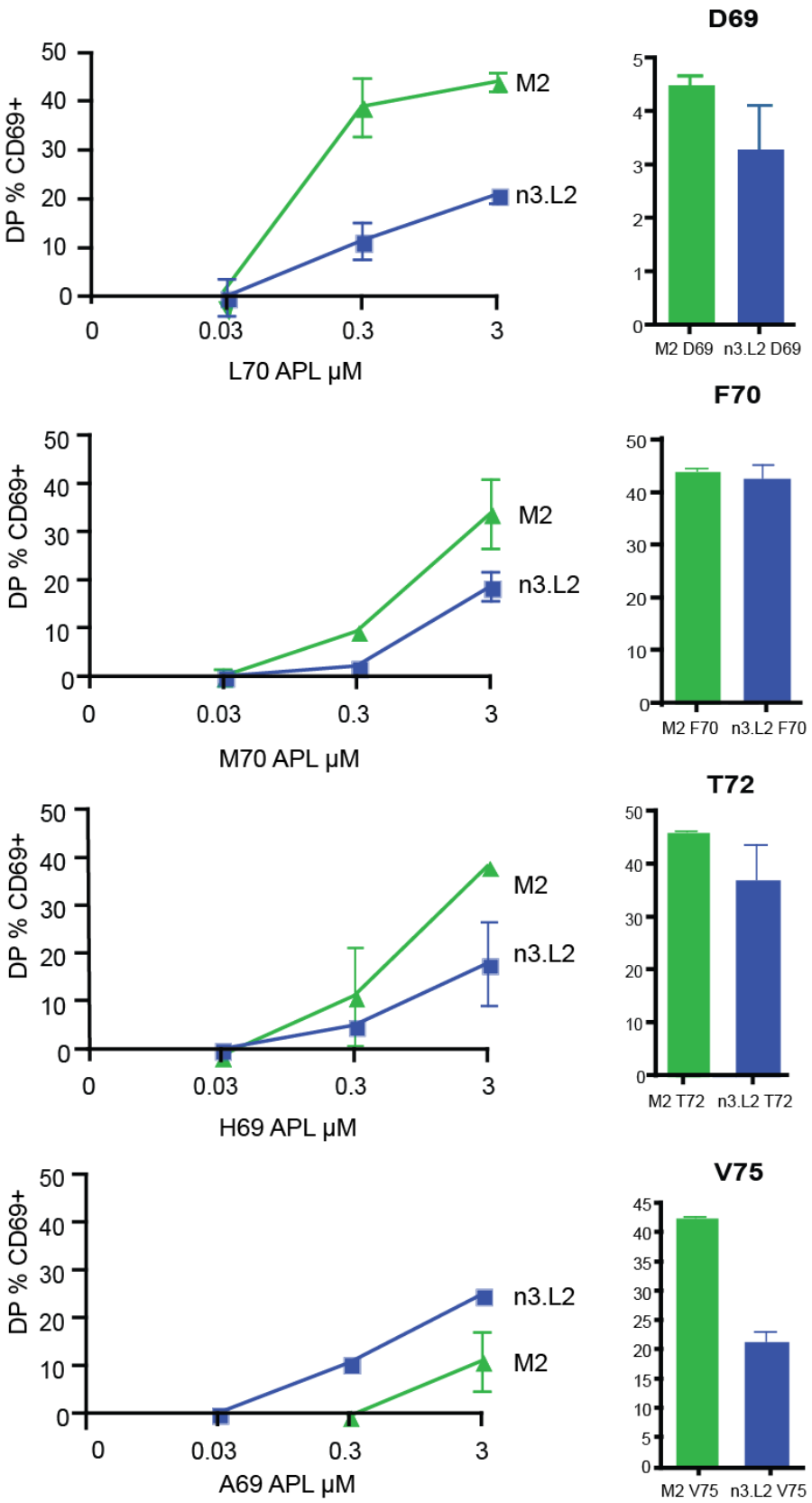


Figure 2.11. CD69 upregulation by DP thymocytes in response to APLs

**Table 2.1 Kinetics of n3.L2 and M2 scTCRs binding Hb(64-76)/I-$E^k$**

Kinetics of n3.L2 and M2 were measured by surface plasmon resonance using scTCRs binding to Hb(64-76)/I-$E^k$ dimers. Measurements of n3.L2 and M2 kinetics are averages of 5 independent experiments on separate CM5 chips.

| | $k_{on}$ (1/Ms) | $k_{off}$ (1/s) | $K_D$ ($k_{off}/k_{on}$, nM) |
|---|---|---|---|
| n3.L2 | 7,650+2,731 | 0.1081+0.029 | 16,648+9,658 |
| M2 | 18,143+2,390 | 0.0768+0.016 | 4,305+1,137 |

Table 2.1. Kinetics of n3.L2 and M2 scTCRs binding Hb(64-76)/I-Ek

**Table 2.2 Correlation between kinetics and response to APLs**

Kinetics of n3.L2 and M2 were measured by surface plasmon resonance using scTCRs binding to Hb(64-76) or APL loaded I-$E^k$ dimers. Measurements of n3.L2 and M2 kinetics are averages of 1-5 independent experiments on separate CM5 chips. $E_{max}$ and $EC_{50}$ values determined for IL-2 production by n3.L2 and M2 hybridomas stimulated with wildtype Hb or APL pulsed APCs. Correlation between kinetic measurements and IL-2 production was determined using a Pearson's correlation.

| | Surface Plasmon Resonance | | | IL-2 production | |
|---|---|---|---|---|---|
| | **$k_{on}$ (1/Ms)** | **$k_{off}$ (1/s)** | **$K_D$ ($k_{off}/k_{on}$, nM)** | **$E_{max}$ (IL-2 pg/mL)** | **$EC_{50}$ (μM)** |
| **n3.L2** | 7,650+2,731 | 0.10814+.029 | 16,648+9,658 | 494 | 11.06 |
| **M2** | 18,143+2,390 | 0.0768+0.016 | 4,305+1,137 | 497 | 6.22 |
| **n3.L2 G69** | 13,675+7672 | 0.24+0.0 | 20,828+11,685 | 295 | 7.18 |
| **M2 G69** | 4,000+382 | 0.2975+0.0304 | 74,351+504 | 91.4 | 6.27 |
| **n3.L2 V69** | 6,970 | 0.379 | 54,375.8967 | | |
| **M2 V69** | 8,540 | 0.149 | 17,447.30679 | | |
| **n3.L2 E70** | 15,900 | 0.468 | 29,433.96226 | 57.6 | >100 |
| **M2 E70** | 4,600 | 0.242 | 52,608.69565 | 425 | >100 |
| **n3.L2 H70** | 3,915+544 | 0.6095+0.070 | 158,459+39,918 | 1.10 | >100 |
| **M2 H70** | 12,250+1,626 | 0.447+0.078 | 37,239+11,293 | 140 | 5.40 |

Correlation between $k_{off}$ and $E_{max}$: $p = 0.0015$; Pearson's $r = -0.914$
No correlation found between $E_{max}$ or $EC_{50}$ and other parameters

Table 2.2. Correlation between kinetics and response to APL

# CHAPTER 3

# $k_{on}$ of TCR:pMHC affinity drives changes in selection and activation of CD4 T cells

## Introduction

The TCR affinity for pMHC regulates outcomes of T cell selection in the thymus and activation of T cells in the periphery (1-4). Agonist peptides induce full T cell activation through strong interactions with the TCR (3, 5). Weaker TCR:pMHC interactions can result in partial T cell activation (6) or anergy (7, 8). Positive selecting, TCR:endogenous pMHC interactions are also of very low affinity (9). The affinity ($K_D$) of the TCR:pMHC complex is determined by the dissociation rate ($k_{off}$) and association rate ($k_{on}$). Kinetic and thermodynamic parameters for the TCR:pMHC interaction have been correlated with T cell activation (12, 39, 41-45, 47, 48), however there is no consensus for one parameter being a predictor of a peptide's ability to stimulate a TCR (46). A few studies have suggested a role for $k_{on}$. Recently, it was shown that a stimulatory pMHC with a fast $k_{off}$ could compensate with a fast $k_{on}$ resulting in sufficient interaction between the TCR and pMHC for full activation (47, 48). These studies clearly revealed that changes in $k_{on}$ can affect the ability of a peptide to stimulate a T cell, but these conclusions were based on TCR:pMHC combinations in which there were changes in both $k_{on}$ and $k_{off}$. Therefore, it remains important to understand the individual contribution $k_{on}$ makes in determining T cell selection and activation.

The TCR:pMHC binding footprint is a specific but flexible structure (20). TCR specificity for pMHC is encoded in the variable CDR loops, which form the binding footprint for TCR to contact the pMHC complex (23, 24). TCR specificity for MHC is primarily through interactions with CDRs 1 and 2 (25, 26), though CDR3 can directly contact MHC (158). It is thought that the highly conserved CDRs 1 and 2 have "germline

encoded" interaction with an MHC. This is best defined for T cells using Vβ8.2 in which a set of conserved interactions exist between two tyrosines and a glutamic acid residue of the TCR CDR2β and the MHC class II α chain (26-28). Mutations in the CDR 1 and 2 loops can result in generation of high affinity TCRs (29, 30), potentially as a consequence of an optimal binding conformation or enhanced TCR:pMHC stability (16, 20, 31, 32). In the general diagonal orientation of the TCR on pMHC, the CDR3 loops are positioned across from the peptide in the MHC binding groove providing direct interactions with specific amino acid side chains (17, 22, 35). The sum of binding energetics between the TCR and pMHC dictate the overall affinity of the complex and determine how a T cell will respond to a specific peptide presented on MHC in both the thymus and periphery (19).

There is an affinity continuum of a TCR for endogenous pMHC that regulates selection of T cells in the thymus (67). T cells must have sufficient affinity for endogenous pMHC above the threshold for positive selection but below the threshold for negative selection (9, 68, 69). T cells on the low end of the affinity spectrum fail to recognize pMHC and die from neglect (70). The threshold for positive selection is set by partial or low level T cell activation. High affinity recognition of self pMHC can result in negative selection. High affinity TCR:pMHC interactions have a longer contact time leading to increased signaling through the TCR (78). Negative selection is a digital response due to the accumulation of specific signals downstream of the TCR (87), resulting in apoptosis of high affinity T cells to establish central tolerance (77, 78). While the majority of self-reactive T cells are deleted to generate central tolerance, it is thought that $T_{regs}$ can develop from these self-reactive, high affinity TCRs (159). $T_{reg}$

development is not merely a consequence of a high affinity TCR, however, as specific environmental cues and TCR sequences may also be required (160, 161). A complex set of distinct signals regulates positive and negative selection (76, 119), tuning T cell responsiveness in the periphery.

Negative selection is an incomplete process, however, and some high affinity T cells escape to the periphery where they can cause autoimmune disease (122). While failure to eliminate these cells leaves a population of potentially self-reactive cells, a back-up system is in place to prevent autoimmunity (162). Potentially autoreactive T cells can be rendered unresponsive to antigenic stimulation (123) or deleted in the periphery to establish peripheral tolerance (78) against antigens that are in low concentrations or not available during thymic selection. Anergy, a state of hyporesponsiveness characterized by low IL-2 production and inhibited proliferation (123), has been induced in naive T cells through lack of costimulation (125), exposure to APLs (6, 8, 77), or low stimulation through the TCR as a result of either low affinity interactions (86, 128, 129) or unstable pMHC complexes (128). *In vivo*, a high affinity interaction can lead to an attenuated T cell response by altering intracellular signaling (134), or rapidly deleting the T cells (163). Activation following suboptimal stimulation, such as in the absence of costimulation or with high immunosuppressive signals, results in a phenotype akin to anergy (124). Anergized T cells downregulate TCR and costimulatory receptors to maintain the hyporeactive state (130). Low expression of a TCR in the thymus results in reduced positive selection in addition to anergy in the periphery (86). Because of the dual role of T cell affinity in selection and activation, the

propensity for T cells to undergo tolerance may be set in the thymus by the affinity of the expressed TCR for self pMHC.

We have generated a novel system to examine how the $k_{on}$ of the TCR binding pMHC regulates T cell selection and activation. This system compares two TCRs recognizing the same cognate antigen, Hb(64-76)/I-$E^k$. In the mouse, the Hb protein exists in two naturally occurring allelic variants, $Hb^d$ and $Hb^s$, such that T cells can develop normally in $Hb^s$ strains and be reactive to cells from $Hb^d$ mice. The n3.L2 TCR was generated against the $Hb^d$ version of the (64-76) peptide (62). A yeast display system was utilized to generate higher affinity variants of the n3.L2 receptor (137, 138). The highest affinity variant, M15, has previously been studied. M15 recognized Hb(64-76) with the same sensitivity as the original n3.L2 TCR (137, 140). Because of its increased affinity, M15 had broader recognition of Hb APLs and had sufficient affinity to respond to weak n3.L2 ligands (138). While providing insight into the sensitivity of the TCR for low affinity pMHC, these studies were only conducted *in vitro* and failed to answer questions about how kinetics regulate the TCR in a naturally selected T cell. Additionally, the increased affinity of M15 is due to changes in both the $k_{on}$ and $k_{off}$. Therefore, the question of the contribution of $k_{on}$ in selection and activation of T cells remains.

A second variant, M2, has two amino acid changes in the CDR1α region resulting in a 3.7 fold higher affinity due specifically to a faster $k_{on}$. We generated an M2 TCR transgenic mouse to test the effects of $k_{on}$ *in vivo*. While the measured affinity of M2 for Hb(64-76)/I-$E^k$ is within the range of naturally occurring T cells (1-50μM), M2 T cells underwent negative selection as a result of the faster $k_{on}$ in the recognition of pMHC. M2

T cells that escaped negative selection to generate the peripheral T cell population were hyporesponsive to Hb stimulation. The faster $k_{on}$ for M2 binding pMHC may set the affinity of M2 for I-$E^k$ near the threshold for activation, increasing TCR stimulation by pMHC during selection and activation. Therefore, the $k_{on}$ for TCR binding pMHC influences signaling through the TCR and thereby regulates T cell selection and activation outcomes.

## Materials and Methods

*Generation of the M2 TCR transgenic mouse line*

The M2 mouse was generated using the method described for the n3.L2 mouse (79). The n3.L2 V-Jα plasmid was mutated by PCR to express the two amino acid changes in the M2 CDR1α chain. The M2α chain was cloned into the TCR shuttle vector. TCRα and β minigene constructs were coinjected into C57/BL/6 pronuclei in the Washington University Department of Pathology and Immunology's Transgenic Core Facility. Transgenic mice were identified by PCR amplification of the M2α and β transgenes from tail DNA. Expression of the M2α chain was confirmed by sequencing the founders' genomic DNA. One founder expressed both the M2α and β transgenes and was bred to the B6.K strain to provide the selecting MHC. Peripheral CD4 T cells in the M2/B6.K mouse stained with the clonotypic antibody, CAb. M2 and n3L.2 mice were further crossed to a Rag-$1^{-/-}$ background producing n3.L2/B6.K/$Rag1^{-/-}$ and M2/B6.K/$Rag1^{-/-}$ mice. Mice were used at 4-8 weeks of age in these studies, unless otherwise noted. All mice were bred and maintained in a pathogen-free barrier facility within Washington

University in St Louis following a protocol approved by and in accordance with guidelines from the Washington University Division of Comparative Medicine.

*Generation of n3.L2 and M2 hybridomas*

n3.L2 and M2 TCRα and β chains were cloned into a p2A retroviral vector with an IRES-GFP tag (pMIIG) developed by the Vignali lab (149), which places the α and β chains as a single polypeptide linked by the p2A peptide. No stability mutations were added into the sequence. The 2A peptide (p2A) is cleaved posttranslationally, ensuring equal expression of the α and β chains and resulting in efficient expression of transduced αβ TCRs. Viral particles were packaged in the PlatE cell line spinfected with 30μg retrovirus. Purified retrovirus containing supernatants from PlatE cells were used to infect the 58 $\alpha^-\beta^-$ $CD4^+$ hybridoma cell line. M2 and n3.L2 expressing hybridomas were generated simultaneously, sorted for comparable high GFP expression, and equal expression of the n3.L2 and M2 TCRs. Cells were sorted a second time to generate a population with stable TCR expression. Equivalent expression levels of CD3, CD4, and TCR between n3.L2 and M2 hybridomas were confirmed by flow cytometry. Surface TCR levels were assessed with CAb, Vβ8.3, and H57. Hybridomas were cultured in RPMI + 10% FCS + 1% β-2-mercaptoethanol + 1% Glutamax + 0.5% gentamycin.

*T cell IL-2 production and proliferation assays*

For isolated T cell stimulation, single cell suspensions were made from pooled lymph nodes and spleen from transgenic mice. $CD4^+$ cells were isolated by negative selection using a Miltenyi CD4 II isolation kit (Miltenyi Biotec). Non-$CD4^+$ cells were

depleted by binding to a Miltenyi AutoMACS column. Purity was tested by flow cytometry analysis for percent $CD4^+$ $CAb^+$. To account for minor variations in the purity between n3.L2 and M2 isolation, cell numbers were normalized to the percent $CD4^+$ $CAb^+$ cells to ensure the same number of specific CD4 cells were plated in each well of the IL-2 or proliferation assays. $1x10^5$ specific CD4 cells were plated in $I10^+$ (IMDM + 10% FCS + 1% L-glutamine + 1% non-essential amino acids + 1% β2-mercaptoethanol + 0.5% gentamycin) with $5x10^5$ irradiated B6.K splenocytes and varying concentrations of purified Hb(64-76) peptide from 0.0001-100μM. 18-20 hours after at 37°C 5% $CO_2$, supernatants were assayed using an IL-2 ELISA. Briefly, IL-2 was captured using an anti-IL-2 antibody (BioLegend) and detected with a second, biotinylated anti-IL-2 antibody (BioXCell). Biotin-labeled IL-2 was detected by a streptavidin conjugated horseradish peroxidase antibody (Southern Biotech) followed by TMB substrate for accurate detection of 5-500 pg/mL of IL-2 (1-step Ultra TMB ELISA, Thermo Scientific). After stopping the reaction with 2M sulfuric acid, absorbance was read at 450nm. Absorbance levels were converted into amount of IL-2 based on a regression analysis of IL-2 standards using GraphPad Prism (GraphPad Software). To measure proliferation, CD4 T cells were isolated and cultured as in the IL-2 production assay. After 72 hours in culture at 37°C 5% $CO_2$, each well was pulsed with 0.4μCi $^3H$ thymidine and maintained in culture. After an additional 24 hours, plates were harvested and measured for $^3H$ thymidine incorporation.

*$Ca^{2+}$ imaging and analysis*

Peptide loaded I-$E^k$ dimers were plated on 8-chambered culture slides overnight in PBS. Slides were washed with $Ca^{2+}$ free Ringer's solution (150mM NaCl + 10mM glucose + 5mM HEPES + 5mM KCl + 1mM $MgCl_2$ + 2mM $CaCl_2$, pH 7.4) prior to imaging. CD4 T cells were isolated from n3.L2 and M2 TCR-tg mice and either cultured with irradiated B6.K splenocytes loaded with 10μM Hb antigen for 6 days to form T cell blasts or kept as naive cells at 37°C. To image $Ca^{2+}$ fluxing, M2 and n3.L2 naive T cells or blasts were labeled in Ringer's solution with 1μM Fura-2 AM, a $Ca^{2+}$ specific indicator dye, immediately before imaging. $1x10^6$ cells were resuspended in 1mL Ringer's solution with 1μM Fura-2 AM and incubated for 30 minutes at 37°C. Cells were washed 1x in Ringer's, resuspended in Ringer's, and quenched for 30 minutes at 37°C. Cells were added to washed wells of the chamber slide and imaged by transmitted light and for emission of 340 and 380 nm fluorescence at 3-second intervals for at least 30 minutes. Data was expressed as a 340/380 ratio to account for loading variation. Between imaging $Rag^{+/+}$ and $Rag1^{-/-}$ T cells, the microscope underwent repairs and was recalibrated. The 340/380 rations differ in levels as a result. While the values differ, the trends can be compared.

Images were analyzed using Metamorph. Regions were drawn around each responding cell (above background intensity ratio of 200) and tracked at each timepoint. Average and maximal intensities for each ratio were recorded for each timepoint in Excel. Maximal intensity for the entire time course was identified and tracks were aligned using an align program (written by E.A. Yttri, using R) to provide data sets for characterization of the $Ca^{2+}$ flux pattern. Peak (max) intensity, average sustained intensity

(post peak), and oscillations (deviation from linear regression of post peak intensities) were compared by ANOVA using Graph Pad Prism.

*Generation of bone marrow chimeras*

Bone marrow was isolated from tibias and femurs of n3.L2 and M2 TCR transgenic mice. Bone marrow was flushed out using a syringe and culture media. Bone marrow homogenate was filtered to remove bone and other particulate or clumps. RBC were lysed using ACK lysis buffer, which does not lyse lymphocytes or precursors. 20 $x10^6$ total bone marrow cells were injected *i.v.* into lethally irradiated recipients. Recipients were irradiated with 900 rad one day prior to bone marrow transfer. For mixed chimeras, $10^6$ n3.L2 and $10^6$ M2 or B6.K control cells were mixed together and transferred into recipients. Mixed bone marrow was analyzed by flow cytometry to record the exact percent derived from each mouse type. Chimeras were maintained on antibiotic treated water for 8-12 weeks until tissues were collected and analyzed by flow cytometry. The initial sets of chimeras, using $Rag^{+/+}$ donors, were analyzed after 8 weeks, according to protocols used previously in the lab. The $Rag1^{-/-}$ chimeras were analyzed at 12 weeks after recommendations from Takeshi Egawa.

*I-$E^k$ Ig dimers*

I-$E^k$ dimers were produced in Drosophila S2 cells, as previously described (150). Amino acid residues chosen for mutagenesis were located on the top of the α and β helices as potential TCR contact residues. To generate mutant I-$E^k$ dimers, mutations were introduced into I-$E^k$ constructs at one of 4 MHCα and 3 MHCβ residues chosen from a

subset of mutants expressed in CHO cells (164). Wildtype and mutant I-$E^k$-Ig dimer constructs were transfected into Drosophila S2 cells. Dimers were isolated from culture supernatants by binding to Protein A. Dimers were exposed to acidic pH to remove the endogenous, weakly binding peptides and maintained in excess amounts of soluble peptide to substitute the desired peptide into the peptide binding groove. To assay the TCR:pMHC binding footprint, 96 well plates were coated overnight with Hb(64-76)-loaded I-$E^k$ Ig dimers. After 20 hours, plates were washed to remove unbound dimer, 5 x $10^5$ hybridomas were added, and activation was assayed after 20 hours using the IL-2 ELISA described above.

**Results**

*Generation of M2 TCR transgenic mice*

To determine if increased $k_{on}$ affected T cell development and normal function of naturally occurring mature T cells, we generated an M2 TCR transgenic mouse. The n3.L2 TCR transgenic mouse has previously been described (79). Work generating retroviral bone marrow chimeras with M2 T cells suggested that M2 would be positively selected but not negatively selected in the presence of I-$E^k$ on APCs (data not shown). M2 α and β chain constructs were coinjected into B6.K eggs. This initial implantation produced a low fecundity, with one mouse positive for the α chain out of 45 tested. Therefore, the M2 TCR α and β transgenes were coinjected onto the B6 background. One founder was generated that co-expressed the M2α and β chains. A second founder was generated that expressed only the M2α chain. The M2α mouse was crossed to mice

expressing the n3.L2 β chain, which is common between the n3.L2 and M2 TCRs. The M2α/n3.L2β did not transmit the transgenes to offspring and therefore was not used further. The M2αβ founder was the source for all M2 mice used in these experiments. The M2αβ founder was crossed to the B6.K and B6.K/Rag1$^{-/-}$ background to provide the proper selecting environment for M2 T cells and to eliminate any potential complications from secondary TCRα rearrangements. The n3.L2 mouse was simultaneously crossed to a Rag1$^{-/-}$ background. The thymocytes and T cells of Rag$^{+/+}$ and Rag1$^{-/-}$ mice were analyzed by flow cytometry.

*M2 CD4 T cells on a Rag$^{+/+}$ background are mature but express low TCR levels*

M2 T cells were present in the periphery of the M2 TCR transgenic mice (Figure 3.1A). While these T cells had the same level of CD4 and CD3 (Figure 3.1A, B), M2 CD4$^{+}$ T cells had lower levels of TCR, measured by our clonotypic antibody, CAb. Additionally while the total spleen size was the same, the M2 mouse had a significant reduction in the CD4 population (Table 3.1). The CAb high population in the M2 mouse was depleted, suggesting the reduced population size was due to removal of the TCR high population. Other maturation markers, such as PD-1, CD5, CD62L and CD44, were expressed at the same level on M2 and n3.L2 transgenic CD4 cells (Figure 3.1B). There did not appear to be any skewing in other lymphocyte populations (B cells, NK cells, $T_{regs}$, γδ T cells).

In the thymus, the M2 CD4 SP population was reduced (Figure 3.2A) and also had a lower percent of TCR high cells (Figure 3.2B). Interestingly, fewer of these T cells were CD69$^{+}$ than the same CD4 SP population in the n3.L2 mouse but otherwise there

was no difference in surface marker expression (Figure 3.2B). While there did not appear to be drastic skewing in the M2 thymus, the DP population was significantly reduced and the DN population significantly larger than in the n3.L2 mouse (Table 3.1). Aside from the lower TCR level, the DP populations were phenotypically the same between the two transgenic mice (Figure 3.2C). The M2 DN population had a slight increase in the $CD25^+$ $CD44^-$ DN3 population (Figure 3.3A). The M2 DN thymocytes were able to express the transgenic TCR, similar to the n3.L2 DN thymocytes, indicating no block in selection of the Vβ8.3 TCRβ chain (Figure 3.3B).

*M2 CD4 T cells on a $Rag1^{-/-}$ background undergo negative selection*

Mature $CD4^+$ T cells developed and were present in the periphery of the M2 $Rag1^{-/-}$ transgenic mouse (Figure 3.4A). These cells were completely mature and expressed high levels of TCR, CD3, CD4, and other maturation markers (Figure 3.4B). However, the $CD4^+$ cell number was greatly reduced in the M2 $Rag1^{-/-}$ mouse in comparison to n3.L2 (Table 3.1), like was seen in the $Rag^{+/+}$ TCR transgenic mouse. The decreased CD4 population suggested a difference in T cell selection. In the thymus, both the M2 $Rag1^{-/-}$ and n3.L2 $Rag1^{-/-}$ mice had a mature CD4 SP population (Figure 3.5A). The CD4 SP populations expressed the same levels of TCR, CD4, CD3 and some maturation markers (Figure 3.5B). Very few $T_{reg}$ cells developed from the transgenic T cells either in the thymus or by peripheral conversion (Figure 3.6). There was no detectable γδ TCR expression (Figure 3.6).

M2 $Rag1^{-/-}$ mice had dramatically reduced thymus cellularity in comparison to n3.L2 $Rag1^{-/-}$ (Table 3.1), suggesting a difference in T cell selection. The M2 $Rag1^{-/-}$

thymus had an increased proportion of DN cells (Table 3.1), arrested at the DN3 stage of development (Figure 3.5, Figure 3.7A). While this developmental block indicated inefficient selection of the M2 TCR, the transgenic Vβ8.3 was highly expressed on a small population at the same level as in the n3.L2 Rag1$^{-/-}$ mouse (Figure 3.7B). The same TCRβ chain was expressed on a larger population in the n3.L2 mice (Figure 3.7B), suggesting the TCRβ transgene is not efficiently expressed in the M2 Rag1$^{-/-}$ mouse, blocking a large percentage of the M2 thymocytes at DN3. The DN population that does express Vβ8.3 developed into DP, SP, and peripheral T cells, permitting further analysis of those populations. Due to the increased DN population in the M2 Rag1$^{-/-}$ transgenic mouse, the number and percentage of DP thymocytes was also reduced in comparison to the n3.L2 Rag1$^{-/-}$ transgenic mouse (Table 3.1). In spite of fewer DP cells, the M2 Rag1$^{-/-}$ and n3.L2 Rag1$^{-/-}$ mice had the same proportion of CD4 single positive cells. Therefore, despite alterations in selection, M2 CD4$^{+}$ T cells developed and persisted in the periphery in M2 Rag1$^{-/-}$ mice. While these cells appeared to be phenotypically normal, we predicted the consequences of a higher affinity interaction with endogenous pMHC in the thymus would alter CD4 function in response to cognate antigen.

*M2 Rag$^{+/+}$ T cells failed to sustain activation, potentially as a result of earlier initiation of signaling*

Following recognition of agonist pMHC, CD4 T cells are programmed to secrete IL-2 and proliferate. IL-2 production occurs rapidly after initiation of signaling cascades downstream of the TCR (165). Proliferation is a later consequence, usually occurring within days following antigen stimulation. Since the M2 TCR had a faster $k_{on}$ for binding

Hb(64-76)/I-$E^k$, the timing of signaling events may be shifted to favor an earlier onset. To test this hypothesis, $CD4^+$ T cells were isolated from n3.L2 and M2 $Rag^{+/+}$ mice and cultured *in vitro* with Hb pulsed irradiated B6.K splenocytes. Cell cultures were pulsed with $^3H$ after 24 or 72 hours to measure T cell proliferation. Cultures were harvested 20 hours later to assess $^3H$ incorporation, indicating level of proliferation. IL-2 production by n3.L2 and M2 T cells was the same 20 hours post incubation. Proliferation of n3.L2 and M2 T cells 48 hours post incubation was equivalent (Figure 3.8A). Interestingly, while n3.L2 T cells continued to proliferate 4 days after exposure to antigen, the M2 cells had reduced levels of proliferation at this timepoint (Figure 3.8B). This suggests that the faster $k_{on}$ of M2 T cells recognizing Hb(64-76)/I-$E^k$ is of sufficient affinity to overcome the threshold for activation but either alters prolonged levels of signaling or results in earlier onset of activation followed by T cell burnout.

*M2 $Rag1^{-/-}$ T cells are hyporesponsive to Hb(64-76) in the periphery*

The immune system has developed multiple mechanisms to ensure self tolerance in the periphery in order to prevent autoimmunity. High affinity T cells that escape negative selection become unresponsive in the periphery (7, 166). Induction of anergy can be programmed in the thymus by selection or conferred by stimulation in the periphery (131, 167, 168). Exposure to low affinity APLs either in the thymus or periphery results in suboptimal activation of T cells and failure to proliferate. Isolated M2 and n3.L2 $Rag1^{-/-}$ $CD4^+$ T cells had the same sensitivity in producing IL-2 in response to Hb(64-76)-I-$E^k$ presented on irradiated B6.K splenocytes after 18-20 hours of culture (Figure 3.9A); however, the M2 T cells produced significantly lower levels of IL-2 in comparison to

n3.L2 T cells. Interestingly, isolated M2 Rag1$^{-/-}$ T cells failed to proliferate at day 4 in response to Hb(64-76) stimulation in contrast to the strong proliferation of n3.L2 T cells (Figure 3.9B). The reduced ability to produce IL-2 and inhibition of proliferation is a classic pattern of T cell anergy (8).

An anergic state is often accompanied by downregulation of the TCR or costimulatory molecules on the T cell surface (130). M2 and n3.L2 T cells retained high TCR levels in the periphery of the transgenic mice (Figure 3.4). CD3 and CD4 levels were the same on n3.L2 and M2 cells (Figure 3.4), suggesting the unresponsive nature of M2 T cells is not due simply to low TCR and CD4 levels. Levels of CD25 (IL-2R), CD28, PD-1, and CTLA-4 were also similar on n3.L2 and M2 CD4 cells (Figure 3.4). As the induction of anergy did not appear to be due to decreased costimulation or increased inhibitory signals, M2's hyporesponsive phenotype may be set in the thymus as a result of different T cell selection in comparison to n3.L2.

*Early signaling is maintained but differs downstream of the M2 and n3.L2 TCRs*

While the proliferative response of M2 T cells to agonist peptide was inhibited, T cells that are rendered anergic may maintain early signaling events. One of these early signaling responses is a flux of $Ca^{2+}$ inside the cell. To measure the intracellular $Ca^{2+}$ flux, we labeled isolated M2 and n3.L2 T cells with the ratiometric dye Fura-2 AM and imaged their response to plate bound Hb(64-76)/I-E$^{k}$ dimers. Interestingly, the percentage of responding cells was the same for n3.L2 and M2 T cells. However, the characteristics of the $Ca^{2+}$ signal differed. CD4 T cells isolated from the Rag$^{+/+}$ transgenic mice differed in their sustained signal, with the n3.L2 T cells having a higher level post peak $Ca^{2+}$ spike

(Figure 3.10). The interactions that n3.L2 T cells made with the I-$E^k$ dimers promoted a more sustained signal. When $Rag1^{-/-}$ cells were used, the M2 and n3.L2 T cells differed in the oscillatory nature of the signal after the initial $Ca^{2+}$ spike (Figure 3.11). M2 $Rag1^{-/-}$ T cells had more variation in the level of $Ca^{2+}$ post peak, measured as deviation from a predicted linear regression. Taken together, the differences in $Ca^{2+}$ fluxes in n3.L2 and M2 T cells suggests that the kinetics of TCR interactions with agonist pMHC are tuned to sustain signals in the T cell and changes in $k_{on}$ of the interaction result in qualitatively different signaling patterns. By altering the cascades downstream of the TCR, M2 T cells can be rendered anergic.

*Stronger selection signal sensed by M2 expressing thymocytes*

T cell selection in the thymus is dependent upon recognition of endogenous pMHC by the TCR. A T cell that receives a strong signal during selection can be targeted for anergy if not deleted by negative selection. We hypothesized that M2 thymocytes would be more sensitive to signals from endogenous selecting pMHCII as a consequence of a lower threshold for selection due to M2's faster $k_{on}$. The level of CD5 is proportional to the strength of signal through the TCR during positive selection (169). The M2 $Rag1^{-/-}$ CD4 SP cells had higher surface levels of CD5 in comparison to n3.L2 $Rag1^{-/-}$ CD4 SP cells (Figure 3.12A). The CD5 level was the same on CD4 SP cells in the M2 and n3.L2 $Rag^{+/+}$ mice (Figure 3.2), which could be a consequence of selection based on a second TCR expressing a non transgenic $\alpha$ chain. CD69 is upregulated on the surface of DP thymocytes that have received a selection signal (152). Since the fate of DP thymocytes that upregulate CD69 post selection is variable, we tested the ability of n3.L2 and M2

thymocytes to recognize self-peptides *in vitro*. DP thymocytes isolated from n3.L2 Rag1$^{-/-}$ and M2 Rag1$^{-/-}$ transgenic mice were cultured with irradiated B6.K splenocytes without the addition of peptide and assayed for CD69 upregulation by flow cytometry. After 18 hours in culture, a larger percentage of M2 Rag1$^{-/-}$ DP thymocytes were CD69$^{+}$ (Figure 3.12B), indicating these cells recognized endogenous peptides presented by the B6.K APCs (74) that were not recognized by n3.L2 DP cells. The higher CD5 level on M2 Rag1$^{-/-}$ SP cells combined with more DP thymocytes upregulating CD69 in response to endogenous antigen suggest a stronger affinity for self pMHC. Therefore, the mutations resulting in the increased affinity of the M2 TCR for Hb(64-76)-I-E$^{k}$ may also raise the affinity of M2 for self pMHC and produce stronger signaling through the TCR. A subset of high affinity T cells developing in the thymus upregulate expression of FoxP3. These $T_{regs}$ develop in response to a strong interaction with self-peptides that does not result in negative selection (170). There was no increase in the percentage of FoxP3$^{+}$ $T_{regs}$ in the n3.L2 or M2 mice (Figure 3.6) indicating that while the affinity of the M2 TCR for self-peptide may be stronger than for n3.L2, the transgenic TCR does not promote development of $T_{regs}$. We attempted to identify a self-peptide that differentially selected n3.L2 and M2 thymocytes. We screened 95 self-peptides for their ability to upregulate CD69 on M2 and n3.L2 DP thymocytes but were unable to find any stimulatory peptides (data not shown). This was not surprising as peptides involved in positive selection are highly specific (74). Even so, the CDR1$\alpha$ mutations in the M2 TCR may lessen the energetic requirement for sufficient contact with endogenous pMHC. This would increase the level of positive selection of M2 thymocytes through stronger affinity interactions or by increasing the number of positively selecting peptides, as was seen with

the Hb(64-76) APLs (Figure 2.11). However, the increased strength of signaling through the M2 TCR might be above the threshold for negative selection, resulting in elimination of these strongly responding T cells. What is most intriguing is that the M2 TCR retained an affinity well within the reported normal range of TCRs binding antigen. The specific change of $k_{on}$ in the M2 system could account for this incongruity, suggesting T cell selection is more sensitive to $k_{on}$ than previously thought.

*M2 T cells are deleted when exposed to Hb(64-76) as an endogenous peptide*

In addition to testing the thymocyte response *in vitro*, we wanted to measure selection changes in response to Hb(64-76) as an endogenous ligand. A strong signal during T cell selection can result in deletion of T cells by negative selection (78, 128). This theory correlates well with the reduced peripheral CD4 population in the M2 transgenic mouse. We took advantage of the mouse Hb antigen system to directly examine selection of M2 and n3.L2 T cells *in vivo* in response to Hb(64-76) as an endogenous self-peptide. Neither T cell was reactive to $Hb^s$ (data not shown). A B6.K/$Hb^d$ congenic line was bred to the n3.L2 and M2 $Rag^{+/+}$ TCR transgenic mice. Due to the high level of agonist antigen present in these mice, we predicted that n3.L2 and M2 T cells would be deleted by negative selection. Surprisingly, a small number of n3.L2 $Rag^{+/+}$ $CD4^+$ T cells were present in the periphery of the n3.L2 x $Hb^d$ mice (Figure 3.13A). While some specific T cells were deleted due to recognition of $Hb^d$(64-76) as self-peptide, the n3.L2 affinity for $Hb^d$(64-76) was apparently not above the threshold for complete negative selection. By 4 weeks of age, these mice developed autoimmune hemolytic anemia as measured by the presence of anti RBC antibodies (Figure 3.13B). In

the n3.L2 x $Hb^d$ mice, we suggest that the small population of Hb specific T cells induce production of anti-$Hb^d$ antibodies by B cells in the spleen. Antibodies are then deposited on RBCs resulting in their lysis and the mice develop autoimmune hemolytic anemia. We can use antibody labeling of RBCs as readout for onset of anemia.

In contrast to the n3.L2 x $Hb^d$ mice, the M2 x $Hb^d$ mice completely lacked M2 specific cells in the periphery, though $CAb^+$ cells were found in the thymus (Figure 3.13A). M2 x $Hb^d$ mice failed to develop anemia due to complete elimination of the M2 population (Figure 3.13B). While the percentage of CD4 cells found in the periphery of M2 x $Hb^d$ mice was not different from non-transgenic controls, a population below detection by CAb could still be present. In this case, the M2 CD4 T cells must be anergized as hemolytic anemia did not develop up to 10 weeks of age. An anergic phenotype would be consistent with stimulation results of CD4 T cells from the M2 $Rag1^{-/-}$ mice since these T cells failed to proliferate in response to Hb(64-76). In the M2 $Rag1^{-/-}$ mouse some M2 T cells escape negative selection (Figure 3.4A), whereas in the M2 x $Hb^d$ mouse they are completely eliminated (Figure 3.13A). Thus, the affinity of M2 for Hb(64-76)/I-$E^k$ is above the negative selection threshold while the affinity of M2 for endogenous pMHCII must be at or slightly below the limit for negative selection.

*Development of n3.L2 and M2 T cells in mixed bone marrow chimeras does not reveal competition between the two TCRs*

Restriction of the TCR rearrangement changes the development of the T cell repertoire. To compare development of n3.L2 and M2 T cells in the same mouse, we generated mixed bone marrow chimeras. Bone marrow cells were isolated from the congenically

marked n3.L2 and M2 TCR transgenic mice, combined 1:1, and injected *intravenously* into lethally irradiated recipients. After 8-12 weeks, development of n3.L2 and M2 T cells was assessed in the thymus and periphery of chimeras. When $Rag^{+/+}$ bone marrow was used to reconstitute chimeras, both n3.L2 and M2 T cells were found in the thymus and periphery of the mixed chimeras (Figure 3.14). Interestingly, the CAb high, CD4 SP population was derived solely from the n3.L2 bone marrow. In contrast, the majority of the CAb low population developed from M2, with a reduced proportion from n3.L2. The TCR high population that develops expressing the M2 TCR was eliminated from the bone marrow chimeras. This same population was missing in the M2 $Rag^{+/+}$ transgenic mouse. CD4 T cells in the n3.L2 $Rag^{+/+}$ transgenic mouse express high levels of the transgenic TCR. Therefore, there did not appear to be any competition between development of n3.L2 and M2 T cells.

Since development of M2 T cells differed between the $Rag^{+/+}$ and $Rag1^{-/-}$ backgrounds, mixed bone marrow chimeras were generated using bone marrow isolated from the n3.L2 and M2 $Rag1^{-/-}$ transgenic mice. The $CAb^{+}$ CD4 population in the spleen developed primarily from the n3.L2 bone marrow (Figure 3.15). Less than 6% developed from M2 bone marrow. Initially the low percent of M2 expressing T cells suggested that the n3.L2 TCR was preferentially selected over the M2 TCR. In fact, the percentage of M2 cells developing in the mixed bone marrow chimeras was lower than in chimeras using only M2 bone marrow (Table 3.2). However, the percent and number of M2 progenitors in the DP population was also decreased in the mixed chimeras. By calculating the predicted percentage of M2 cells based on the DP population, the low percentage of M2 CD4 T cells that develop was the same as predicted by the DP

breakdown (Table 3.2). Therefore, the presence of developing n3.L2 T cells did not influence the development of M2 CD4 T cells and vice versa.

*In vivo activation of n3.L2 and M2 CD4 T cells leads to development of anemia, though with different disease kinetics*

When the TCR transgenic mice were crossed to express $Hb^d$ endogenously, both n3.L2 and M2 T cells were depleted. An alternative way to test induction of anemia involved transferring T cells into $Hb^d$ $C\alpha^{-/-}$ mice. Transfer of antigen specific T cells into lymphoreplete mice as has been used to study induction of arthritis (171), diabetes (172), and experimental autoimmune encephalitis (173) without suppressive signals from $T_{regs}$ or complication of endogenous T cells. Interestingly, both n3.L2 and M2 T cells induce anemia and mice eventually succumb to the disease (Figure 3.16). By transferring M2 T cells into a lymphopenic environment, these CD4 T cells are rescued from a tolergenic state and able to activate in response to the endogenous $Hb^d$. A similar phenomenon was recently reported for tolerized $CD8^+$ T cell that developed in the presence of cognate antigen and gained activity when transferred into irradiated, lymphopenic recipients (174). Given this scenario, both the n3.L2 and M2 T cells undergo homeostatic proliferation to fill the T cell niche. The presence of the $Hb^d$ antigen would enhance proliferation and generate a sufficient T cell population to amplify production of anti RBC antibodies by B cells and exacerbate disease. In the GAG system, CD8 T cells were retolerized when endogenous T cells returned (174). This could explain why induction of anemia fails in the $Hb^d$ $C\alpha^{+/+}$ recipients. In the presence of endogenous T cells, including $T_{regs}$, the transferred transgenic CD4 T cells would be unable to proliferate either through

competition for proinflammatory signals or the presence of suppressive ones. While both n3.L2 and M2 T cells perpetuate anemia, the M2 T cells have a delay in both detection of anti RBC antibodies and in eventual death of recipients (Figure 3.16). Since the n3.L2 T cells are fully functional when isolated from the transgenic mouse, it seems the M2 T cells require two additional days to recover from their tolerized state and respond to the endogenous $Hb^d$. It was not determined if there are additional differences in the phenotype or course of disease development.

*CDR1α of M2 stabilizes the TCR to maintain activation despite mutations in the MHCIIα chain*

We wanted to begin to understand the structural basis for how changing the $k_{on}$ for TCR:pMHC could result in the dramatic changes seen in the M2 CD4 population. The CDR1 loop can interact with the MHC molecule, sometimes without directly contacting the peptide itself. Changes in the CDR1α loop could alter the orientation or direct interactions between TCR:pMHC. We used a set of mutant I-$E^k$ dimers, each containing a single amino acid substitution at a potential TCR contact site, to measure changes in the TCR:pMHCII binding footprint (164). Mutant I-$E^k$ dimers were loaded with Hb(64-76) peptide and used to stimulate IL-2 production by the n3.L2 and M2 hybridomas. Mutations that completely inhibited IL-2 production (> 80% reduction) were considered critical for the TCR:pMHCII interaction. All 3 mutations in the MHCIIβ chain completely inhibited IL-2 secretion for both n3.L2 and M2 hybridomas (Figure 3.17) suggesting interactions with the MHCIIβ are highly specific and critical for formation of the TCR:pMHCII complex. The n3.L2 hybridomas failed to recognize α53, α55, and α57

mutations, indicating these MHCIIα residues are critical for the n3.L2 interaction (Figure 3.17). Interestingly, M2 hybridomas maintained stimulation by all MHCIIα chain mutants. Therefore the n3.L2 TCR contact with the MHCIIα mutants was below the threshold for IL-2 production while the M2 CDR1α mutations maintained sufficient affinity to overcome the activation threshold. It is unclear whether the enhanced affinity dictated by CDR1α is directly through generation of new contacts or through enhanced interactions with key amino acid residues.

**Discussion**

The role of $k_{on}$ in influencing signaling outcomes of specific TCR:pMHC interactions has previously been suggested but not directly determined. Ours is the first system to measure the effect of specifically changing the $k_{on}$ *in vitro* and *in vivo*, without compensatory changes in $k_{off}$. Here we show that an increased $k_{on}$ significantly affects T cell selection and activation. The M2 TCR has a 3.7 fold higher affinity for Hb(64-76)/I-$E^k$ than n3.L2 due to a faster $k_{on}$. As a consequence, signaling through the transgenic TCR is stronger in M2 DP thymocytes, indicated by higher CD5 levels and increased CD69 upregulation than on n3.L2 thymocytes. Because of a higher affinity for endogenous pMHCII, M2 thymocytes are subjected to increased negative selection. In the M2 $Rag^{+/+}$ mouse, the M2 CD4 T cells proliferate early after activation but fail to sustain the response. When these T cells are restricted to selection on the transgenic TCR, the few CD4 cells that escape negative selection in M2 $Rag1^{-/-}$ mice are hyporesponsive to Hb(64-76)/I-$E^k$ stimulation. Similarly M2 and n3.L2 CD4 T cells differ in the pattern

of $Ca2^{+}$ flux, suggesting that the difference in selection of M2 and n3.L2 T cells in the thymus alters signaling downstream of the TCR in the periphery. When $Hb^{d}$ is presented as an endogenous antigen, M2 expressing CD4 T cells are completely deleted by negative selection whereas a small population of n3.L2 cells escape to the periphery and cause autoimmune disease. The difference in selection and activation of M2 cells is likely a consequence of either new or enhanced contacts with the MHCII, as a result of the CDR1α mutations that drive M2's faster $k_{on}$ and an overall stronger affinity for MHCII.

It remains to be seen if $k_{on}$ merely fine-tunes TCR recognition of pMHC, potentially optimizing signaling through the TCR, or if altering $k_{on}$ affects generation of T cell effector and memory cells in the periphery. By increasing $k_{on}$, we generated a T cell that is tolerized to the point of anergy due to increased recognition of pMHCII. While this phenotype is not unique, it is unclear how a faster $k_{on}$ induces anergy. What is unique about our system is that the M2 TCR has a higher affinity due to two amino acid changes in the CDR1α loop. The CDR3 loops interact with the peptide, conferring the cross-reactive property of T cells, and therefore have been the main focus in determining what makes a T cell potentially autoreactive (37, 38, 175). With M2, mutations in the CDR1α loop not only generate a higher affinity TCR (29) but also regulate activation through the TCR. The stability of the TCR or the TCR:pMHC complex conferred by the CDR1α mutations may maintain an affinity closer to the threshold for T cell activation. As a result, M2 T cells can potentially recognize a larger number of selecting peptides in the thymus. While the CDR1α loop is very flexible (33), we cannot determine if changes in peptide fine specificity are due to greater flexibility or merely the result of stronger affinity interactions.

The increased level of negative selection of M2 cells may be a consequence of broader recognition of selecting peptides or stronger interactions with self-peptides that select n3.L2. By increasing the affinity of the TCR for self pMHC complexes, peptides which were low affinity, inducing positive selection, would have high enough affinity to overcome the threshold for negative selection. Therefore, the CDR1α mutations that increased the $k_{on}$ for the M2 TCR may in fact be generating a TCR with stronger recognition of MHCII in the thymus. While we were unable to identify a positively selecting peptide, this does not disprove M2's higher affinity for endogenous pMHCII, as positively selecting peptides are highly specific and do not reflect the structural features of agonists (70, 73-75). High affinity TCRs that escape negative selection are potentially selected using different binding conformations from those used for recognition of antigen in the periphery (38). Inherent TCR flexibility is an effective mechanism for generating a sufficient T cell repertoire to target infections and tumors but can go awry generating autoimmunity (10, 21).

As a mechanism to prevent autoimmune disease, high affinity TCRs can be tolerized, leaving a population of autoreactive T cells unresponsive to agonist stimuli. M2 T cells develop in an environment lacking the $Hb^d$ agonist peptide and do not respond to $Hb^s$ stimulation (data not shown), both indicators that M2 (and n3.L2) T cells are unlikely to become autoreactive in the transgenic mouse. Even so, the TCR high population is deleted from the M2 $Rag^{+/+}$ mouse presumably due to increased negative selection. Those cells that escape negative selection in the M2 $Rag1^{-/-}$ mice are anergized in the periphery. Since M2 T cells are not above physiological affinity for pMHCII, the 4μM affinity may reflect a maximal level of CD4 responsiveness, as has been seen with CD8 cells (176).

Weak agonist TCR:pMHC interactions, such as is measured with some APLs, often result in incomplete T cell activation and induction of anergy (5, 6, 8, 110, 131, 133). Rechallenge with an agonist after anergy induction by APL stimulation leads to an inability to proliferate but restored IL-2 production both *in vitro* and *in vivo* (124). M2 T cells that escape negative selection following selection by a weakly stimulatory peptide would be hyporesponsive when exposed to Hb(64-76) agonist. Early signaling events downstream of the hyporesponsive M2 TCR may be insufficient to trigger full IL-2 production and proliferation, as has been seen with cytolytic activity of CD8 T cells (177), but maintain early signaling events such as $Ca^{2+}$ (108, 110). The developmental programming imposed on these cells in the thymus leads to an altered and attenuated response, despite the sufficient affinity for full activation by an agonist peptide.

The signaling program downstream of the TCR is clearly different between n3.L2 and M2 CD4 T cells. Upon recognition of Hb(64-76)/I-$E^k$ the n3.L2 T cells can respond with full T cell activation leading to sustained $Ca^{2+}$ levels inducing strong IL-2 production and proliferation. M2 CD4 T cells produce low IL-2 and fail to proliferate 4 days after exposure to antigen. $Ca^{2+}$ is a critical second messenger of signal transduction in the T cell and the strength and sustained level of $Ca^{2+}$ signaling can differentially activate transcription factors (178). Interestingly, the pattern of intracellular $Ca^{2+}$ levels can regulate the induction of T cell anergy. A sustained $Ca^{2+}$ signal with low-level oscillations is required for NFAT dephosphorylation leading to transcription of cytokines such as IL-2 (179). Alternatively, tolerizing signals, such as in the absence of costimulation or due to ionomycin treatment, lead to unregulated increases in intracellular $Ca^{2+}$ and formation of NFAT homodimers which can induce transcription of proteins that

suppress IL-2 production and T cell proliferation leading to an anergic phenotype (180, 181). A similar genetic program could be induced with suboptimal stimulation, such as with an antagonist APL. The features of productive versus suppressive $Ca^{2+}$ signaling may reflect the differences between signals measured in n3.L2 and M2 CD4 T cells. Uncovering this level of genetic regulation during selection of the M2 T cells would give further credence to the role development plays in peripheral T cell response.

The optimized M2 TCR structure has a faster $k_{on}$ for binding Hb(64-76) I-$E^k$. The CDR1α region stabilizes the TCR with pMHC by contributing energetically to the overall complex as a result of contact with MHC or directly influencing the CDR3α contact with peptide (22, 32, 33). Since mutations on the I-$E^k$ α chain maintained sufficient interaction with M2 for IL-2 production but not n3.L2, the M2 CDR1α mutations may result in new or stronger contacts with the MHCII, decreasing the requirement for others. An altered binding footprint is unlikely, as structures of high affinity variants in the 2C system do not show altered footprints (182). Instead the faster $k_{on}$ of M2 binding pMHC may reflect an optimal conformation for association with MHC, maintaining affinity above the threshold for T cell activation with a broad range of peptides. A crystal structure of the M2: Hb/I-$E^k$ co-complex would identify the exact structural changes induced by the M2 CDR1α mutations. While the CDR1α mutations increase the $k_{on}$ for M2:Hb(64-76)/I-$E^k$, productive signaling through the TCR is dampened during T cell selection. Therefore, a strong affinity and sustained TCR:pMHC complex must be finely tuned, potentially by $k_{on}$, to produce a mature and responsive T cell.

**Figure 3.1 Characterization of the CD4 T cell populations in the periphery of n3.L2 and M2 Rag$^{+/+}$ TCR transgenic mice**

**A.** Flow cytometry analysis of populations in the spleen of n3.L2 (left) and M2 (right) Rag$^{+/+}$ TCR transgenic mice. The clonotypic antibody, CAb, was generated against the n3.L2 TCR and labels both n3.L2 and M2 expressing cells. Plots were gated on live lymphocytes. The percentage of specific transgenic CD4 (CAb$^{+}$ CD4$^{+}$) cells in the lymphocyte population is noted on each dot plot. Plots are representative of 10 mice. **B.** Overlays of CD4$^{+}$ CAb$^{+}$ populations shown in A in the spleen of representative n3.L2 (black) and M2 (histograms) mice.

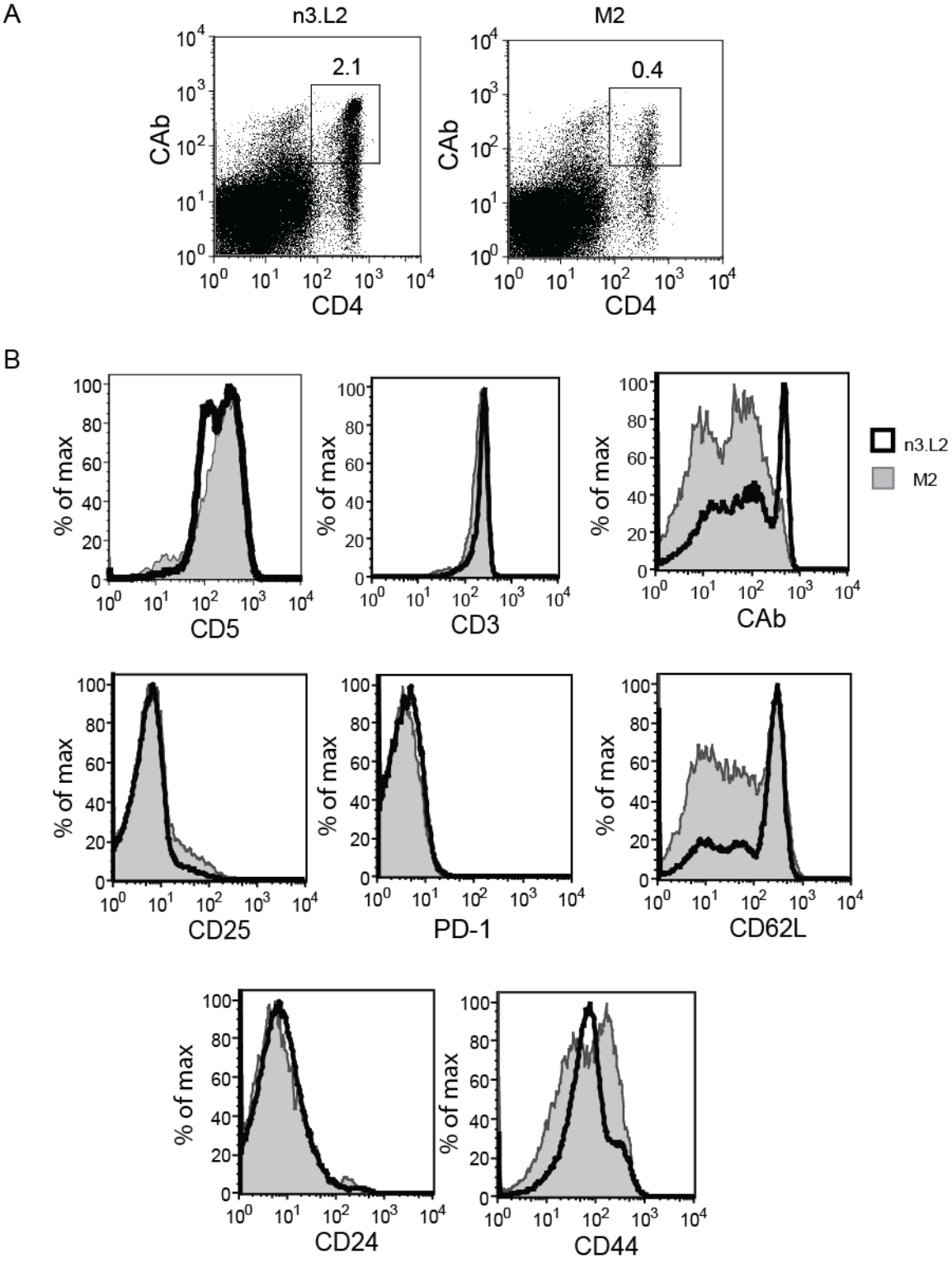


Figure 3.1. Characterization of the CD4 T cell populations in the periphery of n3.L2 and M2 Rag+/+ TCR transgenic mice

**Figure 3.2 Characterization of Rag$^{+/+}$ TCR transgenic thymus populations**

**A.** Labeling of representative thymus from age matched n3.L2 (left) and M2 (right) Rag$^{+/+}$ transgenic mice for CD4 and CD8 expression. Percentage of DN, DP, CD4 and CD8 SP populations are listed. n = 10 mice for each group. **B.** Analysis of the CD4 SP populations from A. Shown percentages are for CAb high and CAb low populations from n3.L2 (left) and M2 (right) mice. Representative overlays of surface levels of activation and selection markers are for the full CD4 SP population for n3.L2 (black histogram) and M2 (filled histogram). **C.** Analysis of DP thymocytes gated in A for the CAb populations shown in B, CD3 and CD69 for n3.L2 (black histogram) and M2 (filled histogram) mice.

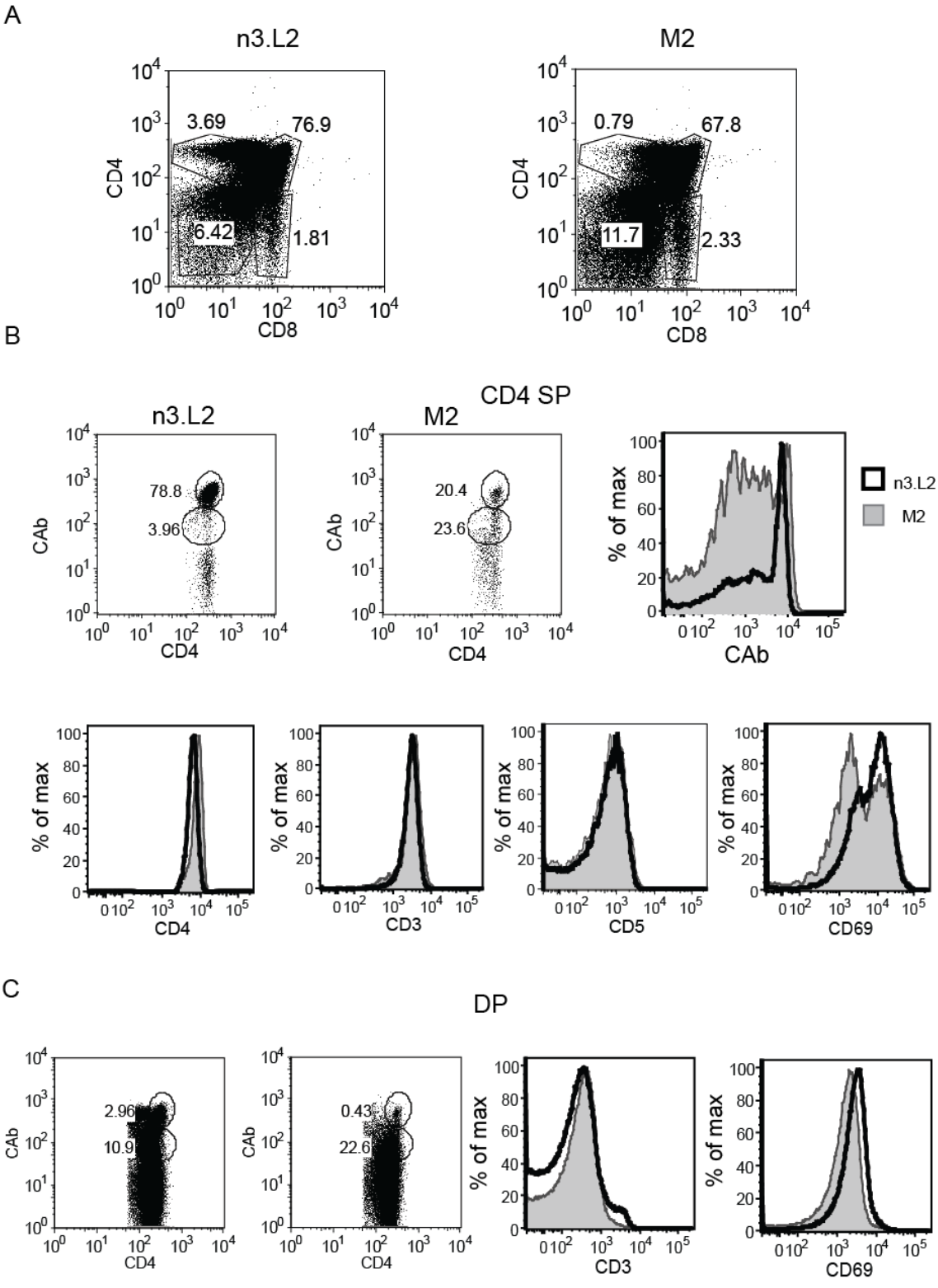


Figure 3.2. Characterization of Rag+/+ TCR transgenic thymus populations.

**Figure 3.3 Analysis of DN populations in the M2 Rag$^{+/+}$ transgenic mouse**

**A.** Characterization of DN populations shown in Figure 3.2A. Percentage of DN1, DN2, DN3 and DN4 populations are shown (top) for n3.L2 (left) and M2 (right) Rag$^{+/+}$ mice. Level of TCR expression, measured by CAb, on total DN cells is noted on bottom plots.

**B.** Overlay of TCRβ chain expression on DN cells from n3.L2 (black histogram) and M2 (filled histogram) mice.

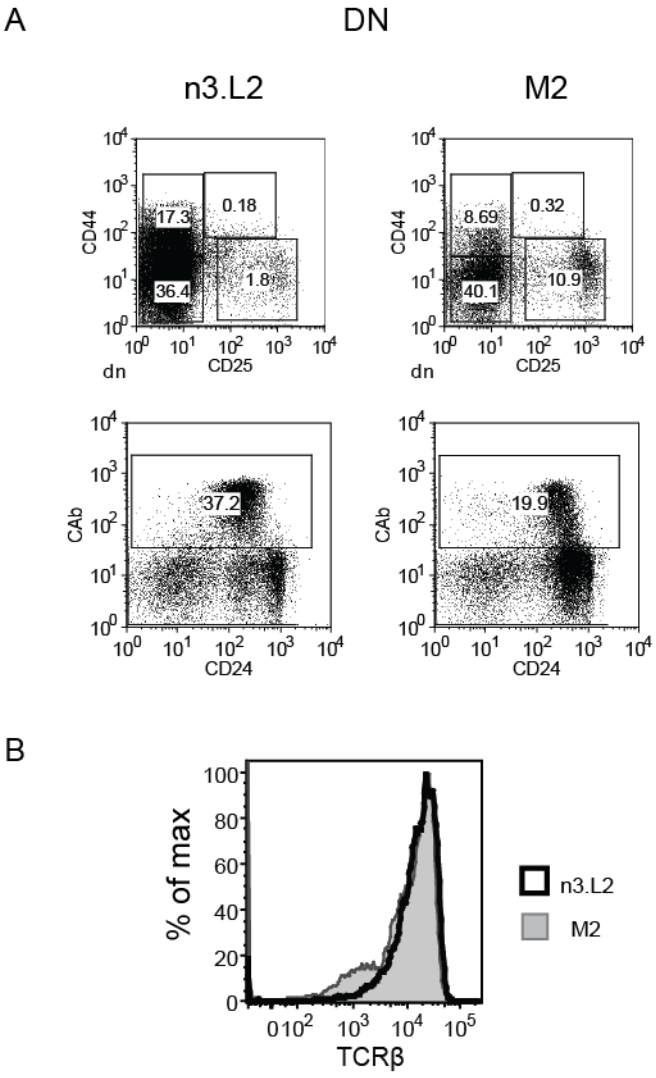


Figure 3.3 Analysis of DN populations in the M2 Rag+/+ transgenic mouse

**Figure 3.4 Characterization of the CD4 T cell populations in the periphery of n3.L2 and M2 Rag1$^{-/-}$ transgenic mice**

**A.** Flow cytometry analysis of the transgenic CD4 population in the spleens of age matched n3.L2 (left) and M2 (right) transgenic mice. CAb labels both n3.L2 and M2 expressing cells. Plots were gated on live lymphocytes. The percentage of specific transgenic CD4 (CAb$^{+}$ CD4$^{+}$) cells in the lymphocyte population is noted on each dot plot. Representative plots from 10 mice. **B.** Histogram overlays showing TCR, CD3, CD4 and maturation markers on naive cells from the spleen of n3.L2 (black line) and M2 (filled histogram) TCR transgenic mice. Splenocytes were gated on live lymphocytes followed by CAb$^{+}$ CD4$^{+}$ cells.

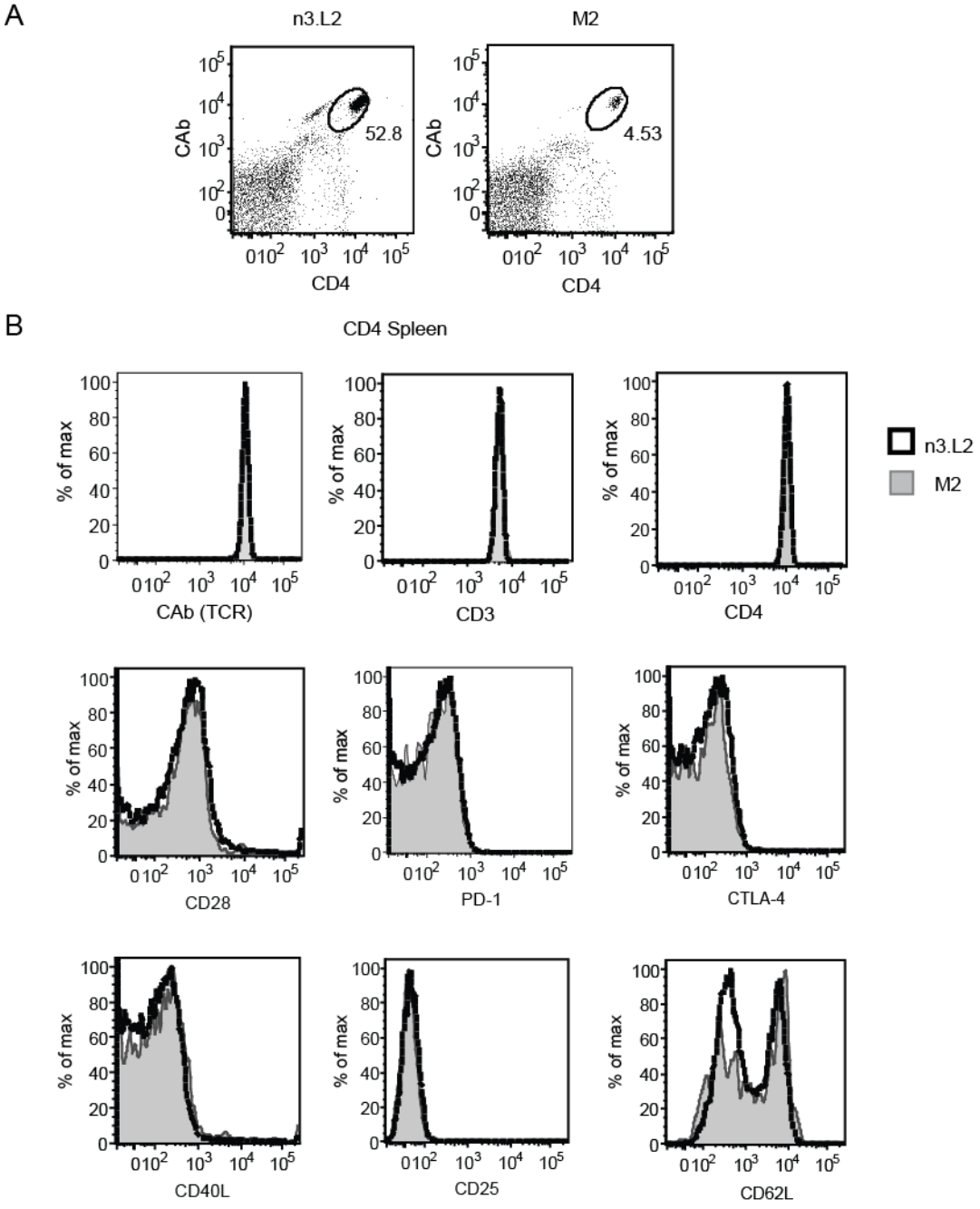


Figure 3.4. Characterization of the CD4 T cell populations in the periphery of n3.L2 and M2 Rag1-/- transgenic mice

**Figure 3.5 Characterization of thymocytes in n3.L2 and M2 Rag1$^{-/-}$ transgenic mice**

**A.** Labeling of representative thymus from age matched n3.L2 (left) and M2 (right) transgenic mice for CD4 and CD8 expression. Percentage of DN, DP, CD4 and CD8 SP populations are listed. n = 10 mice for each group. **B.** Overlays of TCR, CD3, CD4, CD25 and CD44 levels on gated n3.L2 (black line) and M2 (filled histogram) CD4 SP populations from panel A.

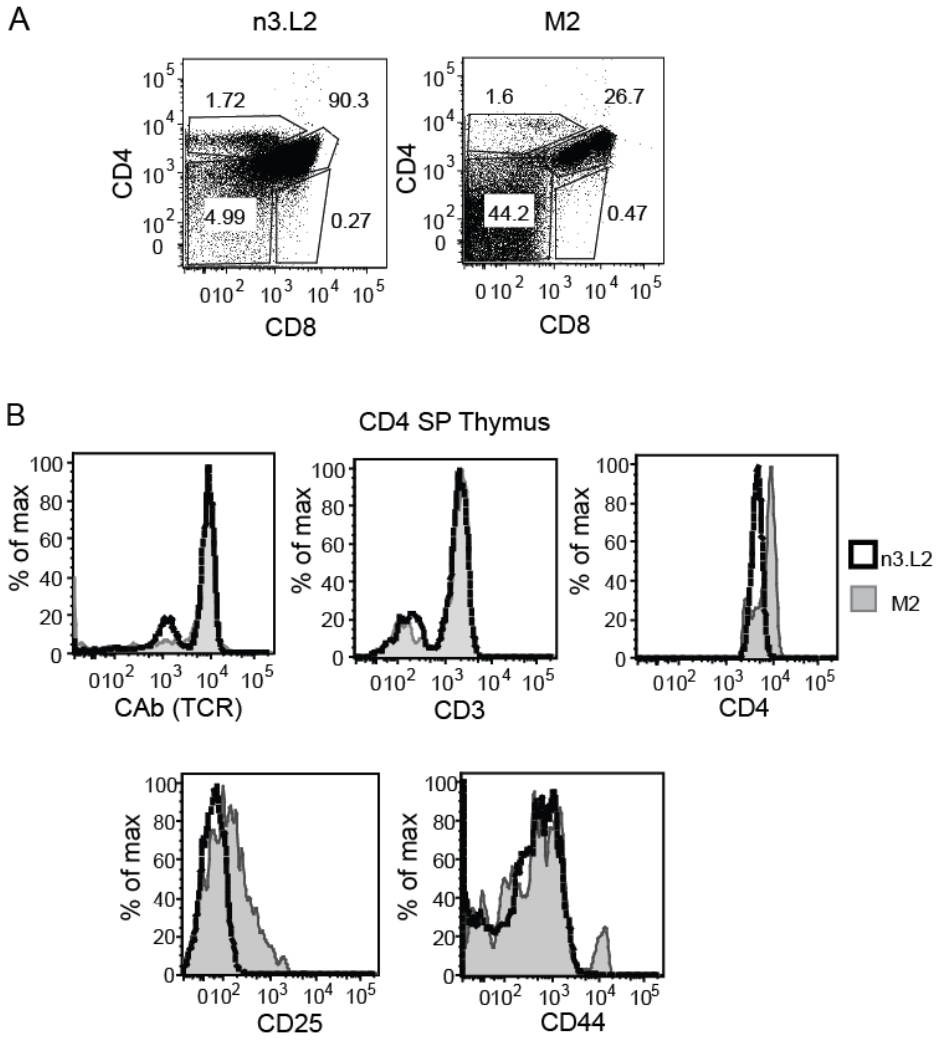


Figure 3.5. Characterization of thymocytes in n3.L2 and M2 Rag1-/- transgenic mice

**Figure 3.6 Development of alternative T cell populations in n3.L2 and M2 Rag1$^{-/-}$ mice**

Expression of FoxP3 in thymus and spleen CD4 cells. Plots were gated on CAb$^{+}$ CD4 SP cells and assayed for CD25 and FoxP3 levels. Gates were determined based on B6.K control populations, which have a normal $T_{reg}$ population. Representative plots from 5 mice in 3 independent experiments. The same gating scheme was used to measure the FoxP3$^{+}$ population in the spleen of the n3.L2 and M2 TCR transgenic mice. As no CD25$^{+}$ cells were identified, shown gates are for the FoxP3$^{+}$ population. Levels were equivalent to negative control labeling, indicating the few FoxP3 cells detected are due to non-specific antibody labeling. γδ T cells did not develop in the n3.L2 (black) or M2 (filled) transgenic mice, indicating the transgenic TCRs are specific for development of CD4$^{+}$ αβ T cells. Representative plots from 5 mice in 3 independent experiments.

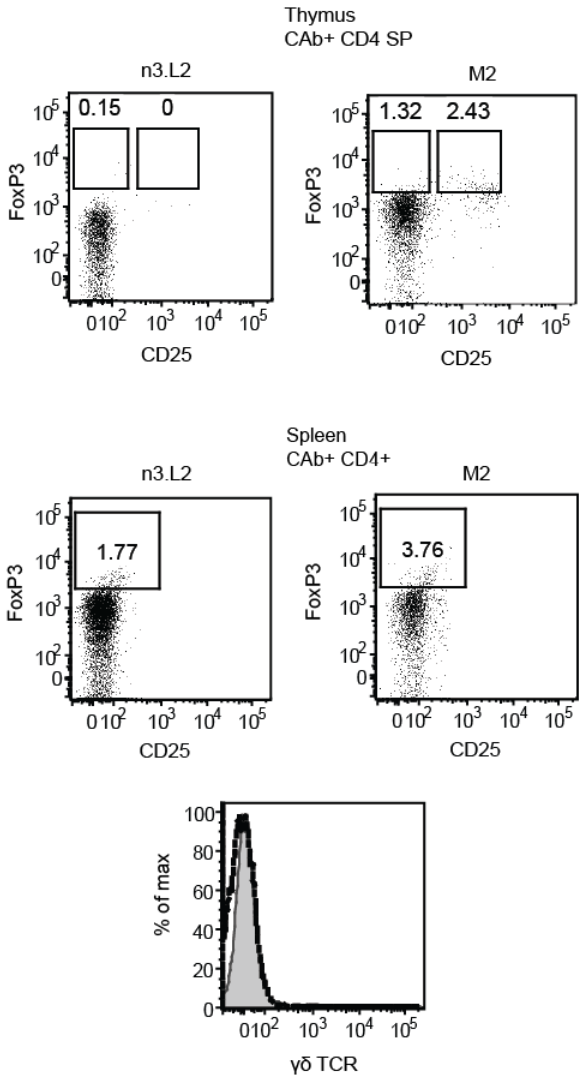


Figure 3.6. Development of alternative T cell populations in n3.L2 and M2 Rag1-/- mice

**Figure 3.7 TCRβ is expressed in n3.L2 and M2 Rag1$^{-/-}$ DN thymocytes**

**A.** Analysis of the DN population from the thymus plot and gating shown in Figure 3.5. The M2 TCR transgenic mouse had a large population of CD25$^{+}$ CD44$^{-}$ cells. **B.** Intracellular staining for the transgenic Vβ8.3 TCRβ chain. N3.L2 (black) and M2 (filled) DN cells expressed equivalent levels of Vβ8.3, though the population of TCRβ$^{+}$ cells was reduced in the M2 TCR transgenic mouse. The n3.L2 (black) and M2 (filled) CD4 SP populations all expressed high levels of the TCRβ chain. Representative plots from 5 mice in 3 independent experiments.

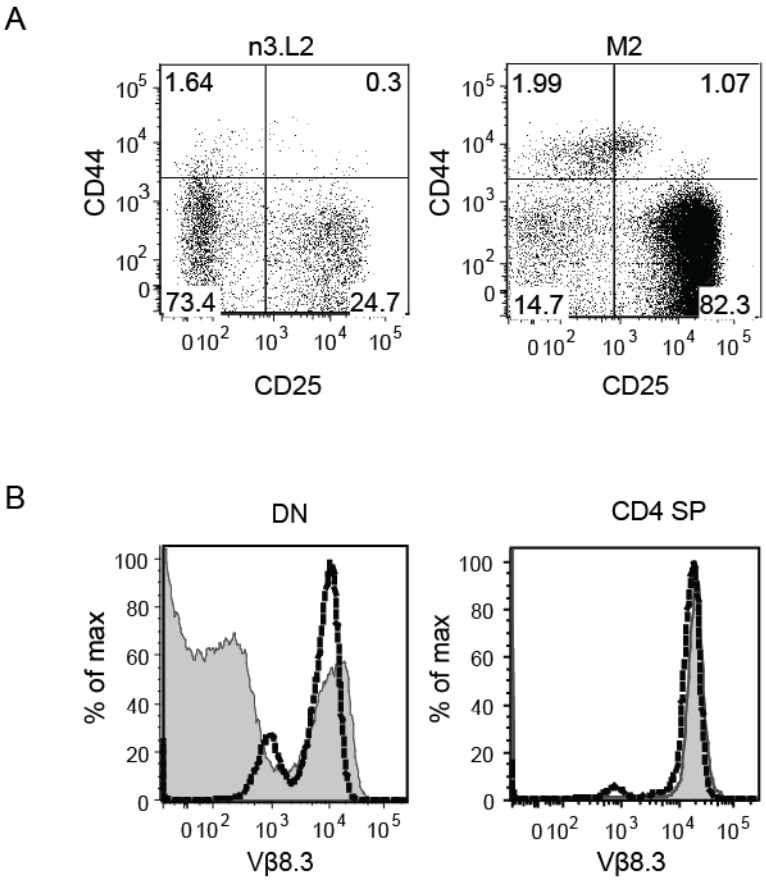


Figure 3.7. TCRβ is expressed in n3.L2 and M2 Rag-/- DN thymocytes

**Figure 3.8 M2 Rag$^{+/+}$ CD4 T cells proliferate 2 days after culture with Hb(64-76) but cannot sustain the proliferative response 4 days after culture**

**A.** CAb$^{+}$ CD4$^{+}$ cells isolated from n3.L2 (blue square) and M2 (green triangle) mice were cultured in triplicate overnight with irradiated B6.K splenocytes pulsed with indicated concentrations of purified Hb(64-76) peptide. Cultures were pulsed with 0.2μCi $^{3}$H and harvested 20 hours later. Dose curves are mean + SEM for 5 independent experiments. **B.** CAb$^{+}$ CD4$^{+}$ cells isolated from n3.L2 (blue square) and M2 (green triangle) mice were cultured with irradiated B6.K splenocytes pulsed with indicated concentrations of purified Hb(64-76) peptide for 72 hours. Cultures were pulsed with 0.2μCi $^{3}$H and harvested 20 hours later. Dose curves are representative mean + SEM for 2 independent experiments.

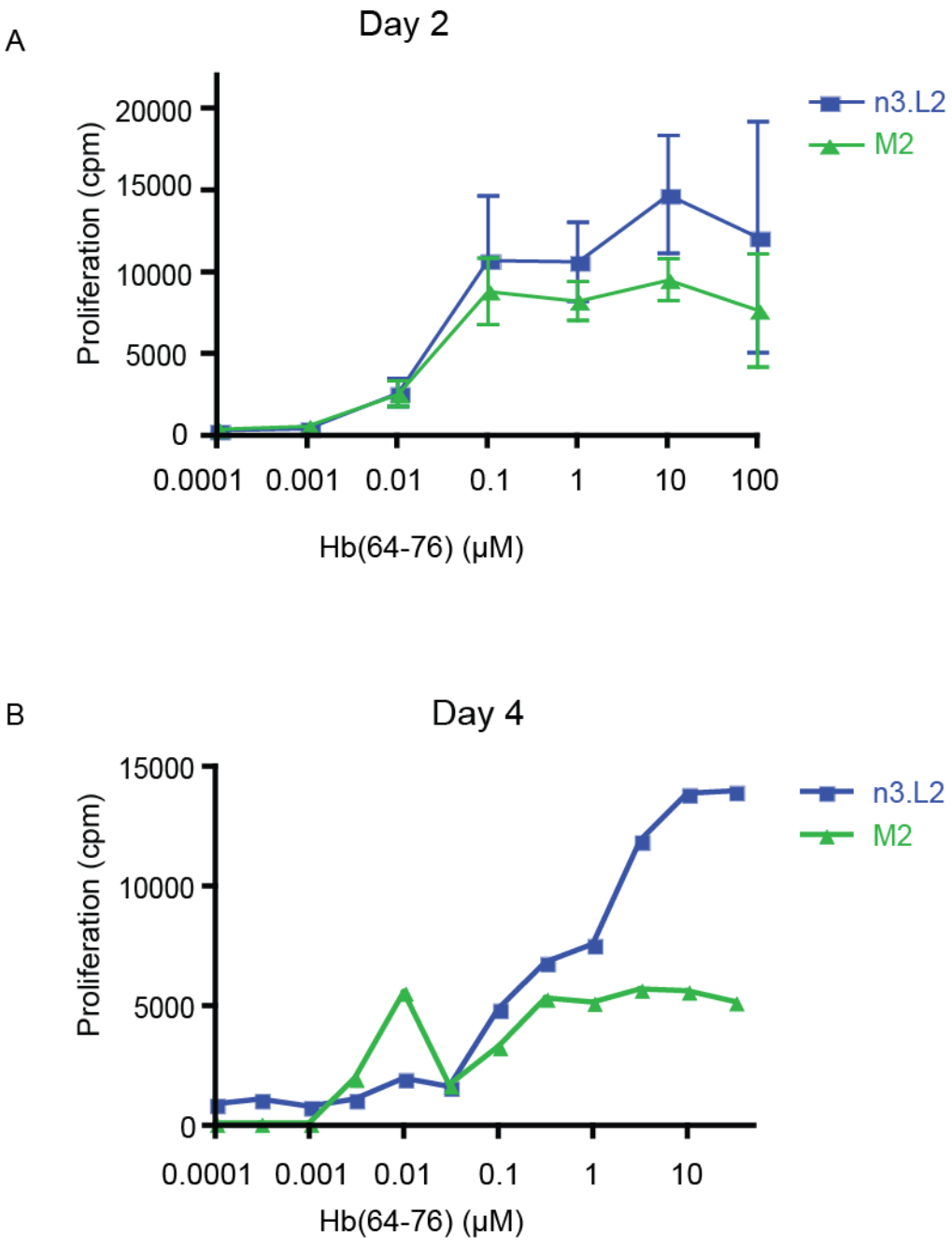


Figure 3.8. M2 Rag+/+ CD4 T cells proliferate 2 days after culture with Hb(64-76) but cannot sustain the proliferative response 4 days after culture

**Figure 3.9 M2 Rag1$^{-/-}$ T cells produce IL-2 but fail to proliferate in response to Hb(64-76)**

**A.** CAb$^{+}$ CD4$^{+}$ cells isolated from n3.L2 (blue square) and M2 (green triangle) Rag1$^{-/-}$ mice were cultured in triplicate overnight with irradiated B6.K splenocytes pulsed with indicated concentrations of purified Hb(64-76) peptide. After 18-20 hours, IL-2 production was assayed by ELISA. Dose curves are mean + SEM of triplicate samples from 3 independent experiments. **B.** The same cells assayed for IL-2 production in panel A were maintained in culture for 72 hours to measure proliferation of isolated n3.L2 (blue square) and M2 (green triangle) cells by $^{3}$H incorporation. Dose curves are mean + SEM of triplicate samples from 3 independent experiments.

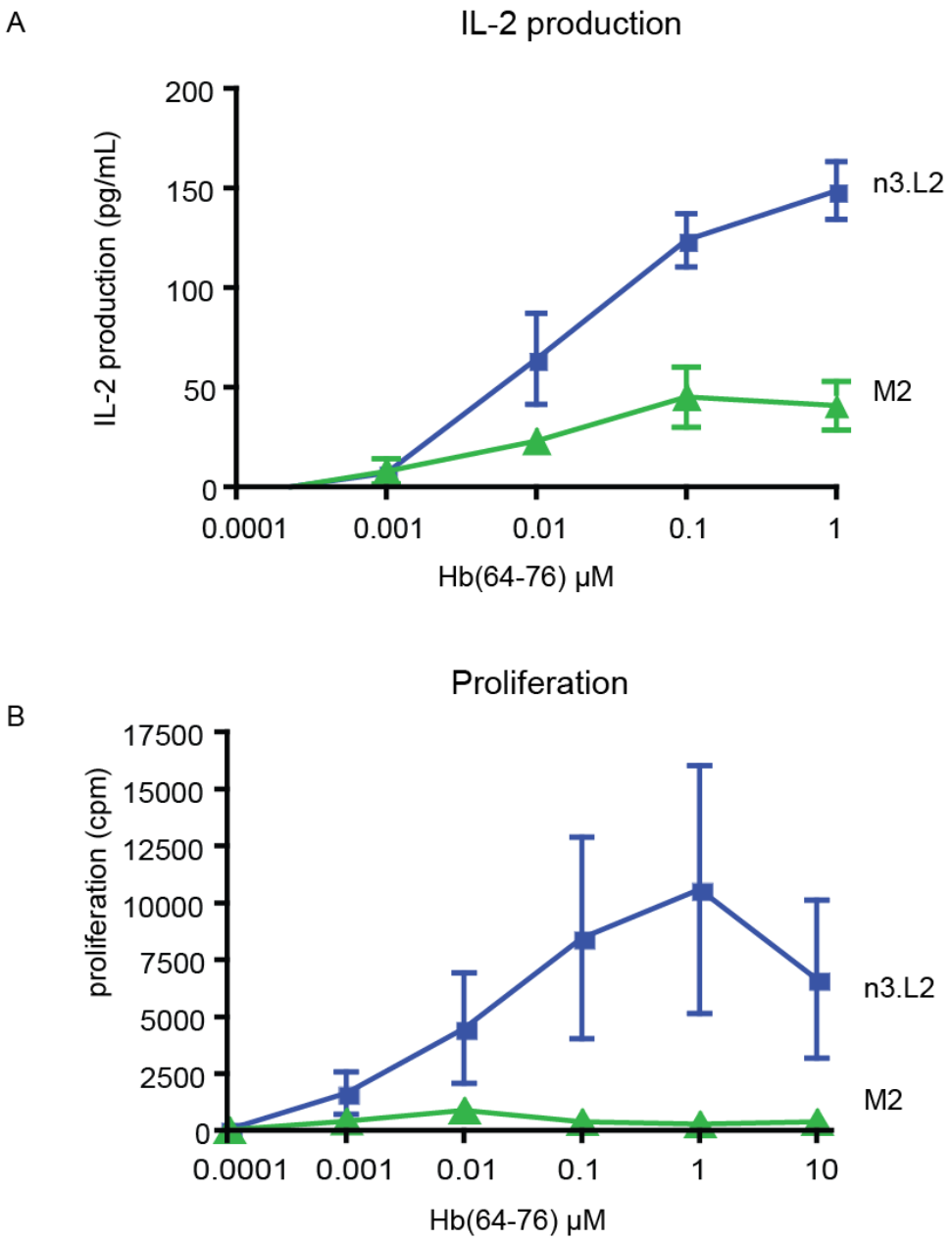


Figure 3.9. M2 Rag1-/- T cells produce IL-2 but fail to proliferate in response to Hb(64-76)

**Figure 3.10 $Ca^{2+}$ signal in $Rag^{+/+}$ CD4 T cells from n3.L2 and M2 mice differ in sustained level**

Isolated $CAb^{+}$ $CD4^{+}$ cells from n3.L2 and M2 $Rag^{+/+}$ mice were labeled with Fura-2 AM and imaged for $Ca^{2+}$ in response to Hb(64-76) or MCC loaded I-$E^{k}$ Ig dimers. Compiled results are from two independent experiments imaged in duplicate timelapses. Data were analyzed by identifying cell regions and measuring the peak (max) intensity of 340/380 ratio, average intensity post peak intensity, and oscillatory behavior (standard deviation from linear regression modeling of post peak intensities). n = 38 for n3.L2 response to 0.3μg/mL Hb (blue); n = 78 for M2 response to 0.3μg/mL Hb (green); n = 40 for response of n3.L2 and M2 to MCC.

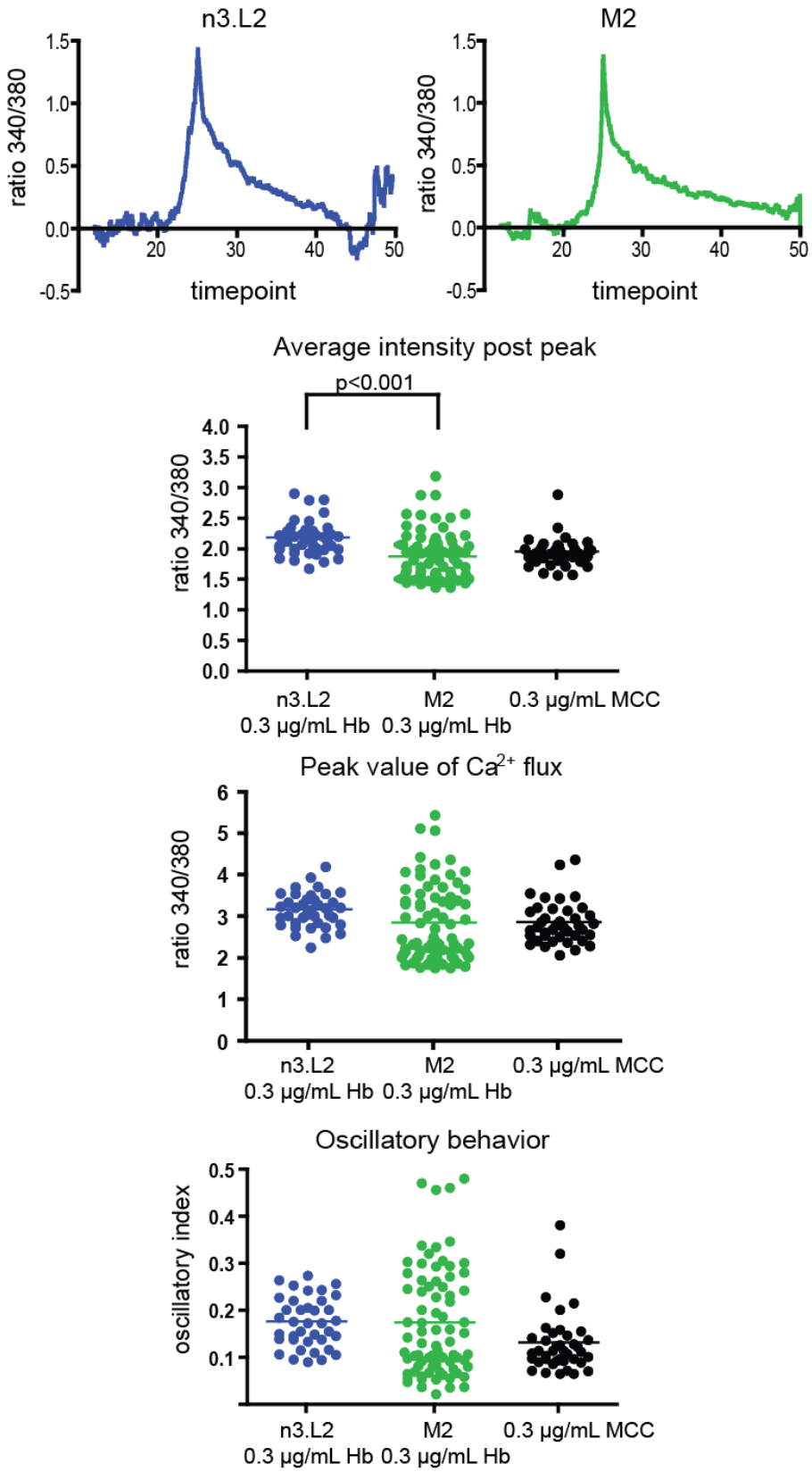


Figure 3.10. Ca2+ signal in Rag+/+ CD4 T cells from n3.L2 and M2 mice differ in sustained level

**Figure 3.11 $Ca^{2+}$ signal in $Rag1^{-/-}$ CD4 T cells from n3.L2 and M2 mice differ in oscillatory behavior**

Isolated $CAb^{+}$ $CD4^{+}$ cells from n3.L2 and M2 $Rag1^{-/-}$ mice were labeled with Fura-2 AM and imaged for $Ca^{2+}$ in response to Hb(64-76) or MCC loaded I-$E^{k}$ Ig dimers. Compiled results are from two independent experiments imaged in duplicate timelapses. Data were analyzed by identifying cell regions and measuring the peak (max) intensity of 340/380 ratio, average intensity post peak intensity, and oscillatory behavior (standard deviation from linear regression modeling of post peak intensities). n = 91 for n3.L2 response to 0.3μg/mL Hb (blue); n = 41 for M2 response to 0.3μg/mL Hb (green); n = 63 for response of n3.L2 and M2 to MCC.

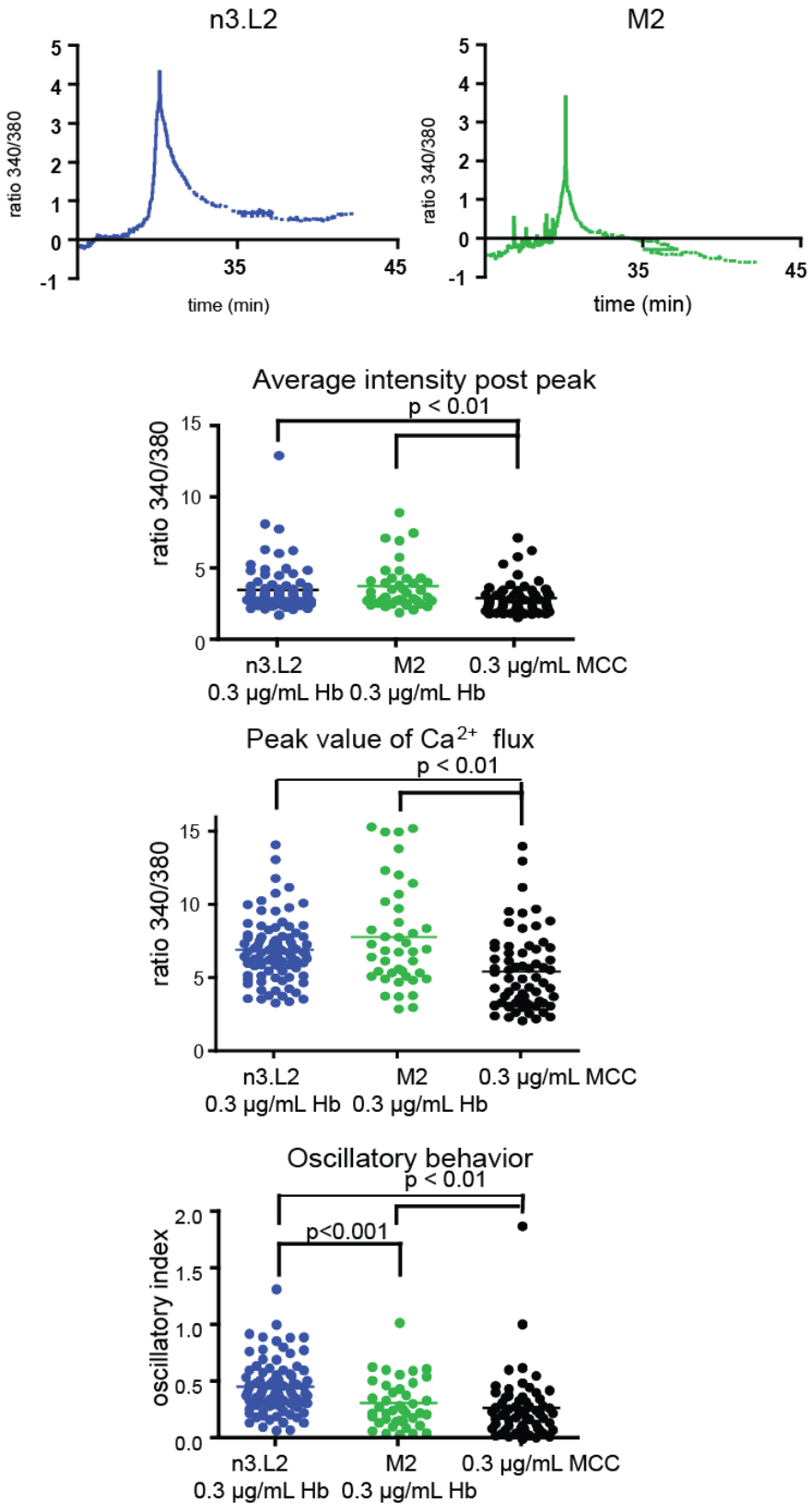


Figure 3.11. Ca2+ signal in Rag1-/- CD4 T cells from n3.L2 and M2 mice differ in oscillatory behavior

**Figure 3.12 M2 thymocytes sense stronger selecting signals**

**A.** Overlay of CD5 levels on CD4 SP populations gated in Figure 3.5 from n3.L2 (black line) and M2 (filled histogram) $Rag1^{-/-}$ transgenic mice. Representative plots from 10 mice. **B.** DP thymocytes isolated from n3.L2 (black) or M2 (grey) thymi were cultured for 18 hours with irradiated B6.K splenocytes. The mean + SEM percentage of DP cells that were $CD69^{+}$ is presented. p values determined by Student's t test. n = 11 from 5 independent experiments.

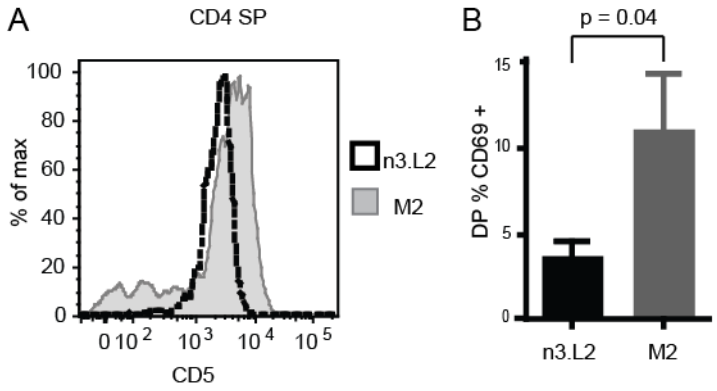


Figure 3.12. M2 thymocytes sense stronger selecting signals

**Figure 3.13 M2 T cells are negatively selected when exposed to endogenous $Hb^d$ and fail to induce anemia**

**A.** n3.L2 and M2 transgenic mice were crossed to congenic $Hb^d$ mice, which express the agonist $Hb^d$ (64-76) as a self-peptide. Thymi and spleens from the crosses were assessed for presence of $CAb^+$ $CD4^+$ cells. Percent $CAb^+$ $CD4^+$ shown for representative n3.L2, M2, n3.L2 x $Hb^d$, M2 x $Hb^d$, and transgenic negative $Hb^d$ littermate mice, aged 6 weeks. 6 n3.L2 x $Hb^d$ and 6 M2 x $Hb^d$ mice were characterized for development of transgenic T cells. **B.** n3.L2 x $Hb^d$ and M2 x $Hb^d$ mice were monitored for development of anemia by deposition of antibodies on RBC. Peripheral blood from 5 week old n3.L2 x $Hb^d$ (black line) and M2 x $Hb^d$ (filled histogram) mice was labeled with a PE-pan Ig antibody. Overlays show levels of anti-Ig on gated RBCs for 3 n3.L2 x $Hb^d$ and 3 M2 x $Hb^d$ mice.

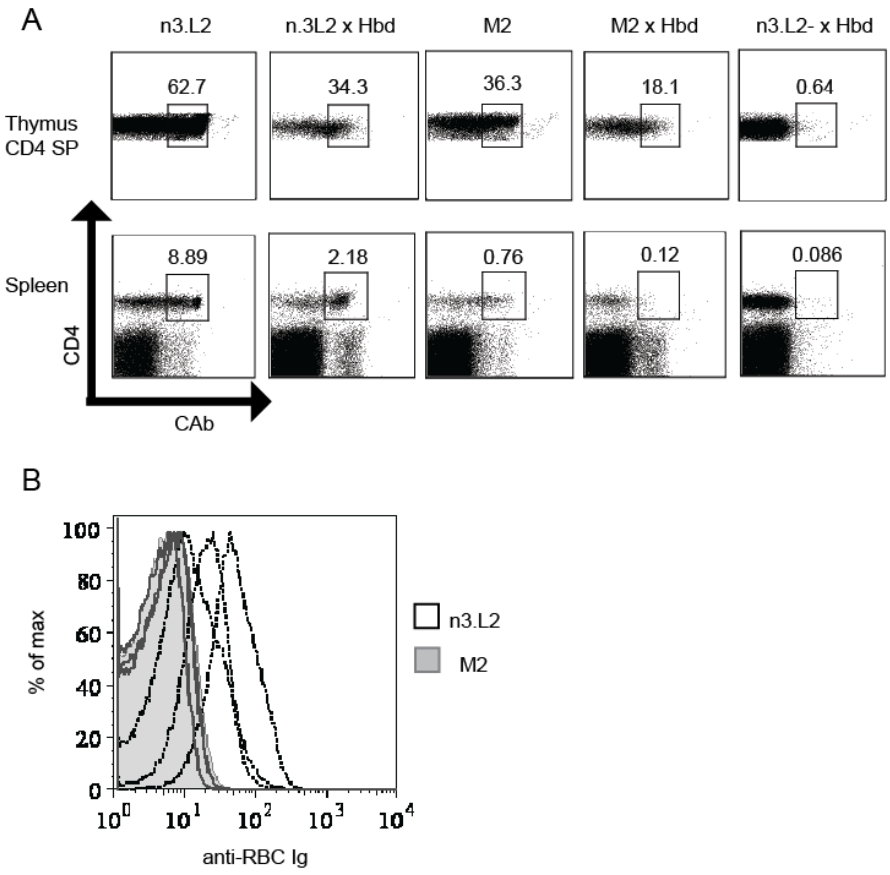


Figure 3.13. M2 T cells are negatively selected when exposed to endogenous Hbd and fail to induce anemia

**Figure 3.14 Chimerism in BMCMs using Rag$^{+/+}$ transgenic donor bone marrow**

Bone marrow chimeras were generated by transferring bone marrow isolated from n3.L2 Ly5.1 and M2 Thy1.1 Rag$^{+/+}$ transgenic mice into irradiated B6.K recipients. Bone marrow was mixed at a 1:1 ratio from the two transgenics or each transgenic and B6.K bone marrow as controls. After 8 weeks, chimeric mice were analyzed for development of transgenic populations in the thymus and spleen using the CAb antibody. From the CD4 population, both CAb high and CAb low populations developed. The contribution of n3.L2 and M2 progenitors to CAb populations is indicated in gates. Plots are representative of n = 9 n3.L2 x M2; n = 7 n3.L2 x B6.K; n = 5 M2 x B6.K made at 3 independent times.

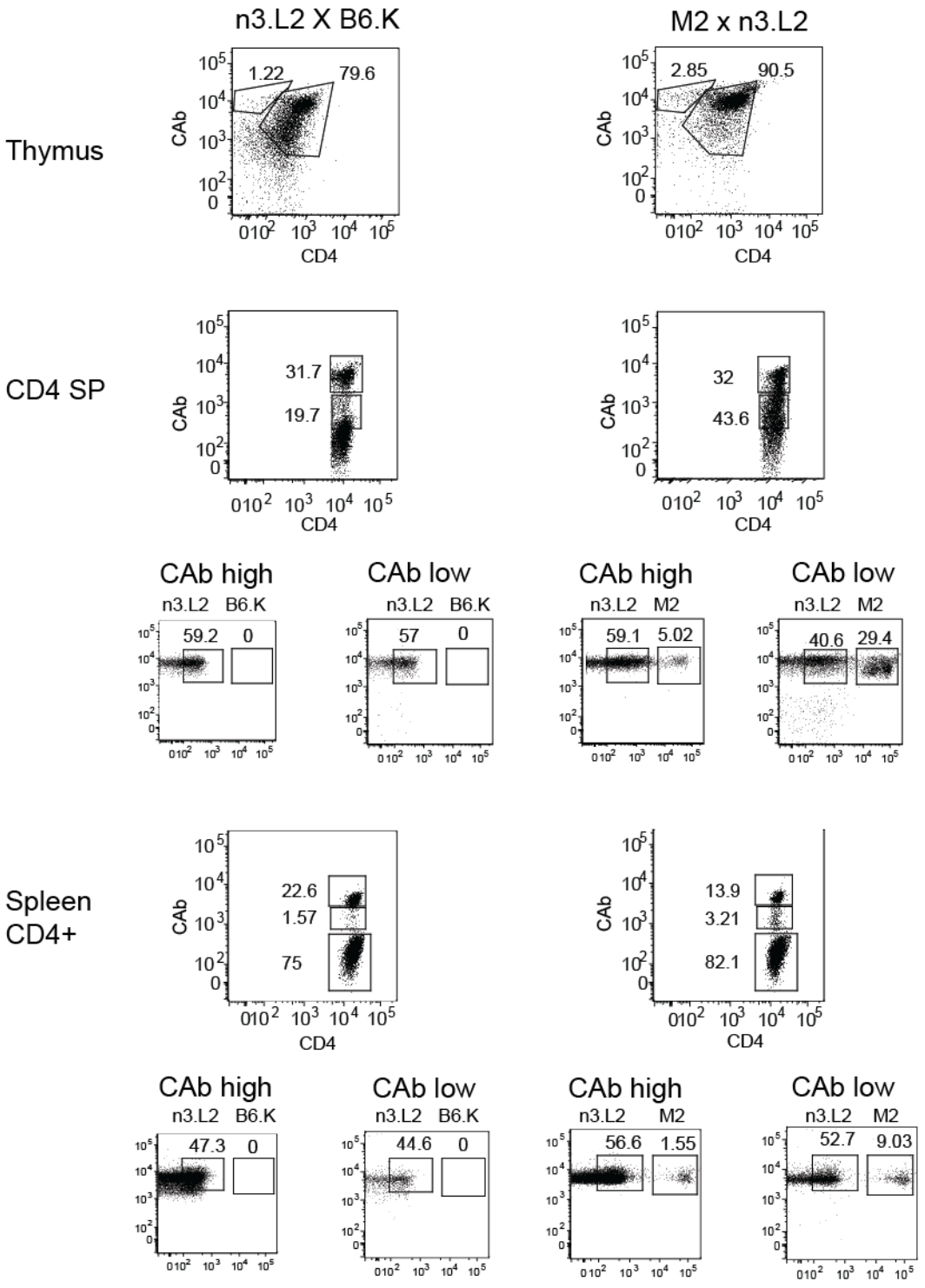


Figure 3.14 Chimerism in BMCMs using Rag+/+ transgenic donor bone marrow

**Figure 3.15 Chimerism in BMCMs using Rag1$^{-/-}$ transgenic donor bone marrow**

Bone marrow was isolated from n3.L2 Ly5.1 and M2 Thy1.1 Rag1$^{-/-}$ mice and mixed at a 1:1 ratio before being transferred into irradiated hosts. As a control, transgenic bone marrow was mixed with B6.K bone marrow. After 12 weeks, chimeric mice were analyzed for the development of CAb$^{+}$ transgenic populations in the thymus and spleen. For DP, CAb$^{+}$ CD4 SP, and splenic CAb$^{+}$ CD4 populations, the percent derived from n3.L2, M2, or B6.K bone marrow is indicated. Plots are representative of n = 16 n3.L2 x M2 mixed chimeras; n = 7 n3.L2 x B6.K; n = 9 M2 x B6.K made in 3 independent sets.

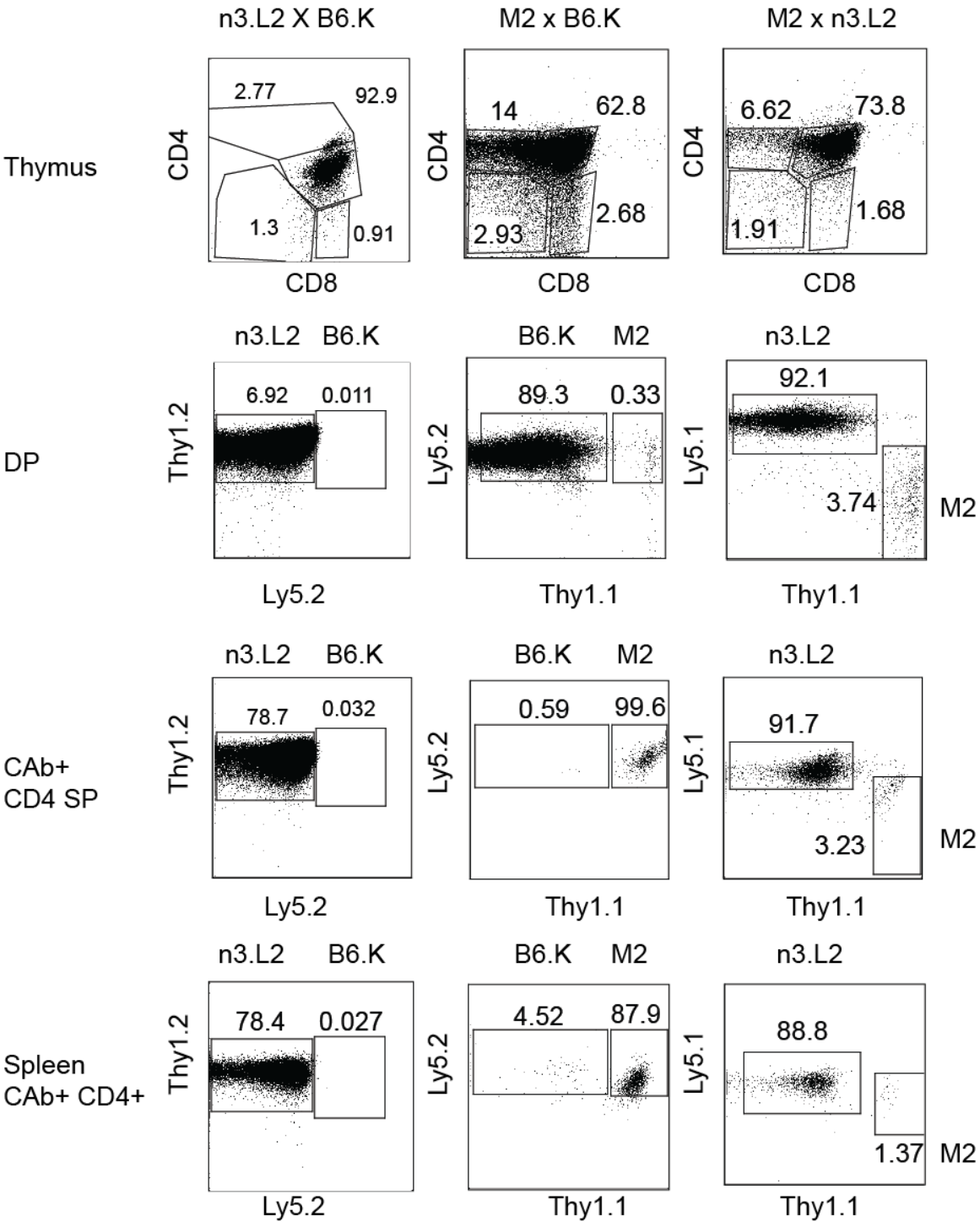


Figure 3.15 Chimerism in BMCMs using Rag-/- transgenic donor bone marrow

**Figure 3.16 $Hb^d$ $C\alpha^{-/-}$ mice succumb to anemia after transfer of n3.L2 or M2 CD4 T cells**

1 x $10^6$ isolated $CAb^+$ $CD4^+$ T cells from n3.L2 and M2 mice were transferred into $Hb^d$ $C\alpha^{-/-}$ mice. Mice were monitored for death due to development of anemia as a consequence of transferred cells. n = 15 for transfer of M2 cells; n = 14 for n3.L2. p =0.04 for log-rank test of survival curves.

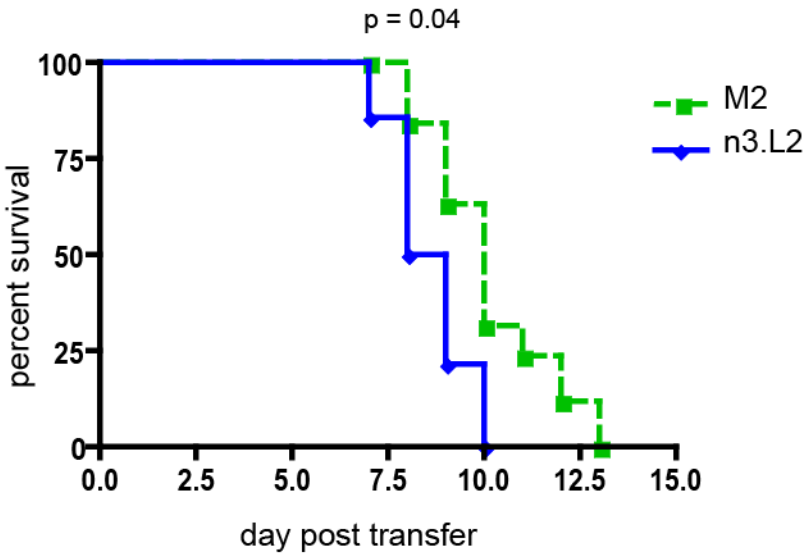


Figure 3.16. Hbd Cα-/- mice succumb to anemia after transfer of n3.L2 or M2 CD4 T cells

**Figure 3.17 Characterization of the footprint of n3.L2 and M2 binding Hb(64-76)/I-$E^k$**

Plate bound Hb-loaded mutant I-$E^k$ dimers were used to stimulate IL-2 production by n3.L2 and M2 hybridomas. We tested the response to 4 mutations in the I-$E^k$ α chain and 3 mutations in the I-$E^k$ β chain. MHC residues were considered critical if mutation at that position inhibited >80% of IL-2 production. Critical contact residues are highlighted by red circles on a surface model of the crystal structure of Hb bound to I-$E^k$ (Protein DataBank accession code, 1FNG). The MHCIIα mutation at position 64 did not alter IL-2 production by n3.L2 or M2 and is not indicated on the model. Green ovals represent the general contact area for TCR CDR1α loops, where the two amino acid differences between n3.L2 and M2 are located. Summarized results are based on 3 independent experiments.

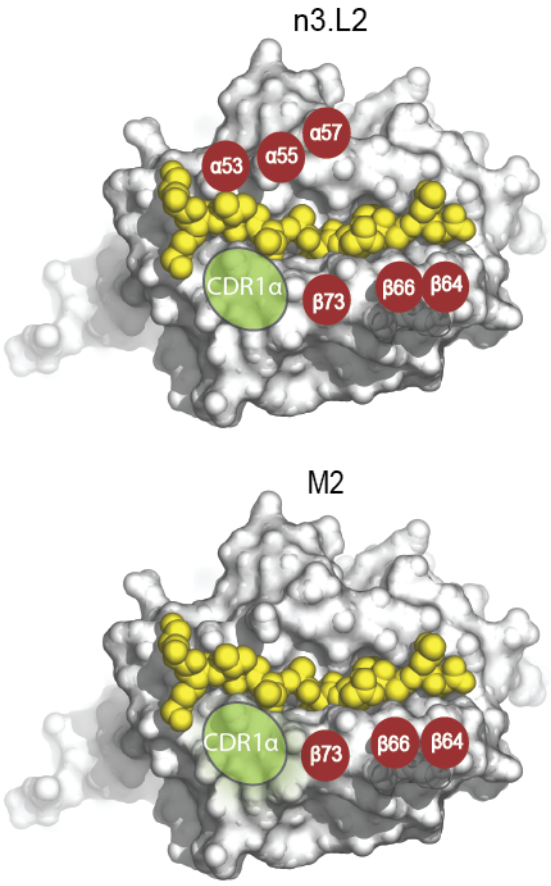


Figure 3.17. Characterization of the footprint of n3.L2 and M2 binding Hb(64-76)/I-Ek

**Table 3.1 Percentage of populations in the thymus and periphery of TCR transgenic mice**

Compilation of thymus and spleen populations in the n3.L2 and M2 transgenic mice. Plots were gated as in Figures 3.1-3.5 and percentages of each population were recorded. Shown is mean + SEM. p values determined by T-test comparing each population in the n3.L2 and M2 mice. n = 6 for n3.L2 $Rag^{+/+}$; n = 14 for n3.L2 $Rag1^{-/-}$; n = 11 for M2 $Rag^{+/+}$; n = 16 for M2 $Rag1^{-/-}$

| | total thymus | cd4 sp % | cd8 sp% | dp % | dn% | total spleen | cd4 sp % |
|---|---|---|---|---|---|---|---|
| **n3.L2 Rag+/+** | 110.8+61.93 | 6.893+7.54 | 3.075+1.558 | 73.37+10.15 | 6.555+4.77 | 140+45.35 | 7.528+3.623 |
| **M2 Rag+/+** | 74.24+25.58 | 3.585+3.51 | 2.909+1.837 | 75.61+13.09 | 8.985+8.979 | 118.8+29.45 | 1.935+0.98 |
| | p = 0.103 | p = 0.50 | p = 0.773 | p = 0.0149 | p = 0.0311 | p = 0.39 | p = 0.0027 |
| **n3.L2 Rag1-/-** | 218.7+62.92 | 2.059+2.14 | 0.4548+.386 | 84.41+12.28 | 8.116+10.53 | 68.51+55.99 | 20.41+13.85 |
| **M2 Rag1-/-** | 15.96+10.72 | 8.445+16.65 | 1.038+1.4 | 24.55+13.61 | 34.92+20.47 | 62.36+29.95 | 7.995+11.61 |
| | p < 0.0001 | p = 0.138 | p = 0.216 | p < 0.0001 | p = 0.0001 | p = 0.754 | p = 0.0063 |

Table 3.1. Percentage of populations in the thymus and periphery of TCR transgenic mice

**Table 3.2 Percentage of cell populations in bone marrow chimeras developing from n3.L2 and M2 Rag1$^{-/-}$ bone marrow**

Percentage of thymic and spleen populations derived from n3.L2 or M2 Rag1$^{-/-}$ bone marrow in chimeras after 12 weeks. Populations were gated as in Figure 3.15. n = 16 for n3.L2 x M2 mixed chimeras; n = 7 n3.L2 x B6.K; n = 9 M2 x B6.K. p values determined by Student's T test comparing the mixed and single transgenic chimera percentages.

| | %CD4 thymus | %DP thymus | SP/DP ratio | %CD4 spleen |
|---|---|---|---|---|
| **n3.L2 mixed** | 52.44+12.22 | 61.77+8.57 | 0.829+0.159 | 74.84+7.66 |
| **n3.L2 only** | 70.46+5.56 | 31.22+14.87 | 5.67+2.34 | 63.23+15.81 |
| | p = 0.268 | p = 0.086 | p = 0.0324 | p = 0.463 |
| **M2 mixed** | 26.7+15.07 | 1.67+0.46 | 1.78+0.456 | 5.84+2.51 |
| **M2 only** | 52.63+15.78 | 31.81+14.27 | 2.27+1.57 | 63.91+11.37 |
| | p = 0.26 | p = 0.042 | p = 0.75 | p < 0.0001 |

Table 3.2. Percentage of cell populations in bone marrow chimeras developing from n3.L2 and M2 Rag-/- bone marrow

# CHAPTER 4

# Future Directions

*Selection by antagonist and weak agonist APLs may alter signaling downstream of the TCR and dampen the peripheral T cell response*

M2 thymocytes had increased reactivity to APLs and self-peptides during selection, resulting in negative selection of M2 T cells. The most logical explanation is that the M2 TCR had a stronger affinity for self pMHC expressed on thymic epithelial cells as a consequence of a faster rate of association with pMHC. In the case of the M2 x $Hb^d$ mice, transgenic T cell development may be skewed by the high level of agonist antigen in the thymus, exacerbating the level of negative selection by other endogenous peptides alone. This system cannot differentiate between the signals from the high affinity of one TCR:$Hb^d$ interaction versus integration of signals from multiple, different TCR:pMHC interactions, an important distinction when evaluating a kinetic model for T cell selection. Decreasing the amount of $Hb^d$ available to developing TCRs by further crossing the M2 x $Hb^d$ mice to B6.K would identify if the high level of negative selection is a consequence of the small M2 population or due specifically to the kinetics of TCR:$Hb^d$/I-$E^k$ interaction, as has previously been suggested (78).

Based on the function of peripheral M2 CD4 T cells and the increased thymocyte sensitivity to APLs and endogenous peptides, the developmental skewing of M2 T cells is most likely the consequence of exposure to an antagonist ligand in the thymus. While antagonists in the periphery will dampen a specific response to agonist antigen, in the thymus these same APLs can be recognized as selecting peptides. Previously, mice were generated that expressed membrane bound Hb(64-76) APLs in addition to endogenous peptides (78, 154, 183). These APL transgenic mice were used to identify the strength of selecting peptides in the thymus when crossed to the n3.L2 TCR transgenic mouse. The

same APL mice crossed to M2 would highlight differences in the selection of these two T cells. For instance, Q72, a null peptide in the periphery, enhanced positive selection of n3.L2 CD4 T cells whereas A72, an antagonist, induced negative selection and E72, another null peptide, had no effect (78). Given the pattern of APL activation in the periphery and with DP thymocytes, we would predict that M2 T cells might undergo negative selection by Q72 and potentially positive selection by E72. These transgenic mice would provide further insight into the relationship between affinity and selecting endogenous peptides. Interestingly, n3.L2 T cells that developed in the presence of A72 failed to proliferate *in vivo* but did respond to wildtype Hb(64-76) *ex vivo* (154, 183). While this confirms the role of A72 as an antagonist for n3.L2, it suggests that induction of anergy in M2 T cells may reflect more than just an increased affinity for APLs. Interestingly, n3.L2 T cells that developed in the presence of I72, a weaker antagonist, failed to proliferate upon exposure to wildtype Hb(64-76) but did produce IL-2 (124), potentially mimicking the profile of M2 CD4 T cells. A selecting peptide does not have to be an antagonist to alter the responsiveness of T cells in the periphery. Selection by a weak agonist can decrease cytokine production and cytolytic activity by CD8 T cells in response to the selecting ligand (184). Therefore, the affinity of a TCR for pMHC in the thymus does fine tune T cell responsiveness in the periphery. Crossing the M2 transgenic mouse to the APL mice would provide a way to directly test whether antagonism in the thymus results in anergy or just further antagonism in the periphery. Should M2 T cells be anergic after selection by A72 or I72, the difference between n3.L2 and M2 T cells may be a consequence of signaling changes downstream of the TCR.

In addition to examining the amount and nature of selecting peptides, the signaling regulation between positive and negative selection has not been compared for n3.L2 and M2 thymocytes. The affinity threshold between a positively selecting and negatively selecting peptide is very small, only a 1.2 fold difference (67), but the accumulation of signals downstream of the TCR differs (185). Lck is thought to be present in a consitutively active state (186). Upon binding of the TCR, Lck is recruited to the TCR:pMHC complex via coreceptor engagement and then phosphorylates ITAMs on the CD3ζ chains. While CD4 T cells are less dependent on the coreceptor for enhancing activation (81), selection of M2 and n3.L2 T cells may differ as a result of changes in early signaling downstream of the TCR. Since negatively selecting peptides induce faster and higher accumulation of Lck (187), M2 may recruit more Lck following stimulation with self pMHC because of a faster $k_{on}$. Higher levels of CD3ζ phosphorylation recruit high levels of ZAP-70 (188). As a consequence, the pattern of ZAP-70 phosphorylation changes, inducing negative selection due to enhanced activity (76). Interestingly, mutation of ZAP-70, inhibiting its activation, skews both positive and negative selection of T cells, resulting in failure to eliminate autoreactive T cells (189). Since development of M2 and n3.L2 was restricted in the $Rag1^{-/-}$ mice, the levels of ZAP-70 would not be decreased by expression of a secondary TCR. However, the fast $k_{on}$ for M2 binding pMHC may result in more or differential phosphorylation of ZAP-70, something that can easily be tested by western blot of thymocyte populations. The activation state of ZAP-70 leads to a specific pattern of $Ca^{2+}$ and ERK signaling, and pERK localization that results in negative selection (67). High levels of pERK are only induced with strong peptide stimulation. Isolated n3.L2 and M2 DP thymocytes can be imaged for $Ca^{2+}$ flux using

Fura-2 AM, as was done with peripheral T cells. pERK can be measured in a flow cytometry assay using fluo-4 AM. The pattern of $Ca^{2+}$ and pERK may give a clue as to how negative selection in the thymus sets anergy in peripheral T cells. Transient ERK phosphorylation may be regulated by the activation of Ras. Cellular and theoretical studies have identified that positively selecting ligands activate Ras by Ras-GRP (67, 87). When a high affinity TCR:pMHC interaction occurs, Ras can be activated by a second pathway through recruitment of Grb2/SOS to the plasma membrane. This creates a positive feedback loop, which increases the level of Ras-GTP above a threshold leading to negative selection. By comparing the levels and activation states of these signaling components in n3.L2 and M2, we can generate a signaling profile for T cells undergoing positive and negative selection. Additionally, we can compare the response of n3.L2 and M2 thymocytes to APLs to further characterize how changes in kinetic parameters, such as $k_{on}$, alter signal transduction during T cell selection. The same profile could provide insight into how the signals leading to negative selection can alternatively induce anergy in T cells that escape deletion.

*Examination of signaling downstream of the TCR that leads to anergy induction and alteration of n3.L2 versus M2 responsiveness in the periphery*

Induction of anergy in a T cell has been shown to be dependent on the stability of the TCR:pMHC complex (128, 190) and may be induced in the absence of costimulation. The M2 affinity for Hb(64-76)/I-$E^k$ indicates that a stable complex can be formed between soluble scTCR and pMHC complexes. Originally, the M2 TCR was selected for increased stability on the surface of yeast (137), lending further evidence against an

unstable TCR:pMHC complex. *In vivo*, there may be a difference in the stability of the TCR:pMHC complex that inhibits formation of the immune synapse and productive, sustained signaling (190). However, as the M2 $Rag^{+/+}$ T cells do respond to antigen stimulation, complex instability is unlikely to be the cause of anergy induction in M2 $Rag1^{-/-}$ T cells. The geometric shape of the synapse can augment signaling downstream of the TCR (191, 192). When TCR:pMHC complexes are restricted from forming the cSMAC, $Ca^{2+}$ and tyrosine phosphorylation levels both were increased (191), though whether this leads to enhanced activation or, more likely, inhibition of T cell activation has not been determined. The formation of a synapse can be imaged with isolated n3.L2 and M2 T cells on lipid bilayers containing pMHC, with and without the addition of costimulation, and may provide insight into how changes in the TCR:pMHC affinity affect clustering and downstream signaling (51). A difference in the level of costimulation also seems unlikely since n3.L2 and M2. T cells had equivalent levels of all costimulatory and inhibitory receptors measured. One thought would be that the levels of these molecules, such as CTLA-4, PD-1 or CD28, would change after activation (reviewed in (7)). Perhaps the anergic M2 T cells have a high proportion of CTLA-4 on the surface to outcompete CD28 and dampen costimulation. While this may be a simple explanation of the difference between n3.L2 and M2 T cells, the more intriguing possibility is that changes in intracellular signaling downstream of the TCRs control the propensity for tolerance.

Tolerance induction has been linked to phosphorylation of CD3ζ, ERK, ZAP-70, and formation of NFAT dimers (7, 128, 145, 179-181, 190, 193). Low levels of pZAP-70 can disregulate levels of ERK and change the intracellular $Ca^{2+}$ level. Since $Ca^{2+}$ is a

critical second messenger in many signaling pathways, the level and characteristics of $Ca^{2+}$ flux regulate diverse outcomes, including anergy. The n3.L2 and M2 T cells differ in intracellular $Ca^{2+}$ pattern. As a consequence, n3.L2 and M2 T cells may differ in activation of NFAT, required for production of IL-2. The amplitude, duration and oscillations of intracellular $Ca^{2+}$ activate specific sets of transcription factors leading to complex patterns of gene expression (178, 194, 195). Most likely this is through regulation of NFAT dimer formation (180) and the balance of activating NFAT versus NFκB (178, 195). The anergic M2 T cells had a more oscillatory signal that was lower than n3.L2's sustained signal. Interestingly, NFAT activation requires rapid oscillations that result in a low, sustained level of intracellular $Ca^{2+}$ (178, 179). In contrast, a large transient rise with infrequent oscillations preferentially stimulates NFκB. Perhaps the sustained $Ca^{2+}$ level in n3.L2 T cells leads to transcription of NFAT dependent genes, including IL-2, and can account for the maintained responsive state of these T cells. In contrast, while M2 T cells have a more oscillatory phenotype, these oscillations are rather small and may not be enough to sustain NFAT transcription of IL-2. As a consequence, NFAT may form homodimers that inhibit association with AP-1 and lead to the activation of anergy-inducing genes (180, 181). It would be interesting to see if n3.L2 and M2 CD4 T cells differ in activation of NFAT and NFκB. Since the initial $Ca^{2+}$ studies were done in the absence of costimulation, the addition of CD28 ligands may alter the phenotype, providing evidence as to the importance of costimulation in sustained intracellular $Ca^{2+}$ levels and production of IL-2.

A consequence of differential gene transcription is skewed production of cytokines. In a state of anergy, NFAT preferentially induces production of suppressive

cytokines, such as IL-10, though the level may differ in Th1 versus Th2 cells (181). Different cytokines are induced by subtle changes in secondary signal messengers, such as $Ca^{2+}$, and have varying requirements for costimulation (113). Cytokine production by n3.L2 and M2 T cells was not examined aside from IL-2. While n3.L2 was originally a Th1 clone, the stronger affinity M2 may produce a different cytokine profile upon activation by agonist peptides. If M2 favors suppressive signals, this would account for the development of an anergic $Rag1^{-/-}$ population and failure to sustain activation in $Rag^{+/+}$ T cells. In addition to assaying cytokine production *in vitro*, measuring *in vivo* production in the $Hb^{d}$ $C\alpha^{-/-}$ transfer system may provide insight into the delayed disease induction by M2 CD4 T cells.

*Skewing of T cell differentiation and memory formation as a consequence of differences in T cell signaling*

In addition to controlling cytokine production, levels of NFAT family members control the differentiation of naive T helper cells. NFATc2 and NFATc3 function to decrease T cell sensitivity to TCR stimulation. T cells deficient in NFATc2 and NFATc3 preferentially develop into Th2 cells and secrete high levels of IL-4 (196). In contrast, NFATc promotes a T cell response by lowering the threshold for activation (197). When unchecked in the absence of suppressive NFAT factors, NFATc induces rampant production of Th2 cytokines, antibodies, and T cell resistance to Fas induced death (197). This skewing occurred both *in vivo* and *in vitro* by the cytokine milleu. In addition to being resistant to activation induced cell death, the T cells had a faster initiation of proliferation dependent on $Ca^{2+}$ signaling (196). The early but unsustained proliferation

of M2 $Rag^{+/+}$ CD4 T cells may also reflect faster signaling downstream of the TCR because of a lower activation threshold, potentially altering the function of these cells. Instead of TCR sequence, costimulatory signals regulate the differentiation of effector T cell populations (198). CD28 promotes and CTLA-4 inhibits generation of Th2 cells (199). The difference in intracellular $Ca^{2+}$ signal between n3.L2 and M2 T cells may reflect a change in the propensity of these T cells to develop into effector populations, even though the original n3.L2 clone was a Th1 cell. As such, the responses of n3.L2 and M2 T cells to infection or autoantigen may differ.

The strength of the TCR contacting pMHC is critical for naive T cell homeostasis and the generation of memory T cell populations (200). Both processes are critical for maintaining protection against foreign infection. While n3.L2 and M2 CD4 T cells from unmanipulated transgenic mice did not differ in levels of IL-7R or CD44, the difference in sensitivity between n3.L2 and M2 TCRs may result in changes in long term survival of naive T cells or development of memory T cells. Interestingly, an eleveated level of $Ca^{2+}$ from strong TCR signaling induces apoptosis, which can be blocked by Bcl-2, whereas low-level oscillations promote survival (201). Therefore the difference in $Ca^{2+}$ flux measured between n3.L2 and M2 T cells may indicate a difference in survival. When the T cell population is small, the level of antiapoptotic IL-7 is increased, leading proliferation and differentiation into a memory population (202). Tracking the number of transgenic T cells in old M2 and n3.L2 mice could provide information on the homeostatic survival rate of the two different T cells, especially given the difference in thymus sizes at 8 weeks of age. Since isolated M2 T cells were anergic to *ex vivo* stimulation, it is unlikely that we would be able to monitor T cell proliferation *in vivo*.

Transfer of the M2 T cells to a lymphopenic host might induce homeostatic expansion due to increased levels of IL-7.

Since CD4 T cells undergo less homeostatic proliferation than CD8s, a better question may be to identify if an increased $k_{on}$ for pMHC binding alters generation of a memory population. We sought to use a Hb-expressing *Listeria monocytogenes* mutant to examine n3.L2 and M2 activation and recall response to an infection. However, we were unable to induce proliferation of either T cell to stimulation by infected macrophages *in vitro* or immunization *in vivo*. Presumably the system we used induced tolerance of both n3.L2 and M2 T cells. In the lymphopenic $Hb^d$ $C\alpha^{-/-}$ mice, both n3.L2 and M2 T cells seem to expand to fill the T cell niche and induce autoimmune disease, though the transferred cells were not characterized for phenotypic markers of activation or memory. Using the $Hb^d$ $C\alpha^{-/-}$ transfer system, we can identify how differences in the TCR:pMHC affinity alter the rates of T cell expansion or change the activation or memory state of CD4 T cells. The development of memory cells may reflect the affinity of naive T cells for self pMHC in the periphery, however the maintenance of this population is primarily due to cytokines (200, 203). The generation of effector memory cells, which have an activated phenotype, is dependent on the strength of TCR affinity for pMHC. The M2 TCR may generate a larger or more sensitive effector memory population as a consequence of a higher affinity for pMHC. The altered memory population would confer better protection from secondary infection but also increase the possibility of responding to endogenous antigen (200, 203).

*The correlation of TCR:pMHC kinetics to T cell selection and activation, and improving the measurement of this relationship*

The affinity measurements presented in this thesis are derived from measurements of 3D kinetics using purified scTCR and pMHC molecules for SPR. While this system provides a way to make conclusions based on kinetic paramenters of the TCR:pMHC complex, 3D kinetic measurements may not accurately reflect *in vivo* interactions. Recent studies have suggested that 2D kinetics more accurately reflect *in vivo* activation phenotypes and have proposed this as a better system to generate conclusions as to how kinetics regulate T cell activation (25, 153). We are currently using 2D $K_D$ measurements to assess the affinity of TCR for selecting peptide and in a Listeria specific TCR system. Similar measurements could be obtained for n3.L2 and M2 and provide a stronger correlation between activation and kinetics. One caveat is that this may alter the conclusion that M2's increased affinity for Hb(64-76)/I-$E^k$ is due to a change in $k_{on}$. However, in the original reports using the 2D $K_D$ system (153) and in reports using a FRET based system *in vivo* (41), the largest differences between 3D kinetics and these other methods are measured for $k_{on}$, suggesting the relationship we reported for n3.L2 versus M2 may be maintained, though with a different magnitude.

Even though large structural changes in the TCR:pMHC complex have not been observed with higher affinity TCRs (182), a fast $k_{on}$ may reflect optimized molecular conformations for clustering of TCR:pMHC molecules upon activation. Formation of clusters amplifies signals downstream of the TCR but is not required for effective activation of a T cell, including $Ca^{2+}$ signaling (204). As the TCR:pMHC interaction is transient *in vivo*, a faster $k_{on}$ may alter serial engagement of a TCR or the formation of the

cSMAC, which detunes the level of activation (109). A consequence of an increased $k_{on}$ could then be strong signaling through the TCR leading to amplification of inhibitory signals and development of anergy (51), as seen for the M2 T cells. While the studies presented in this thesis suggest a definitive role for $k_{on}$ in regulating CD4 T cell selection and activation, additional systems examining changes solely in $k_{on}$ need to be generated to extend these studies to a general T cell population. By examining changes in the duration and structure of $k_{on}$ driven TCR:pMHC interactions and the propagation of signaling in the T cell, we can understand the sensitive regulation of T cell activation and uncover new ways to enhance, or inhibit, T cell mediated immunity.

REFERENCES


1. Gakamsky, D. M., I. F. Luescher, and I. Pecht. 2004. T cell receptor-ligand interactions: a conformational preequilibrium or an induced fit. *Proc. Natl. Acad. Sci. U. S. A.* 101:9063-9066.
2. McKeithan, T. W. 1995. Kinetic proofreading in T-cell receptor signal transduction. *Proc. Natl. Acad. Sci. U. S. A.* 92:5042-5046.
3. Rabinowitz, J. D., C. Beeson, D. S. Lyons, M. M. Davis, and H. M. McConnell. 1996. Kinetic discrimination in T-cell activation. *Proc. Natl. Acad. Sci. U. S. A.* 93:1401-1405.
4. Valitutti, S., and A. Lanzavecchia. 1997. Serial triggering of TCRs: a basis for the sensitivity and specificity of antigen recognition. *Immunol. Today* 18:299-304.
5. Lyons, D. S., S. A. Lieberman, J. Hampl, J. J. Boniface, Y. Chien, L. J. Berg, and M. M. Davis. 1996. A TCR binds to antagonist ligands with lower affinities and faster dissociation rates than to agonists. *Immunity* 5:53-61.
6. Evavold, B. D., J. Sloan-Lancaster, and P. M. Allen. 1993. Tickling the TCR: selective T-cell functions stimulated by altered peptide ligands. *Immunol. Today* 14:602-609.
7. Macian, F., S. H. Im, F. J. Garcia-Cozar, and A. Rao. 2004. T-cell anergy. *Curr. Opin. Immunol.* 16:209-216.
8. Sloan-Lancaster, J., B. D. Evavold, and P. M. Allen. 1993. Induction of T-cell anergy by altered T-cell-receptor ligand on live antigen-presenting cells. *Nature* 363:156-159.
9. Hogquist, K. A., S. C. Jameson, W. R. Heath, J. L. Howard, M. J. Bevan, and F. R. Carbone. 1994. T cell receptor antagonist peptides induce positive selection. *Cell* 76:17-27.
10. Garcia, K. C., C. G. Radu, J. Ho, R. J. Ober, and E. S. Ward. 2001. Kinetics and thermodynamics of T cell receptor- autoantigen interactions in murine experimental autoimmune encephalomyelitis. *Proc. Natl. Acad. Sci. U. S. A.* 98:6818-6823.
11. Davis-Harrison, R. L., F. K. Insaidoo, and B. M. Baker. 2007. T cell receptor binding transition states and recognition of peptide/MHC. *Biochemistry* 46:1840-1850.
12. Krogsgaard, M., N. Prado, E. J. Adams, X. L. He, D. C. Chow, D. B. Wilson, K. C. Garcia, and M. M. Davis. 2003. Evidence that structural rearrangements and/or flexibility during TCR binding can contribute to T cell activation. *Mol. Cell* 12:1367-1378.
13. Holler, P. D., and D. M. Kranz. 2003. Quantitative analysis of the contribution of TCR/pepMHC affinity and CD8 to T cell activation. *Immunity* 18:255-264.
14. Davis, M. M., and Y. Chien. 1993. Topology and affinity of T-cell receptor mediated recognition of peptide-MHC complexes. *Curr. Opin. Immunol.* 5:45-49.
15. Qi, S., M. Krogsgaard, M. M. Davis, and A. K. Chakraborty. 2006. Molecular flexibility can influence the stimulatory ability of receptor-ligand interactions at cell-cell junctions. *Proc. Natl. Acad. Sci. U. S. A.* 103:4416-4421.
16. Holler, P. D., and D. M. Kranz. 2004. T cell receptors: affinities, cross-reactivities, and a conformer model. *Mol. Immunol.* 40:1027-1031.

17. Davis, M. M., J. J. Boniface, Z. Reich, D. Lyons, J. Hampl, B. Arden, and Y. Chien. 1998. Ligand recognition by alpha beta T cell receptors. *Annu. Rev. Immunol.* 16:523-544.
18. Yang, J., C. P. Swaminathan, Y. Huang, R. Guan, S. Cho, M. C. Kieke, D. M. Kranz, R. A. Mariuzza, and E. J. Sundberg. 2003. Dissecting cooperative and additive binding energetics in the affinity maturation pathway of a protein-protein interface. *J. Biol. Chem.* 278:50412-50421.
19. Robbins, P. F., Y. F. Li, M. El-Gamil, Y. Zhao, J. A. Wargo, Z. Zheng, H. Xu, R. A. Morgan, S. A. Feldman, L. A. Johnson, A. D. Bennett, S. M. Dunn, T. M. Mahon, B. K. Jakobsen, and S. A. Rosenberg. 2008. Single and dual amino acid substitutions in TCR CDRs can enhance antigen-specific T cell functions. *J. Immunol.* 180:6116-6131.
20. Willcox, B. E., G. F. Gao, J. R. Wyer, J. E. Ladbury, J. I. Bell, B. K. Jakobsen, and P. A. van der Merwe. 1999. TCR binding to peptide-MHC stabilizes a flexible recognition interface. *Immunity* 10:357-365.
21. Basu, D., S. Horvath, L. O'Mara, D. Donermeyer, and P. M. Allen. 2001. Two MHC surface amino acid differences distinguish foreign peptide recognition from autoantigen specificity. *J. Immunol.* 166:4005-4011.
22. Borg, N. A., L. K. Ely, T. Beddoe, W. A. Macdonald, H. H. Reid, C. S. Clements, A. W. Purcell, L. Kjer-Nielsen, J. J. Miles, S. R. Burrows, J. McCluskey, and J. Rossjohn. 2005. The CDR3 regions of an immunodominant T cell receptor dictate the 'energetic landscape' of peptide-MHC recognition. *Nat. Immunol.* 6:171-180.
23. Huseby, E. S., F. Crawford, J. White, P. Marrack, and J. W. Kappler. 2006. Interface-disrupting amino acids establish specificity between T cell receptors and complexes of major histocompatibility complex and peptide. *Nat. Immunol.* 7:1191-1199.
24. Collins, E. J., and D. S. Riddle. 2008. TCR-MHC docking orientation: natural selection, or thymic selection? *Immunol. Res.* 41:267-294.
25. Adams, J. J., S. Narayanan, B. Liu, M. E. Birnbaum, A. C. Kruse, N. A. Bowerman, W. Chen, A. M. Levin, J. M. Connolly, C. Zhu, D. M. Kranz, and K. C. Garcia. 2011. T cell receptor signaling is limited by docking geometry to peptide-major histocompatibility complex. *Immunity* 35:681-693.
26. Marrack, P., K. Rubtsova, J. Scott-Browne, and J. W. Kappler. 2008. T cell receptor specificity for major histocompatibility complex proteins. *Curr. Opin. Immunol.* 20:203-207.
27. Feng, D., C. J. Bond, L. K. Ely, J. Maynard, and K. C. Garcia. 2007. Structural evidence for a germline-encoded T cell receptor-major histocompatibility complex interaction 'codon'. *Nat. Immunol.* 8:975-983.
28. Scott-Browne, J. P., J. White, J. W. Kappler, L. Gapin, and P. Marrack. 2009. Germline-encoded amino acids in the alphabeta T-cell receptor control thymic selection. *Nature* 458:1043-1046.
29. Chlewicki, L. K., P. D. Holler, B. C. Monti, M. R. Clutter, and D. M. Kranz. 2005. High-affinity, peptide-specific T cell receptors can be generated by mutations in CDR1, CDR2 or CDR3. *J. Mol. Biol.* 346:223-239.
30. Manning, T. C., E. A. Parke, L. Teyton, and D. M. Kranz. 1999. Effects of complementarity determining region mutations on the affinity of an alpha/beta T

cell receptor: measuring the energy associated with CD4/CD8 repertoire skewing. *J. Exp. Med.* 189:461-470.

31. Dai, S., E. S. Huseby, K. Rubtsova, J. Scott-Browne, F. Crawford, W. A. Macdonald, P. Marrack, and J. W. Kappler. 2008. Crossreactive T Cells spotlight the germline rules for alphabeta T cell-receptor interactions with MHC molecules. *Immunity* 28:324-334.
32. Burrows, S. R., Z. Chen, J. K. Archbold, F. E. Tynan, T. Beddoe, L. Kjer-Nielsen, J. J. Miles, R. Khanna, D. J. Moss, Y. C. Liu, S. Gras, L. Kostenko, R. M. Brennan, C. S. Clements, A. G. Brooks, A. W. Purcell, J. McCluskey, and J. Rossjohn. 2010. Hard wiring of T cell receptor specificity for the major histocompatibility complex is underpinned by TCR adaptability. *Proc. Natl. Acad. Sci. U. S. A.* 107:10608-10613.
33. Armstrong, K. M., K. H. Piepenbrink, and B. M. Baker. 2008. Conformational changes and flexibility in T-cell receptor recognition of peptide-MHC complexes. *Biochem. J.* 415:183-196.
34. Krummel, M., C. Wulfing, C. Sumen, and M. M. Davis. 2000. Thirty-six views of T-cell recognition. *Philosophical transactions of the Royal Society of London. Series B, Biological sciences* 355:1071-1076.
35. Kersh, G. J., and P. M. Allen. 1996. Structural basis for T cell recognition of altered peptide ligands: a single T cell receptor can productively recognize a large continuum of related ligands. *J. Exp. Med.* 184:1259-1268.
36. Jones, L. L., L. A. Colf, A. J. Bankovich, J. D. Stone, Y. G. Gao, C. M. Chan, R. H. Huang, K. C. Garcia, and D. M. Kranz. 2008. Different thermodynamic binding mechanisms and peptide fine specificities associated with a panel of structurally similar high-affinity T cell receptors. *Biochemistry* 47:12398-12408.
37. Reiser, J. B., C. Darnault, C. Gregoire, T. Mosser, G. Mazza, A. Kearney, P. A. van der Merwe, J. C. Fontecilla-Camps, D. Housset, and B. Malissen. 2003. CDR3 loop flexibility contributes to the degeneracy of TCR recognition. *Nat. Immunol.* 4:241-247.
38. Yin, Y., Y. Li, M. C. Kerzic, R. Martin, and R. A. Mariuzza. 2011. Structure of a TCR with high affinity for self-antigen reveals basis for escape from negative selection. *EMBO J.* 30:1137-1148.
39. Matsui, K., J. J. Boniface, P. Steffner, P. A. Reay, and M. M. Davis. 1994. Kinetics of T-cell receptor binding to peptide/I-Ek complexes: correlation of the dissociation rate with T-cell responsiveness. *Proc. Natl. Acad. Sci. U. S. A.* 91:12862-12866.
40. Telmer, P. G., and B. H. Shilton. 2003. Insights into the conformational equilibria of maltose-binding protein by analysis of high affinity mutants. *The Journal of biological chemistry* 278:34555-34567.
41. Huppa, J. B., M. Axmann, M. A. Mortelmaier, B. F. Lillemeier, E. W. Newell, M. Brameshuber, L. O. Klein, G. J. Schutz, and M. M. Davis. 2010. TCR-peptide-MHC interactions in situ show accelerated kinetics and increased affinity. *Nature* 463:963-967.
42. Kersh, G. J., E. N. Kersh, D. H. Fremont, and P. M. Allen. 1998. High- and low-potency ligands with similar affinities for the TCR: the importance of kinetics in TCR signaling. *Immunity* 9:817-826.

43. Dushek, O., M. Aleksic, R. J. Wheeler, H. Zhang, S. P. Cordoba, Y. C. Peng, J. L. Chen, V. Cerundolo, T. Dong, D. Coombs, and P. A. van der Merwe. 2011. Antigen potency and maximal efficacy reveal a mechanism of efficient T cell activation. *Sci. Signal.* 4:ra39.
44. Lee, J. K., G. Stewart-Jones, T. Dong, K. Harlos, K. Di Gleria, L. Dorrell, D. C. Douek, P. A. van der Merwe, E. Y. Jones, and A. J. McMichael. 2004. T cell cross-reactivity and conformational changes during TCR engagement. *J. Exp. Med.* 200:1455-1466.
45. Ely, L. K., T. Beddoe, C. S. Clements, J. M. Matthews, A. W. Purcell, L. Kjer-Nielsen, J. McCluskey, and J. Rossjohn. 2006. Disparate thermodynamics governing T cell receptor-MHC-I interactions implicate extrinsic factors in guiding MHC restriction. *Proc. Natl. Acad. Sci. U. S. A.* 103:6641-6646.
46. Tian, S., R. Maile, E. J. Collins, and J. A. Frelinger. 2007. CD8+ T cell activation is governed by TCR-peptide/MHC affinity, not dissociation rate. *J. Immunol.* 179:2952-2960.
47. Govern, C. C., M. K. Paczosa, A. K. Chakraborty, and E. S. Huseby. 2010. Fast on-rates allow short dwell time ligands to activate T cells. *Proc. Natl. Acad. Sci. U. S. A.* 107:8724-8729.
48. Aleksic, M., O. Dushek, H. Zhang, E. Shenderov, J. L. Chen, V. Cerundolo, D. Coombs, and P. A. van der Merwe. 2010. Dependence of T cell antigen recognition on T cell receptor-peptide MHC confinement time. *Immunity* 32:163-174.
49. Sadir, R., E. Forest, and H. Lortat-Jacob. 1998. The heparan sulfate binding sequence of interferon-gamma increased the on rate of the interferon-gamma-interferon-gamma receptor complex formation. *J. Biol. Chem.* 273:10919-10925.
50. Andersen, P. S., C. Geisler, S. Buus, R. A. Mariuzza, and K. Karjalainen. 2001. Role of the T cell receptor ligand affinity in T cell activation by bacterial superantigens. *The Journal of biological chemistry* 276:33452-33457.
51. Sykulev, Y. 2010. T cell receptor signaling kinetics takes the stage. *Sci. Signal.* 3:pe50.
52. Faroudi, M., R. Zaru, P. Paulet, S. Muller, and S. Valitutti. 2003. Cutting edge: T lymphocyte activation by repeated immunological synapse formation and intermittent signaling. *J. Immunol.* 171:1128-1132.
53. Rosette, C., G. Werlen, M. A. Daniels, P. O. Holman, S. M. Alam, P. J. Travers, N. R. Gascoigne, E. Palmer, and S. C. Jameson. 2001. The impact of duration versus extent of TCR occupancy on T cell activation: a revision of the kinetic proofreading model. *Immunity* 15:59-70.
54. Kalergis, A. M., N. Boucheron, M. A. Doucey, E. Palmieri, E. C. Goyarts, Z. Vegh, I. F. Luescher, and S. G. Nathenson. 2001. Efficient T cell activation requires an optimal dwell-time of interaction between the TCR and the pMHC complex. *Nat. Immunol.* 2:229-234.
55. Engelhardt, J. J., and M. F. Krummel. 2008. The importance of prolonged binding to antigen-presenting cells for T cell fate decisions. *Immunity* 28:143-145.
56. Blichfeldt, E., L. A. Munthe, J. S. Rotnes, and B. Bogen. 1996. Dual T cell receptor T cells have a decreased sensitivity to physiological ligands due to reduced density of each T cell receptor. *Eur. J. Immunol.* 26:2876-2884.

57. Ferber, I., G. Schonrich, J. Schenkel, A. L. Mellor, G. J. Hammerling, and B. Arnold. 1994. Levels of peripheral T cell tolerance induced by different doses of tolerogen. *Science* 263:674-676.
58. Reay, P. A., K. Matsui, K. Haase, C. Wulfing, Y. H. Chien, and M. M. Davis. 2000. Determination of the relationship between T cell responsiveness and the number of MHC-peptide complexes using specific monoclonal antibodies. *J. Immunol.* 164:5626-5634.
59. Watanabe, N., H. Arase, M. Onodera, P. S. Ohashi, and T. Saito. 2000. The quantity of TCR signal determines positive selection and lineage commitment of T cells. *J. Immunol.* 165:6252-6261.
60. Boniface, J. J., Z. Reich, D. S. Lyons, and M. M. Davis. 1999. Thermodynamics of T cell receptor binding to peptide-MHC: evidence for a general mechanism of molecular scanning. *Proc. Natl. Acad. Sci. U. S. A.* 96:11446-11451.
61. Goldbaum, F. A., A. Cauerhff, C. A. Velikovsky, A. S. Llera, M. M. Riottot, and R. J. Poljak. 1999. Lack of significant differences in association rates and affinities of antibodies from short-term and long-term responses to hen egg lysozyme. *J. Immunol.* 162:6040-6045.
62. Evavold, B. D., S. G. Williams, B. L. Hsu, S. Buus, and P. M. Allen. 1992. Complete dissection of the Hb(64-76) determinant using T helper 1, T helper 2 clones, and T cell hybridomas. *J. Immunol.* 148:347-353.
63. Evavold, B. D., J. Sloan-Lancaster, K. J. Wilson, J. B. Rothbard, and P. M. Allen. 1995. Specific T cell recognition of minimally homologous peptides: evidence for multiple endogenous ligands. *Immunity* 2:655-663.
64. Sloan-Lancaster, J., T. H. Steinberg, and P. M. Allen. 1996. Selective activation of the calcium signaling pathway by altered peptide ligands. *J. Exp. Med.* 184:1525-1530.
65. Evavold, B. D., J. Sloan-Lancaster, and P. M. Allen. 1994. Antagonism of superantigen-stimulated helper T-cell clones and hybridomas by altered peptide ligand. *Proc. Natl. Acad. Sci. U. S. A.* 91:2300-2304.
66. Jameson, S. C., and M. J. Bevan. 1998. T-cell selection. *Curr. Opin. Immunol.* 10:214-219.
67. Daniels, M. A., E. Teixeiro, J. Gill, B. Hausmann, D. Roubaty, K. Holmberg, G. Werlen, G. A. Hollander, N. R. Gascoigne, and E. Palmer. 2006. Thymic selection threshold defined by compartmentalization of Ras/MAPK signalling. *Nature* 444:724-729.
68. Hogquist, K. A., and M. J. Bevan. 1996. The nature of the peptide/MHC ligand involved in positive selection. *Semin. Immunol.* 8:63-68.
69. Kosmrlj, A., A. K. Jha, E. S. Huseby, M. Kardar, and A. K. Chakraborty. 2008. How the thymus designs antigen-specific and self-tolerant T cell receptor sequences. *Proc. Natl. Acad. Sci. U. S. A.* 105:16671-16676.
70. Jameson, S. C., K. A. Hogquist, and M. J. Bevan. 1994. Specificity and flexibility in thymic selection. *Nature* 369:750-752.
71. Ignatowicz, L., J. Kappler, and P. Marrack. 1996. The repertoire of T cells shaped by a single MHC/peptide ligand. *Cell* 84:521-529.

72. Huseby, E. S., J. W. Kappler, and P. Marrack. 2008. Thymic selection stifles TCR reactivity with the main chain structure of MHC and forces interactions with the peptide side chains. *Mol. Immunol.* 45:599-606.
73. Dao, T., J. M. Blander, and D. B. Sant'Angelo. 2003. Recognition of a specific self-peptide: self-MHC class II complex is critical for positive selection of thymocytes expressing the D10 TCR. *J. Immunol.* 170:48-54.
74. Lo, W. L., N. J. Felix, J. J. Walters, H. Rohrs, M. L. Gross, and P. M. Allen. 2009. An endogenous peptide positively selects and augments the activation and survival of peripheral CD4+ T cells. *Nat. Immunol.* 10:1155-1161.
75. Hogquist, K. A., A. J. Tomlinson, W. C. Kieper, M. A. McGargill, M. C. Hart, S. Naylor, and S. C. Jameson. 1997. Identification of a naturally occurring ligand for thymic positive selection. *Immunity* 6:389-399.
76. Gascoigne, N. R., and E. Palmer. 2011. Signaling in thymic selection. *Curr. Opin. Immunol.* 23:207-212.
77. Klein, L., M. Hinterberger, G. Wirnsberger, and B. Kyewski. 2009. Antigen presentation in the thymus for positive selection and central tolerance induction. *Nat. Rev. Immunol.* 9:833-844.
78. Williams, C. B., D. L. Engle, G. J. Kersh, J. Michael White, and P. M. Allen. 1999. A kinetic threshold between negative and positive selection based on the longevity of the T cell receptor-ligand complex. *J. Exp. Med.* 189:1531-1544.
79. Kersh, G. J., D. L. Donermeyer, K. E. Frederick, J. M. White, B. L. Hsu, and P. M. Allen. 1998. TCR transgenic mice in which usage of transgenic alpha- and beta-chains is highly dependent on the level of selecting ligand. *J. Immunol.* 161:585-593.
80. Sebzda, E., V. A. Wallace, J. Mayer, R. S. Yeung, T. W. Mak, and P. S. Ohashi. 1994. Positive and negative thymocyte selection induced by different concentrations of a single peptide. *Science* 263:1615-1618.
81. Kao, H., and P. M. Allen. 2005. An antagonist peptide mediates positive selection and CD4 lineage commitment of MHC class II-restricted T cells in the absence of CD4. *J. Exp. Med.* 201:149-158.
82. Dave, V. P., Z. Cao, C. Browne, B. Alarcon, G. Fernandez-Miguel, J. Lafaille, A. de la Hera, S. Tonegawa, and D. J. Kappes. 1997. CD3 delta deficiency arrests development of the alpha beta but not the gamma delta T cell lineage. *EMBO J.* 16:1360-1370.
83. Love, P. E., E. W. Shores, M. D. Johnson, M. L. Tremblay, E. J. Lee, A. Grinberg, S. P. Huang, A. Singer, and H. Westphal. 1993. T cell development in mice that lack the zeta chain of the T cell antigen receptor complex. *Science* 261:918-921.
84. Morley, S. C., K. S. Weber, H. Kao, and P. M. Allen. 2008. Protein kinase C-theta is required for efficient positive selection. *J. Immunol.* 181:4696-4708.
85. Pircher, H., K. Burki, R. Lang, H. Hengartner, and R. M. Zinkernagel. 1989. Tolerance induction in double specific T-cell receptor transgenic mice varies with antigen. *Nature* 342:559-561.
86. Girgis, L., M. M. Davis, and B. Fazekas de St Groth. 1999. The avidity spectrum of T cell receptor interactions accounts for T cell anergy in a double transgenic model. *J. Exp. Med.* 189:265-278.

87. Prasad, A., J. Zikherman, J. Das, J. P. Roose, A. Weiss, and A. K. Chakraborty. 2009. Origin of the sharp boundary that discriminates positive and negative selection of thymocytes. *Proc. Natl. Acad. Sci. U. S. A.* 106:528-533.
88. Werlen, G., B. Hausmann, D. Naeher, and E. Palmer. 2003. Signaling life and death in the thymus: timing is everything. *Science* 299:1859-1863.
89. Starr, T. K., S. C. Jameson, and K. A. Hogquist. 2003. Positive and negative selection of T cells. *Annu. Rev. Immunol.* 21:139-176.
90. Kappler, J. W., N. Roehm, and P. Marrack. 1987. T cell tolerance by clonal elimination in the thymus. *Cell* 49:273-280.
91. Burgert, H. G., J. White, H. U. Weltzien, P. Marrack, and J. W. Kappler. 1989. Reactivity of V beta 17a+ CD8+ T cell hybrids. Analysis using a new CD8+ T cell fusion partner. *J. Exp. Med.* 170:1887-1904.
92. Wucherpfennig, K. W., M. J. Call, L. Deng, and R. Mariuzza. 2009. Structural alterations in peptide-MHC recognition by self-reactive T cell receptors. *Curr. Opin. Immunol.* 21:590-595.
93. Freitas, A. A., F. Agenes, and G. C. Coutinho. 1996. Cellular competition modulates survival and selection of CD8+ T cells. *Eur. J. Immunol.* 26:2640-2649.
94. Morgan, D. J., H. T. Kreuwel, and L. A. Sherman. 1999. Antigen concentration and precursor frequency determine the rate of CD8+ T cell tolerance to peripherally expressed antigens. *J. Immunol.* 163:723-727.
95. Itoh, Y., B. Hemmer, R. Martin, and R. N. Germain. 1999. Serial TCR engagement and down-modulation by peptide:MHC molecule ligands: relationship to the quality of individual TCR signaling events. *J. Immunol.* 162:2073-2080.
96. Chan, C., A. J. George, and J. Stark. 2001. Cooperative enhancement of specificity in a lattice of T cell receptors. *Proc. Natl. Acad. Sci. U. S. A.* 98:5758-5763.
97. Valitutti, S., M. Dessing, K. Aktories, H. Gallati, and A. Lanzavecchia. 1995. Sustained signaling leading to T cell activation results from prolonged T cell receptor occupancy. Role of T cell actin cytoskeleton. *J. Exp. Med.* 181:577-584.
98. Korb, L. C., S. Mirshahidi, K. Ramyar, A. A. Sadighi Akha, and S. Sadegh-Nasseri. 1999. Induction of T cell anergy by low numbers of agonist ligands. *J. Immunol.* 162:6401-6409.
99. Gottschalk, R. A., M. M. Hathorn, H. Beuneu, E. Corse, M. L. Dustin, G. Altan-Bonnet, and J. P. Allison. 2012. Distinct influences of peptide-MHC quality and quantity on in vivo T-cell responses. *Proc. Natl. Acad. Sci. U. S. A.* 109:881-886.
100. Thomas, S., S. A. Xue, C. R. Bangham, B. K. Jakobsen, E. C. Morris, and H. J. Stauss. 2011. Human T cells expressing affinity-matured TCR display accelerated responses but fail to recognize low density of MHC-peptide antigen. *Blood* 118:319-329.
101. Campi, G., R. Varma, and M. L. Dustin. 2005. Actin and agonist MHC-peptide complex-dependent T cell receptor microclusters as scaffolds for signaling. *J. Exp. Med.* 202:1031-1036.

102. Varma, R., G. Campi, T. Yokosuka, T. Saito, and M. L. Dustin. 2006. T cell receptor-proximal signals are sustained in peripheral microclusters and terminated in the central supramolecular activation cluster. *Immunity* 25:117-127.
103. Grakoui, A., S. K. Bromley, C. Sumen, M. M. Davis, A. S. Shaw, P. M. Allen, and M. L. Dustin. 1999. The immunological synapse: a molecular machine controlling T cell activation. *Science* 285:221-227.
104. Cemerski, S., J. Das, J. Locasale, P. Arnold, E. Giurisato, M. A. Markiewicz, D. Fremont, P. M. Allen, A. K. Chakraborty, and A. S. Shaw. 2007. The stimulatory potency of T cell antigens is influenced by the formation of the immunological synapse. *Immunity* 26:345-355.
105. Hampl, J., Y. H. Chien, and M. M. Davis. 1997. CD4 augments the response of a T cell to agonist but not to antagonist ligands. *Immunity* 7:379-385.
106. Krummel, M. F., M. D. Sjaastad, C. Wulfing, and M. M. Davis. 2000. Differential clustering of CD4 and CD3zeta during T cell recognition. *Science* 289:1349-1352.
107. Tailor, P., S. Tsai, A. Shameli, P. Serra, J. Wang, S. Robbins, M. Nagata, A. L. Szymczak-Workman, D. A. Vignali, and P. Santamaria. 2008. The proline-rich sequence of CD3epsilon as an amplifier of low-avidity TCR signaling. *J. Immunol.* 181:243-255.
108. Beeson, C., J. Rabinowitz, K. Tate, I. Gutgemann, Y. H. Chien, P. P. Jones, M. M. Davis, and H. M. McConnell. 1996. Early biochemical signals arise from low affinity TCR-ligand reactions at the cell-cell interface. *J. Exp. Med.* 184:777-782.
109. Cemerski, S., J. Das, E. Giurisato, M. A. Markiewicz, P. M. Allen, A. K. Chakraborty, and A. S. Shaw. 2008. The balance between T cell receptor signaling and degradation at the center of the immunological synapse is determined by antigen quality. *Immunity* 29:414-422.
110. Rabinowitz, J. D., C. Beeson, C. Wulfing, K. Tate, P. M. Allen, M. M. Davis, and H. M. McConnell. 1996. Altered T cell receptor ligands trigger a subset of early T cell signals. *Immunity* 5:125-135.
111. Bennett, F., D. Luxenberg, V. Ling, I. M. Wang, K. Marquette, D. Lowe, N. Khan, G. Veldman, K. A. Jacobs, V. E. Valge-Archer, M. Collins, and B. M. Carreno. 2003. Program death-1 engagement upon TCR activation has distinct effects on costimulation and cytokine-driven proliferation: attenuation of ICOS, IL-4, and IL-21, but not CD28, IL-7, and IL-15 responses. *J. Immunol.* 170:711-718.
112. Powell, J. D., J. A. Ragheb, S. Kitagawa-Sakakida, and R. H. Schwartz. 1998. Molecular regulation of interleukin-2 expression by CD28 co-stimulation and anergy. *Immunol. Rev.* 165:287-300.
113. Lerner, C. G., M. R. Horton, R. H. Schwartz, and J. D. Powell. 2000. Distinct requirements for C-C chemokine and IL-2 production by naive, previously activated, and anergic T cells. *J. Immunol.* 164:3996-4002.
114. Nelson, B. H. 2004. IL-2, regulatory T cells, and tolerance. *J. Immunol.* 172:3983-3988.
115. Krummel, M. F., and J. P. Allison. 1995. CD28 and CTLA-4 have opposing effects on the response of T cells to stimulation. *J. Exp. Med.* 182:459-465.

116. Boise, L. H., A. J. Minn, P. J. Noel, C. H. June, M. A. Accavitti, T. Lindsten, and C. B. Thompson. 1995. CD28 costimulation can promote T cell survival by enhancing the expression of Bcl-XL. *Immunity* 3:87-98.
117. Guntermann, C., and D. R. Alexander. 2002. CTLA-4 suppresses proximal TCR signaling in resting human CD4(+) T cells by inhibiting ZAP-70 Tyr(319) phosphorylation: a potential role for tyrosine phosphatases. *J. Immunol.* 168:4420-4429.
118. Inobe, M., and R. H. Schwartz. 2004. CTLA-4 engagement acts as a brake on CD4+ T cell proliferation and cytokine production but is not required for tuning T cell reactivity in adaptive tolerance. *J. Immunol.* 173:7239-7248.
119. Alberola-Ila, J., K. A. Hogquist, K. A. Swan, M. J. Bevan, and R. M. Perlmutter. 1996. Positive and negative selection invoke distinct signaling pathways. *J. Exp. Med.* 184:9-18.
120. Werlen, G., B. Hausmann, and E. Palmer. 2000. A motif in the alphabeta T-cell receptor controls positive selection by modulating ERK activity. *Nature* 406:422-426.
121. McNeil, L. K., T. K. Starr, and K. A. Hogquist. 2005. A requirement for sustained ERK signaling during thymocyte positive selection in vivo. *Proc. Natl. Acad. Sci. U. S. A.* 102:13574-13579.
122. Zehn, D., and M. J. Bevan. 2006. T cells with low avidity for a tissue-restricted antigen routinely evade central and peripheral tolerance and cause autoimmunity. *Immunity* 25:261-270.
123. De Boer, R. J., D. Homann, and A. S. Perelson. 2003. Different dynamics of CD4+ and CD8+ T cell responses during and after acute lymphocytic choriomeningitis virus infection. *J. Immunol.* 171:3928-3935.
124. Edwards, L. J., and B. D. Evavold. 2010. A unique unresponsive CD4+ T cell phenotype post TCR antagonism. *Cell. Immunol.* 261:64-68.
125. Schwartz, R. H. 1996. Models of T cell anergy: is there a common molecular mechanism? *J. Exp. Med.* 184:1-8.
126. Bachmann, M. F., D. E. Speiser, T. W. Mak, and P. S. Ohashi. 1999. Absence of co-stimulation and not the intensity of TCR signaling is critical for the induction of T cell unresponsiveness in vivo. *Eur. J. Immunol.* 29:2156-2166.
127. Falb, D., T. J. Briner, G. H. Sunshine, C. R. Bourque, M. Luqman, M. L. Gefter, and T. Kamradt. 1996. Peripheral tolerance in T cell receptor-transgenic mice: evidence for T cell anergy. *Eur. J. Immunol.* 26:130-135.
128. Mirshahidi, S., L. C. Ferris, and S. Sadegh-Nasseri. 2004. The magnitude of TCR engagement is a critical predictor of T cell anergy or activation. *J. Immunol.* 172:5346-5355.
129. Savage, P. A., J. J. Boniface, and M. M. Davis. 1999. A kinetic basis for T cell receptor repertoire selection during an immune response. *Immunity* 10:485-492.
130. Schonrich, G., U. Kalinke, F. Momburg, M. Malissen, A. M. Schmitt-Verhulst, B. Malissen, G. J. Hammerling, and B. Arnold. 1991. Down-regulation of T cell receptors on self-reactive T cells as a novel mechanism for extrathymic tolerance induction. *Cell* 65:293-304.

131. Garbi, N., G. J. Hammerling, H. C. Probst, and M. van den Broek. 2010. Tonic T cell signalling and T cell tolerance as opposite effects of self-recognition on dendritic cells. *Curr. Opin. Immunol.* 22:601-608.
132. Heissmeyer, V., and A. Rao. 2004. E3 ligases in T cell anergy--turning immune responses into tolerance. *Science's STKE : signal transduction knowledge environment* 2004:pe29.
133. Zehn, D., S. Y. Lee, and M. J. Bevan. 2009. Complete but curtailed T-cell response to very low-affinity antigen. *Nature* 458:211-214.
134. Corse, E., R. A. Gottschalk, M. Krogsgaard, and J. P. Allison. 2010. Attenuated T cell responses to a high-potency ligand in vivo. *PLoS Biol.* 8.
135. Lorenz, R. G., and P. M. Allen. 1988. Direct evidence for functional self-protein/Ia-molecule complexes in vivo. *Proc. Natl. Acad. Sci. U. S. A.* 85:5220-5223.
136. Lorenz, R. G., and P. M. Allen. 1989. Thymic cortical epithelial cells can present self-antigens in vivo. *Nature* 337:560-562.
137. Weber, K. S., D. L. Donermeyer, P. M. Allen, and D. M. Kranz. 2005. Class II-restricted T cell receptor engineered in vitro for higher affinity retains peptide specificity and function. *Proc. Natl. Acad. Sci. U. S. A.* 102:19033-19038.
138. Donermeyer, D. L., K. S. Weber, D. M. Kranz, and P. M. Allen. 2006. The study of high-affinity TCRs reveals duality in T cell recognition of antigen: specificity and degeneracy. *J. Immunol.* 177:6911-6919.
139. Starwalt, S. E., E. L. Masteller, J. A. Bluestone, and D. M. Kranz. 2003. Directed evolution of a single-chain class II MHC product by yeast display. *Protein Eng.* 16:147-156.
140. Persaud, S. P., D. L. Donermeyer, K. S. Weber, D. M. Kranz, and P. M. Allen. 2010. High-affinity T cell receptor differentiates cognate peptide-MHC and altered peptide ligands with distinct kinetics and thermodynamics. *Mol. Immunol.* 47:1793-1801.
141. Kisielow, P., H. S. Teh, H. Bluthmann, and H. von Boehmer. 1988. Positive selection of antigen-specific T cells in thymus by restricting MHC molecules. *Nature* 335:730-733.
142. Sha, W. C., C. A. Nelson, R. D. Newberry, D. M. Kranz, J. H. Russell, and D. Y. Loh. 1988. Positive and negative selection of an antigen receptor on T cells in transgenic mice. *Nature* 336:73-76.
143. Wulfing, C., C. Sumen, M. D. Sjaastad, L. C. Wu, M. L. Dustin, and M. M. Davis. 2002. Costimulation and endogenous MHC ligands contribute to T cell recognition. *Nat. Immunol.* 3:42-47.
144. Kersh, G. J., and P. M. Allen. 1996. Essential flexibility in the T-cell recognition of antigen. *Nature* 380:495-498.
145. Sloan-Lancaster, J., A. S. Shaw, J. B. Rothbard, and P. M. Allen. 1994. Partial T cell signaling: altered phospho-zeta and lack of zap70 recruitment in APL-induced T cell anergy. *Cell* 79:913-922.
146. Fridkis-Hareli, M., P. A. Reche, and E. L. Reinherz. 2004. Peptide variants of viral CTL epitopes mediate positive selection and emigration of Ag-specific thymocytes in vivo. *J. Immunol.* 173:1140-1150.

147. Fridkis-Hareli, M., and E. L. Reinherz. 2004. New approaches to eliciting protective immunity through T cell repertoire manipulation: the concept of thymic vaccination. *Med Immunol* 3:2.
148. Judkowski, V., E. Rodriguez, C. Pinilla, E. Masteller, J. A. Bluestone, N. Sarvetnick, and D. B. Wilson. 2004. Peptide specific amelioration of T cell mediated pathogenesis in murine type 1 diabetes. *Clin. Immunol.* 113:29-37.
149. Holst, J., A. L. Szymczak-Workman, K. M. Vignali, A. R. Burton, C. J. Workman, and D. A. Vignali. 2006. Generation of T-cell receptor retrogenic mice. *Nat. Protoc.* 1:406-417.
150. Masteller, E. L., M. R. Warner, W. Ferlin, V. Judkowski, D. Wilson, N. Glaichenhaus, and J. A. Bluestone. 2003. Peptide-MHC class II dimers as therapeutics to modulate antigen-specific T cell responses in autoimmune diabetes. *J. Immunol.* 171:5587-5595.
151. Shusta, E. V., M. C. Kieke, E. Parke, D. M. Kranz, and K. D. Wittrup. 1999. Yeast polypeptide fusion surface display levels predict thermal stability and soluble secretion efficiency. *J. Mol. Biol.* 292:949-956.
152. Swat, W., M. Dessing, H. von Boehmer, and P. Kisielow. 1993. CD69 expression during selection and maturation of CD4+8+ thymocytes. *Eur. J. Immunol.* 23:739-746.
153. Huang, J., V. I. Zarnitsyna, B. Liu, L. J. Edwards, N. Jiang, B. D. Evavold, and C. Zhu. 2010. The kinetics of two-dimensional TCR and pMHC interactions determine T-cell responsiveness. *Nature* 464:932-936.
154. Williams, C. B., K. Vidal, D. Donermeyer, D. A. Peterson, J. M. White, and P. M. Allen. 1998. In vivo expression of a TCR antagonist: T cells escape central tolerance but are antagonized in the periphery. *J. Immunol.* 161:128-137.
155. Page, D. M., J. Alexander, K. Snoke, E. Appella, A. Sette, S. M. Hedrick, and H. M. Grey. 1994. Negative selection of CD4+ CD8+ thymocytes by T-cell receptor peptide antagonists. *Proc. Natl. Acad. Sci. U. S. A.* 91:4057-4061.
156. Zhao, Y., A. D. Bennett, Z. Zheng, Q. J. Wang, P. F. Robbins, L. Y. Yu, Y. Li, P. E. Molloy, S. M. Dunn, B. K. Jakobsen, S. A. Rosenberg, and R. A. Morgan. 2007. High-affinity TCRs generated by phage display provide CD4+ T cells with the ability to recognize and kill tumor cell lines. *J. Immunol.* 179:5845-5854.
157. McMahan, R. H., J. A. McWilliams, K. R. Jordan, S. W. Dow, D. B. Wilson, and J. E. Slansky. 2006. Relating TCR-peptide-MHC affinity to immunogenicity for the design of tumor vaccines. *The Journal of clinical investigation* 116:2543-2551.
158. McBeth, C., A. Seamons, J. C. Pizarro, S. J. Fleishman, D. Baker, T. Kortemme, J. M. Goverman, and R. K. Strong. 2008. A new twist in TCR diversity revealed by a forbidden alphabeta TCR. *J. Mol. Biol.* 375:1306-1319.
159. Yu, P., C. L. Haymaker, R. D. Divekar, J. S. Ellis, J. Hardaway, R. Jain, D. M. Tartar, C. M. Hoeman, J. A. Cascio, A. Ostermeier, and H. Zaghouani. 2008. Fetal exposure to high-avidity TCR ligand enhances expansion of peripheral T regulatory cells. *J. Immunol.* 181:73-80.
160. Bautista, J. L., C. W. Lio, S. K. Lathrop, K. Forbush, Y. Liang, J. Luo, A. Y. Rudensky, and C. S. Hsieh. 2009. Intraclonal competition limits the fate determination of regulatory T cells in the thymus. *Nat. Immunol.* 10:610-617.

161. Lathrop, S. K., N. A. Santacruz, D. Pham, J. Luo, and C. S. Hsieh. 2008. Antigen-specific peripheral shaping of the natural regulatory T cell population. *J. Exp. Med.* 205:3105-3117.
162. D'Adamio, L., K. M. Awad, and E. L. Reinherz. 1993. Thymic and peripheral apoptosis of antigen-specific T cells might cooperate in establishing self tolerance. *Eur. J. Immunol.* 23:747-753.
163. Engels, B., A. S. Chervin, A. J. Sant, D. M. Kranz, and H. Schreiber. 2012. Long-term Persistence of CD4(+) but Rapid Disappearance of CD8(+) T Cells Expressing an MHC Class I-restricted TCR of Nanomolar Affinity. *Mol. Ther.* 20:652-660.
164. Felix, N. J., D. L. Donermeyer, S. Horvath, J. J. Walters, M. L. Gross, A. Suri, and P. M. Allen. 2007. Alloreactive T cells respond specifically to multiple distinct peptide-MHC complexes. *Nat. Immunol.* 8:388-397.
165. Smith, K. A. 1988. Interleukin-2: inception, impact, and implications. *Science* 240:1169-1176.
166. Kirberg, J., W. Swat, B. Rocha, P. Kisielow, and H. von Boehmer. 1993. Induction of tolerance in immature and mature T cells. *Transplant. Proc.* 25:279-280.
167. Madrenas, J., R. H. Schwartz, and R. N. Germain. 1996. Interleukin 2 production, not the pattern of early T-cell antigen receptor-dependent tyrosine phosphorylation, controls anergy induction by both agonists and partial agonists. *Proc. Natl. Acad. Sci. U. S. A.* 93:9736-9741.
168. Tanchot, C., D. L. Barber, L. Chiodetti, and R. H. Schwartz. 2001. Adaptive tolerance of CD4+ T cells in vivo: multiple thresholds in response to a constant level of antigen presentation. *J. Immunol.* 167:2030-2039.
169. Azzam, H. S., A. Grinberg, K. Lui, H. Shen, E. W. Shores, and P. E. Love. 1998. CD5 expression is developmentally regulated by T cell receptor (TCR) signals and TCR avidity. *J. Exp. Med.* 188:2301-2311.
170. Itoh, M., T. Takahashi, N. Sakaguchi, Y. Kuniyasu, J. Shimizu, F. Otsuka, and S. Sakaguchi. 1999. Thymus and autoimmunity: production of CD25+CD4+ naturally anergic and suppressive T cells as a key function of the thymus in maintaining immunologic self-tolerance. *J. Immunol.* 162:5317-5326.
171. Hickman-Brecks, C. L., J. L. Racz, D. M. Meyer, T. P. LaBranche, and P. M. Allen. 2011. Th17 cells can provide B cell help in autoantibody induced arthritis. *J. Autoimmun.* 36:65-75.
172. Pakala, S. V., M. O. Kurrer, and J. D. Katz. 1997. T helper 2 (Th2) T cells induce acute pancreatitis and diabetes in immune-compromised nonobese diabetic (NOD) mice. *J. Exp. Med.* 186:299-306.
173. Lafaille, J. J., F. V. Keere, A. L. Hsu, J. L. Baron, W. Haas, C. S. Raine, and S. Tonegawa. 1997. Myelin basic protein-specific T helper 2 (Th2) cells cause experimental autoimmune encephalomyelitis in immunodeficient hosts rather than protect them from the disease. *J. Exp. Med.* 186:307-312.
174. Schietinger, A., J. J. Delrow, R. S. Basom, J. N. Blattman, and P. D. Greenberg. 2012. Rescued tolerant CD8 T cells are preprogrammed to reestablish the tolerant state. *Science* 335:723-727.

175. Lang, H. L., H. Jacobsen, S. Ikemizu, C. Andersson, K. Harlos, L. Madsen, P. Hjorth, L. Sondergaard, A. Svejgaard, K. Wucherpfennig, D. I. Stuart, J. I. Bell, E. Y. Jones, and L. Fugger. 2002. A functional and structural basis for TCR cross-reactivity in multiple sclerosis. *Nat. Immunol.* 3:940-943.
176. Schmid, D. A., M. B. Irving, V. Posevitz, M. Hebeisen, A. Posevitz-Fejfar, J. C. Sarria, R. Gomez-Eerland, M. Thome, T. N. Schumacher, P. Romero, D. E. Speiser, V. Zoete, O. Michielin, and N. Rufer. 2010. Evidence for a TCR affinity threshold delimiting maximal CD8 T cell function. *J. Immunol.* 184:4936-4946.
177. Beal, A. M., N. Anikeeva, R. Varma, T. O. Cameron, G. Vasiliver-Shamis, P. J. Norris, M. L. Dustin, and Y. Sykulev. 2009. Kinetics of early T cell receptor signaling regulate the pathway of lytic granule delivery to the secretory domain. *Immunity* 31:632-642.
178. Dolmetsch, R. E., R. S. Lewis, C. C. Goodnow, and J. I. Healy. 1997. Differential activation of transcription factors induced by Ca2+ response amplitude and duration. *Nature* 386:855-858.
179. Baine, I., B. T. Abe, and F. Macian. 2009. Regulation of T-cell tolerance by calcium/NFAT signaling. *Immunol. Rev.* 231:225-240.
180. Soto-Nieves, N., I. Puga, B. T. Abe, S. Bandyopadhyay, I. Baine, A. Rao, and F. Macian. 2009. Transcriptional complexes formed by NFAT dimers regulate the induction of T cell tolerance. *J. Exp. Med.* 206:867-876.
181. Macian, F., F. Garcia-Cozar, S. H. Im, H. F. Horton, M. C. Byrne, and A. Rao. 2002. Transcriptional mechanisms underlying lymphocyte tolerance. *Cell* 109:719-731.
182. Varani, L., A. J. Bankovich, C. W. Liu, L. A. Colf, L. L. Jones, D. M. Kranz, J. D. Puglisi, and K. C. Garcia. 2007. Solution mapping of T cell receptor docking footprints on peptide-MHC. *Proc. Natl. Acad. Sci. U. S. A.* 104:13080-13085.
183. Basu, D., C. B. Williams, and P. M. Allen. 1998. In vivo antagonism of a T cell response by an endogenously expressed ligand. *Proc. Natl. Acad. Sci. U. S. A.* 95:14332-14336.
184. Sebzda, E., T. M. Kundig, C. T. Thomson, K. Aoki, S. Y. Mak, J. P. Mayer, T. Zamborelli, S. G. Nathenson, and P. S. Ohashi. 1996. Mature T cell reactivity altered by peptide agonist that induces positive selection. *J. Exp. Med.* 183:1093-1104.
185. McGargill, M. A., L. L. Sharp, J. D. Bui, S. M. Hedrick, and S. Calbo. 2005. Active Ca2+/calmodulin-dependent protein kinase II gamma B impairs positive selection of T cells by modulating TCR signaling. *J. Immunol.* 175:656-664.
186. Nika, K., C. Soldani, M. Salek, W. Paster, A. Gray, R. Etzensperger, L. Fugger, P. Polzella, V. Cerundolo, O. Dushek, T. Hofer, A. Viola, and O. Acuto. 2010. Constitutively active Lck kinase in T cells drives antigen receptor signal transduction. *Immunity* 32:766-777.
187. Mallaun, M., D. Naeher, M. A. Daniels, P. P. Yachi, B. Hausmann, I. F. Luescher, N. R. Gascoigne, and E. Palmer. 2008. The T cell receptor's alpha-chain connecting peptide motif promotes close approximation of the CD8 coreceptor allowing efficient signal initiation. *J. Immunol.* 180:8211-8221.

188. Graef, I. A., L. J. Holsinger, S. Diver, S. L. Schreiber, and G. R. Crabtree. 1997. Proximity and orientation underlie signaling by the non-receptor tyrosine kinase ZAP70. *EMBO J.* 16:5618-5628.
189. Tanaka, S., S. Maeda, M. Hashimoto, C. Fujimori, Y. Ito, S. Teradaira, K. Hirota, H. Yoshitomi, T. Katakai, A. Shimizu, T. Nomura, N. Sakaguchi, and S. Sakaguchi. 2010. Graded attenuation of TCR signaling elicits distinct autoimmune diseases by altering thymic T cell selection and regulatory T cell function. *J. Immunol.* 185:2295-2305.
190. Teague, R. M., P. D. Greenberg, C. Fowler, M. Z. Huang, X. Tan, J. Morimoto, M. L. Dossett, E. S. Huseby, and C. Ohlen. 2008. Peripheral CD8+ T cell tolerance to self-proteins is regulated proximally at the T cell receptor. *Immunity* 28:662-674.
191. Mossman, K. D., G. Campi, J. T. Groves, and M. L. Dustin. 2005. Altered TCR signaling from geometrically repatterned immunological synapses. *Science* 310:1191-1193.
192. Choudhuri, K., D. Wiseman, M. H. Brown, K. Gould, and P. A. van der Merwe. 2005. T-cell receptor triggering is critically dependent on the dimensions of its peptide-MHC ligand. *Nature* 436:578-582.
193. Utting, O., S. J. Teh, and H. S. Teh. 2000. A population of in vivo anergized T cells with a lower activation threshold for the induction of CD25 exhibit differential requirements in mobilization of intracellular calcium and mitogen-activated protein kinase activation. *J. Immunol.* 164:2881-2889.
194. Feske, S., J. Giltnane, R. Dolmetsch, L. M. Staudt, and A. Rao. 2001. Gene regulation mediated by calcium signals in T lymphocytes. *Nat. Immunol.* 2:316-324.
195. Dolmetsch, R. E., K. Xu, and R. S. Lewis. 1998. Calcium oscillations increase the efficiency and specificity of gene expression. *Nature* 392:933-936.
196. Rengarajan, J., B. Tang, and L. H. Glimcher. 2002. NFATc2 and NFATc3 regulate T(H)2 differentiation and modulate TCR-responsiveness of naive T(H)cells. *Nat. Immunol.* 3:48-54.
197. Ranger, A. M., M. Oukka, J. Rengarajan, and L. H. Glimcher. 1998. Inhibitory function of two NFAT family members in lymphoid homeostasis and Th2 development. *Immunity* 9:627-635.
198. Wang, C., C. M. Sanders, Q. Yang, H. W. Schroeder, Jr., E. Wang, F. Babrzadeh, B. Gharizadeh, R. M. Myers, J. R. Hudson, Jr., R. W. Davis, and J. Han. 2010. High throughput sequencing reveals a complex pattern of dynamic interrelationships among human T cell subsets. *Proc. Natl. Acad. Sci. U. S. A.* 107:1518-1523.
199. Oosterwegel, M. A., D. A. Mandelbrot, S. D. Boyd, R. B. Lorsbach, D. Y. Jarrett, A. K. Abbas, and A. H. Sharpe. 1999. The role of CTLA-4 in regulating Th2 differentiation. *J. Immunol.* 163:2634-2639.
200. Boyman, O., S. Letourneau, C. Krieg, and J. Sprent. 2009. Homeostatic proliferation and survival of naive and memory T cells. *Eur. J. Immunol.* 39:2088-2094.

201. Zhong, F., M. C. Davis, K. S. McColl, and C. W. Distelhorst. 2006. Bcl-2 differentially regulates Ca2+ signals according to the strength of T cell receptor activation. *The Journal of cell biology* 172:127-137.
202. Surh, C. D., and J. Sprent. 2008. Homeostasis of naive and memory T cells. *Immunity* 29:848-862.
203. Purton, J. F., J. T. Tan, M. P. Rubinstein, D. M. Kim, J. Sprent, and C. D. Surh. 2007. Antiviral CD4+ memory T cells are IL-15 dependent. *J. Exp. Med.* 204:951-961.
204. Friedman, R. S., P. Beemiller, C. M. Sorensen, J. Jacobelli, and M. F. Krummel. 2010. Real-time analysis of T cell receptors in naive cells in vitro and in vivo reveals flexibility in synapse and signaling dynamics. *J. Exp. Med.* 207:2733-2749.

VITAE
Jennifer N. Lynch


Mailing Address: 5636 Waterman Blvd #25
St Louis, MO 63112

E-mail Address: jennifer.nicole.lynch@gmail.com


Education: Ph.D., Immunology, expected August 2012

Washington University in St Louis, MO

B.S., Biology, May 2005
The College of William and Mary, Williamsburg, VA

Awards and Honors: AAI Abstract Trainee Award, 2011
American Association of Immunologists
Academy of Science--St Louis Science Educator Award, 2011
Washington University Imaging Sciences Pathway Fellowship, 2006-2008
Nathan P. Jacobs Scholar Award for independent research, 2003
Howard Hughes Medical Institute Undergraduate Research Awards, 2001-2005
Mortar Board Honor Society
Monroe Scholar

Teaching and
Research Experience: Graduate Research Assistant, 2005-2008
Washington University in St Louis
Laboratory of Dr Mark J. Miller

Teaching Assistant, 2006
Neurophysiology Laboratory
Washington University in St Louis

Undergraduate Research Assistant, 2001-2005
The College of William and Mary

Research Intern, 2000-2001
Lombardi Cancer Center, Georgetown University
Laboratory of Dr Dorraya El-Ashry

Service: The Young Scientist Program (ysp.wustl.edu), 2005-2012
Director and Chairperson for YSP 20th Anniversary Symposium, 2011
Summer Research Mentor and Tutor, 2009-2011

Forensics Teaching Team Head, creator, 2005-2009
Research Boot Camp Instructor, 2005-2009
Steering Committee Member, 2005-2012

Publications:

**Lynch, J.N.,** Donermeyer, D.L., Weber, K.S., Kranz, D.M., and Allen, P.M. *A $k_{on}$ mediated increase in TCR:pMHC affinity results in negative selection and anergy in CD4 T cells.* Submitted.

Divekar, R.D., Haymaker, C.L., Cascio, J.A., Guloglu, B.F., Ellis, J.S., Tartar, D.M., Hoeman, C.M., Franklin, C.L., Zinselmeyer, B.H., **Lynch, J.N.**, Miller, M.J., and Zaghouani, H. *T cell dynamics during induction of tolerance and suppression of experimental allergic encephalomyelitis.* J Immunol. 2011.

Aoshi, T., Zinselmeyer, B.H., Konjufca, V., **Lynch, J.N.**, Zhang, X., Koide, Y., and Miller, M.J. *Bacterial entry to the PALS initiates antigen presentation to CD8 T cells.* Immunity. 2008.

Zinselmeyer, B.H., **Lynch, J.N.**, Zhang, X., Aoshi, T., and Miller, M.J. *Video-rate two-photon imaging of mouse footpad - a promising model for studying leukocyte recruitment dynamics during inflammation*. Inflamm Res. 2008.

Riggs, T., Walts, A., Perry, N., Bickle, L., **Lynch, J.N.**, Myers, A., Flynn, J., Linderman, J.J., Miller, M.J., and Kirschner, D.E. *A comparison of random vs. chemotaxis-driven contacts of T cells with dendritic cells during repertoire scanning.* J Theor Biol. 2008.

Beltman, J.B., Marée, A.F., **Lynch, J.N.**, Miller, M.J., and de Boer, R.J. *Lymph node topology dictates T cell migration behavior.* J Exp Med. 2007.

Conference Abstracts:

**Lynch, J.N.**, Donermeyer, D., Weber, K. S., and Allen, P.M. *Increased $k_{on}$ of TCR-pMHC Interaction Influences Activation and Development of $CD4^+$ T Cells*. American Association of Immunologists, Talk and Poster, 2011

**Lynch, J.N.**, Moss, B., Chiappinelli, K., Mosher, J. and Woolsey, T. *The Young Scientist Program (YSP): Successful use of a volunteer based outreach program created by graduate and medical students to improve science education in the St Louis public school system*, American Association of Immunologists, Talk and Poster, 2011

Unlisted: numerous undergraduate and graduate presentations, including fellowship and departmental research seminars, and journal clubs.